# Functions of the Aryl hydrocarbon Receptor (AhR) and the AhR-Repressor (AhRR) in defense against *Salmonella* Typhimurium and *Toxoplasma gondii* infections

Inaugural thesis presented to the Faculty of Mathematics and Natural Sciences of Heinrich Heine University Düsseldorf for

the degree of Doctor of Natural Sciences

By

**Sevgi Can Cengiz**

from Ankara / TURKEY

Düsseldorf, November 2020

From the Life and Medical Science Institute (LIMES),
Department Immunology and Environment
Rheinische Friedrich Wilhelms University, Bonn

Printed by permission of the Faculty of Mathematics and Natural Sciences of
Heinrich Heine University of Düsseldorf

Examiners:

1. Prof. Dr.rer.nat Irmgard Förster

2. Prof. Dr. rer.nat Johannes Hegemann

Date of the oral defense: 24 March 2021

Statutory Declaration

I declare under oath that I have produced my thesis independently and without any undue assistance by third parties under consideration of the ‘Principles for the Safe Guarding of Good Scientific Practice’ at Heinrich Heine University Düsseldorf.

So far, I have not made any unsuccessful doctoral attempts and have not submitted this dissertation in the present or similar form to any other institution.

Date: November 2020 Sevgi Can Cengiz

# Table of contents

# Abstract / Summary

The aryl hydrocarbon receptor (AhR) is a ligand-activated transcription factor, which is required for regulating immune responses and hence needs a strict regulatory mechanism. The AhR-repressor (AhRR) is encoded by target gene of the AhR and regulates AhR activity by negative feedback inhibition. Our group has generated AhRR/eGFP-reporter mice and showed that the AhRR is highly expressed in gut immune cells. In order to study immunoregulatory functions of the AhRR, disease models inducing gut inflammation was used.

Previously, it was shown that AhRR-deficient mice were highly susceptible to dextran sodium sulfate (DSS)-induced colitis, which was accompanied by enhanced Th17/Tc17 and reduced Th1/Tc1 frequencies in the gut. In line, AhRR-deficient mice were susceptible to *Toxoplasma gondii* infection with enhanced intestinal tissue damage. However, in this thesis it was shown that AhRR-deficiency slightly enhanced Th1 and Tc1 response in the small intestine similar to AhR-deficiency in response *Toxoplasma gondii* infection. These findings may partially explain the intestinal damage observed in AhRR-deficient mice upon parasitic infection. However, the differences in T cell ratios in DSS-induced colitis and *Toxoplasma gondii* infection in AhRR-deficient mice is not due to T cell intrinsic actions.

The necessity of the AhRR in regulating intestinal tissue damage could further be underlined using a *Salmonella* Typhimurium infection model. The AhRR is required not systemically but locally in the small intestine during bacterial infection. In the small intestine, the AhRR-deficiency leads to a strong Th1 response and is likely to have more profound effect in inducing intestinal damage upon bacterial infection.

Furthermore, it was shown that the AhR is required for survival upon *Salmonella* Typhimurium infection. Unlike the AhRR, the AhR has only a minor influence on *Salmonella* induced intestinal tissue damage. High serum IFNγ levels in AhR-deficient mice to bacterial challenge correlated with bacterial numbers and disease severity. During infection, the AhR balances extramedullary erythropoiesis by modulating EPO, TPO and IL-6 production. In addition, the AhR is involved in regulating splenic architecture since AhR-deficient mice lose white pulp structure due to decrease in B cell follicles and increase in T cell dislocation in response to *Salmonella* Typhimurium infection. Moreover, the AhR restrict infection induced hyperactivated immune cell response in

spleen by downregulating excess IFNγ expression in T cells and CD69 expression in T cells and myeloid cells.

Overall, this study showed that the AhRR influence on T cell differentiation and tissue damage in small intestine is dependent on the disease context and gives novel insights about the processes that are regulated by the AhR during *Salmonella* Typhimurium infection.

# List of abbreviations

| | |
|---|---|
| **AhR** | Aryl hydrocarbon Receptor |
| **AhRR** | Aryl hydrocarbon Receptor Repressor |
| **AIDS** | Acquired immune deficiency syndrome |
| **AIP** | AhR-interacting protein |
| **ALRs** | AIM2-like receptors |
| **AMPK** | AMP-activated protein kinase |
| **ANOVA** | Analysis of variance |
| **APC** | Antigen presenting cells |
| **ARNT** | AhR nuclear translocator |
| **BCR** | B cell receptor |
| **bHLH** | Basic helix-loop-helix |
| **BSA** | Bovine serum albumin |
| **CAMP** | Cationic antimicrobial peptides |
| **CD** | Crohn's disease |
| **CDC** | Center of Disease Control and Prevention |
| **CFU** | Colony forming unit |
| **CLR** | C-type lectin receptors |
| **CPs** | Cryptopatches |
| **DAPI** | 4',6-diamidino-2-phenylindole |
| **DC** | Dendritic cells |
| **DIM** | 3,3-diindolymethane |
| **dsRNA** | Double-stranded RNA |
| **DSS** | Dextran sulfate sodium |
| **EDTA** | Ethylenediaminetetraacetic acid |
| **EH** | Extramedullary hematopoiesis |
| **ELISA** | Enzyme- linked immunosorbent assay |
| **EPO** | Erythropoietin |

| | |
|---|---|
| **ER** | Estrogen receptor |
| **EtOH** | Ethanol |
| **FACS** | Fluorescence-activated cell sorting |
| **FAE** | Follicle-associated epithelium |
| **FICZ** | 6-formylindolo[3,2-b] carbazole |
| **FOXP3** | Forkhead box P3 |
| **g** | Gram |
| **GALT** | Gut associated lymphoid tissue |
| **GFP** | Green fluorescent protein |
| **GI** | Gastrointestinal |
| **h** | Hour |
| **H&E** | Hematoxylin and eosin |
| **HIF1α** | Hypoxia-inducible-factor 1 α |
| **HSC** | Hematopoietic stem cell |
| **HSP90** | Heat shock protein 90 |
| **I3C** | Indole 3-carbinol |
| **IBD** | Inflammatory bowel diseases |
| **ICZ** | Indole-[3,2-b]-carbazole |
| **IDO** | Indoleamine 2,3-dioxygenase |
| **IEL** | Intraepithelial lymphocytes |
| **IFNγ** | Interferon gamma |
| **Ig** | Immunoglobulin |
| **IL** | Interleukin |
| **ILC** | Innate lymphoid cells |
| **ILFs** | Isolated lymphoid follicles |
| **iNOS** | Inducible nitric oxide synthase |
| **iNTS** | Invasive non-typhoid *Salmonella* |
| **IRGs** | Immunity-related GTPases |
| **LB** | Luria-Bertani |
| **LP** | Lamina propria |
| **LPS** | Lipopolysaccharide |

| | |
|---|---|
| **mg** | Milligram |
| **µm** | Micrometer |
| **mm** | Millimeter |
| **mM** | Millimolar |
| **MACS** | Magnetic cell separation |
| **M cell** | Microfold cell |
| **MALT** | Mucosa-associated lymphoid tissue |
| **MHC** | Major histocompatibility complex |
| **min** | Minute |
| **ml** | Millimeter |
| **mLNs** | Mesenteric lymph nodes |
| **MMM** | Marginal zone metallophilic macrophages |
| **mTOR** | Mammalian target of rapamycin |
| **MZ** | Marginal zone |
| **MZM** | Marginal zone macrophages |
| **NK** | Natural killer |
| **NLR** | NOD like receptors |
| **NO** | Nitric oxide |
| **Nramp1** | Natural resistance-associated protein 1 |
| **O/N** | Overnight |
| **PAS** | PER-ARNT-SIM domains |
| **PBS** | Phosphate buffered saline |
| **PCR** | Polymerase chain reaction method |
| **PFA** | Paraformaldehyde |
| **PLP** | Periodate lysine paraformaldehyde |
| **PPs** | Peyer`s patches |
| **PRR** | Pattern-recognition receptors |
| **RBC** | Red blood cells |
| **RLRs** | RIG-I-like receptors |
| **RORγt** | RAR-related orphan receptor gamma thymus |
| **ROS** | Reactive oxygen species |

| | |
|---|---|
| **RP** | Red pulp |
| **RPM** | Red pulp macrophage |
| **RT** | Room temperature |
| ***S. bongori*** | *Salmonella bongori* |
| ***S. enterica*** | *Salmonella enterica* |
| ***S.Typhimurium*** | *Salmonella* Typhimurium |
| **SCF** | Stem cell factor |
| **SCID** | Severe combined immunodeficiency |
| **SCV** | *Salmonella*- containing vacuoles |
| **SEM** | Standard error of the mean |
| **SNP** | Single nucleotide polymorphism |
| **SPI** | *Salmonella* pathogenicity island |
| **SRC** | Proto-oncogene tyrosine-protein kinase Src |
| ***T.gondii*** | *Toxoplasma gondii* |
| **T3SS** | Type III secretion system |
| **TCDD** | 2,3,7,8-tetrachlorodibenzo-p-dioxin |
| **TCR** | T cell receptor |
| **TF** | Transcription factor |
| **Th** | T helper |
| **TLR** | Toll-like receptors |
| **TNF** | Tumor necrosis factor |
| **TPO** | Thrombopoietin |
| **WHO** | World Health Organization |
| **WP** | White pulp |
| **WT** | Wild type |
| **XLD** | Xylose Lysine Deoxycholate |
| **XRE** | Xenobiotic response elements |

# Table of Figures

# Table of Tables

# 1 Introduction

## 1.1 The immune system

Continuous exposure of complex organisms to diverse challenges from external threats, such as pathogens or toxins, to internal threats, like tumor formation, requires an orchestrated network to defend itself. This network consists of cells, proteins and chemicals with highly specialized functions and is known as the immune system. In order to be effective, the immune system needs to work effectively and if not, various diseases may develop. Thus, the immune system can be weak, overactive, or dysfunctional. A dysfunctional immune system may result from congenital primary immune deficiencies that are present at birth, as for example severe combined immunodeficiency (SCID). A weakening of the immune system may be acquired at later stages in life, which can for example be observed in acquired immune deficiency syndrome (AIDS). An overactive immune system on the other hand may react to substances in the environment, which under normal conditions are harmless. Examples for an overactive immune system include allergies such as asthma, eczema, and hay fever. In autoimmune diseases, like in Lupus erythematosus or Type I diabetes, the immune system attacks normal and healthy tissues (Maidhof & Hilas, 2012; Van Belle et al., 2011).

Depending on the speed and the specificity of the response, the immune response is divided into two parts: innate immunity and adaptive immunity (Murphy, 2011). Innate immunity can be further categorized into immediate and induced innate immunity. Immediate immune responses form the first line of defense against external threats, and can be mechanical, chemical, or microbiological. Skin, gut, lungs, and eyes/nose/oral cavity form our body surfaces and these organs are protected by epithelia. Tight junctions firmly link epithelial cells to each other, and hence serve as mechanical barriers. Mucus secreted by mucosal epithelia in lungs, tears produced in eyes or longitudinal flow of air in skin are also mechanical barriers against pathogens. Epithelial cells can also produce digestive enzymes and antimicrobial peptides all of which are important for creating chemical barriers against pathogens (Marshall et al., 2018). Healthy epithelial surfaces are generally colonized with non-harmful bacteria, known as commensal microbiota, and these harmless bacteria on one hand compete with pathogens for nutrients and on the other hand produce

antimicrobial substances that are important for host defense (Murphy, 2011). If the first line of defense is bypassed, initially induced innate immune system and later antigen specific adaptive immune system is triggered.

## 1.2 Innate immune system

After breaching the first line of defense, pathogens encounter soluble and cellular innate defense mechanisms. The complement system, chemokines, and cytokines make up the main components of the soluble innate defense system. The complement system recognizes and coats pathogens to target them to immune cells for phagocytosis and effective killing. It consists of plasma and membrane-associated serum proteins to regulate inflammatory and cytolytic immune responses against pathogens and tissue damage. Many complement proteins are activated by proteolytic cleavage and the complement system operates through a triggered enzyme cascade. Recent evidence also suggest that the complement system can play an important role in adaptive immunity and facilitates maintenance of immunologic memory (Dunkelberger & Song, 2010; Sarma & Ward, 2011). Cytokines and chemokines are small, secreted proteins and are important for cell-cell communication. Cytokines are crucial mediators of cellular activation and chemokines are necessary for cell migration. Tumor necrosis factor (TNF), Interleukin- 1 (IL-1), Interleukin-6 (IL-6) are important cytokines produced by innate immune cells. Some of the important chemokines during inflammatory responses include CCL1, CCL23, CCL17 and CXCL1 (Cardona et al., 2013; Stutte et al., 2010). Depletion of one or multiple chemokines can impair cell migration (Griffith et al., 2014).

Various cells are involved in innate immune responses with different mechanisms and functions. The innate immune cell types are depicted in **Figure 1-1** and among these macrophages and neutrophils represent phagocytes. Phagocytosis is described as the capacity of a cell to engulf microbes, and expose these microbes to toxic intracellular molecules, including superoxide ions, lysozymes, and nitric oxide (NO). Neutrophils contain granules, and are able to eject nuclear chromatin to entangle bacteria (Kaplan & Radic, 2012; Marshall et al., 2018). Macrophages, in addition to their phagocytic activity have the ability to function as antigen presenting cells (APCs). However, the most potent type of APCs are the dendritic cells (DCs). One of the most crucial function of DCs is to act as a messenger between innate and adaptive immune responses. DCs can

efficiently capture, process and present antigens as well as migrate to lymphoid tissues to select antigen reactive T cell clones. A member of granulocytes, namely eosinophils are necessary in killing parasites by releasing reactive oxygen metabolites to the environment (Klion & Nutman, 2004). Mast cells and basophils initiate acute inflammatory responses and are effectors of allergic inflammation. Natural killer (NK) cells can destroy tumors and virus infected cells, through the release of perforins and granzymes. Innate lymphoid cells (ILCs) are important for tissue homeostasis and inflammation (Delves & Roitt, 2000; Marshall et al., 2018).

Innate immune cells can recognize pathogens or other danger related signals through germline-encoded pattern-recognition receptors (PRRs). Pathogens have conserved microbial patterns, which are recognized by different PRRs. This recognition leads to activation of innate immunity. The PRR family can mainly be grouped in membrane-bound receptors and cytoplasmic receptors. Toll-like receptors (TLRs) and C-type lectin receptors (CLRs) are examples of membrane-bound receptors and they are located either on cell surface or on endosomal membranes. NOD like receptors (NLRs), RIG-I-like receptors (RLRs) and the AIM2-like receptors (ALRs) form the soluble group that hunt intracellular pathogens in the cytosol (Brubaker et al., 2015). In mammalian species, there are more than ten TLRs and all have distinct functions in addition to expression patterns depending on the cell subset. TLR4 is expressed rather broadly, and recognizes lipopolysaccharide (LPS), which is present in outer membrane of gram-negative bacteria (Hoshino et al., 1999). TLR2 recognizes peptidoglycan from gram-positive bacteria and bacterial lipoproteins and dimerizes with TLR1 or TLR6. TLR3 recognizes double-stranded RNA (dsRNA), TLR5 recognizes flagellin, which forms the bacterial flagella and TLR9 recognizes unmethylated CpG motifs in bacterial DNA (Medzhitov, 2001). Dectin-1, which is a member of the CLR family, recognizes β-glucan present in fungal cell walls and it regulates phagocytosis as well as other immune responses. Another member of the CLR family, Dectin-2, on the other hand binds to mannose and promotes production of cytokines (T. H. Li et al., 2019). NOD1 and NOD2 are members of the NLR family, which reside in the cytosol and detect components of bacterial outer membranes and regulate cytokine production (Caruso et al., 2014). RLRs detect the presence of foreign RNA within the cytosol, and ALRs are involved in detection of dsDNA, both of which are important for regulating immune responses to these molecules (Brubaker et al., 2015).

In addition to eliminating pathogens through processes described above, innate immune cells need to send information to adaptive immune cells to help mount an efficient immune response against pathogens and help B cells to produce different kinds of antibodies in response to these pathogens. To do this, an antigen presentation system has evolved in which antigens are presented either by major histocompatibility complex I (MHCI) or MHCII molecules. This mechanism recognizes self and non-self-antigens, however only the latter induce an immune response. Antigens that are detected in the cytosol of all cells are presented by MHC I molecules to $CD8^+$ T cells (cytotoxic T cells) (Rock et al., 2016). These cells are specialized in destroying infected cells. On the other hand, MHC II molecules bind pathogen peptides, which are generated by proteolytic cleavage in endocytic compartments of antigen presenting cells, like macrophages, DCs and B cells and are presented to $CD4^+$ T cells (helper T cells) (Neefjes et al., 2011). The MHC-peptide complex hence is important in regulating adaptive immune responses, which are more specific and effective in eliminating pathogens.

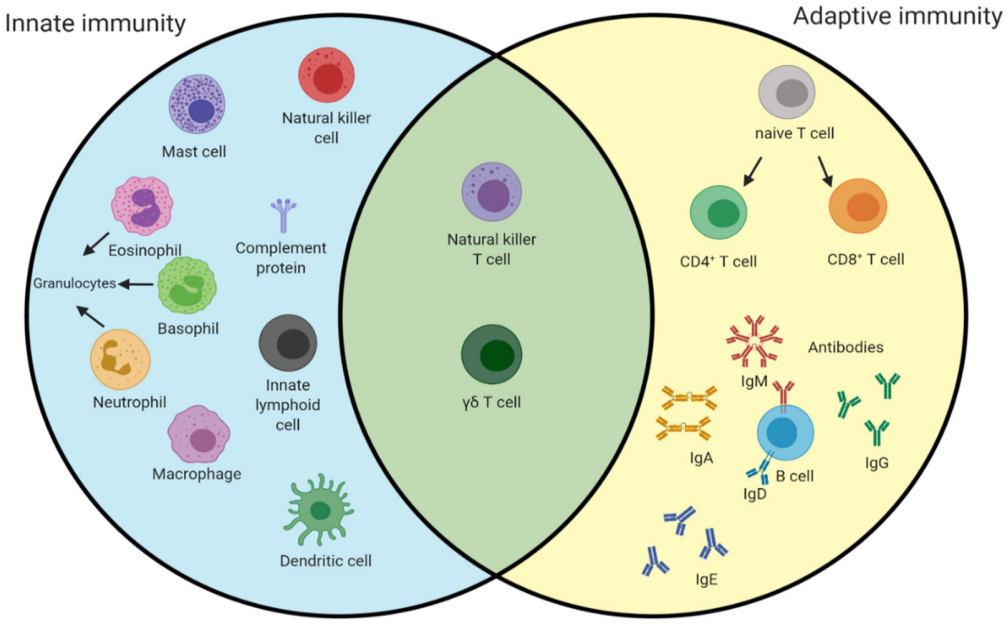


**Figure 1-1: Cell types of the innate and adaptive immune response.**
After bypassing the mechanical barriers, external threats like toxins or pathogens initiate innate immune responses. These responses are rapid and generated by macrophages, NK cells, ILCs, mast cells, dendritic cells, and granulocytes. These cells exert their function by either engulfing the pathogen or creating soluble immune mediators such as cytokines and chemokines. In later stages, adaptive immune responses are generated. B cells secrete antibodies and T cells either help other cells to regulate immune responses ($CD4^+$ T cells) or act directly by killing infected cells ($CD8^+$ T cells).

## 1.3 Adaptive immune system

For initial pathogen restraint, innate immune cells are essential for forming pro-inflammatory responses, but in later stages, adaptive immune cells take over the duty. The main adaptive immune cell types are represented in **Figure 1-1**. Initially, adaptive immune cells fulfill effector functions in the immune response to specifically eliminate the invading pathogen and later, these cells differentiate into a pool of memory cells. Memory cells can persist a very long time and can protect the host against re-infection. These two points make adaptive immune system unique.

B and T lymphocytes are the antigen-responsive cells of the adaptive immune system. Naïve B cells express immunoglobulin D and/or M (IgD, IgM) on their surface. Antigen encounter with the B cell receptor (BCR) initiates B cell activation. B cell activation can occur either via T cell independent or T cell dependent processes. Recognition of T independent antigens by BCR together with TLRs differentiates B cells to plasma cells that secrete IgM (Batista & Harwood, 2009). However, the majority of antibody responses to antigens require T cells. Upon antigen recognition by the BCR, B cells display MHCII-peptide complexes on their surface, which are recognized by $CD4^+$ T cells (Batista & Harwood, 2009). With this direct cellular contact, B cells can differentiate into plasma or memory cells. The plasma cells are important for secreting large amounts of IgA, IgG, IgE, while memory cells are the quick responders upon re-infection.

T cells are activated when the T cell receptor (TCR) recognizes MHC-peptide complexes presented on APCs. The TCR consists of either alpha (α) and beta (β) or gamma (γ) and delta (δ) chains (Murphy, 2011). Together with CD3 and ζ-chain accessory molecules, the TCR complex is formed. The TCR associates with CD3 for initiating intracellular signaling cascades and associates with co-receptors CD4 or CD8 for stabilizing interactions between T cell and APC (Germain, 2002). T cells also require a co-stimulatory signal through CD28 for activation and survival. Signaling through the TCR complex leads to robust IL-2 secretion and this cytokine stimulates T cell proliferation in an autocrine manner (Sojka et al., 2004). Helper T cells express CD4 and are capable of producing cytokines to activate immune cells like macrophages and chemokines to recruit immune cells to the site of infection. Cytotoxic T cells have CD8 and in addition to cytokine production, they are responsible for eliminating infected cells via delivery of cytotoxic granules (Pennock et al., 2013). Depending on the antigen, a diverse cytokine milieu is generated. T cells

differentiate into different subsets in response to these cytokines and form most effective mechanisms for eliminating the pathogen. Important T helper (Th) subsets are Th1, Th2, Th17, Th9, Th22, follicular Th (Tfh) and Tregs, which have different cytokine profiles as seen in **Figure 1-2**. IFNγ is crucial for macrophage activation and are released by Th1 cells. Differentiation of naïve T cells to Th1 cells requires IL-12 in the environment (Szabo et al., 2000).

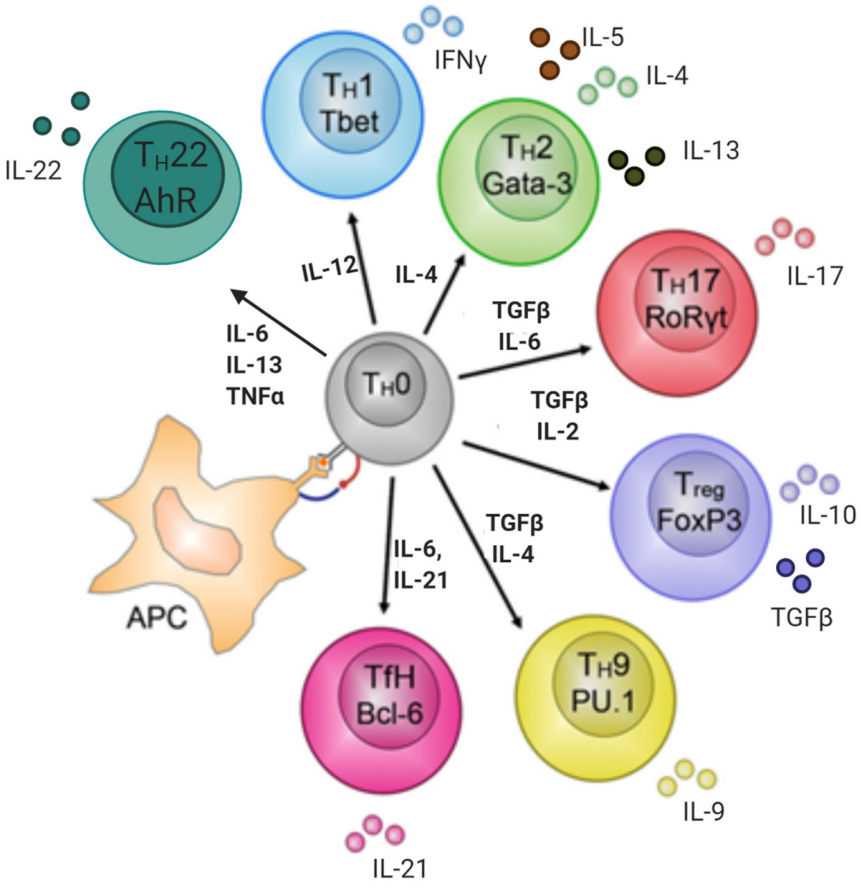


**Figure 1-2: Differentiation of naïve T cells to helper T cell subsets.**
Depending on the type of the antigen presented on APC-MHCII complex and cytokine milieu, naïve T cells are differentiated into T-helper (Th) 1, Th2, Th9, Th17, and Th22, Tfh and Treg subsets. The cytokines required for specific subset differentiation, master transcription factor as well as cytokines produced by different subsets are depicted. (Figure is modified from Russ et al., 2013)

Th2 subset differentiation is mediated in the presence of IL-4, and Th2 cells in turn produce IL-4, IL-5 and IL-13, which mediate parasite elimination by activating eosinophils, mast cells and

basophils (Mosmann & Coffman, 1989; Taylor-Robinson & Phillips, 1992). Th9 cells are generated in the presence of IL-4 and TGFβ and this subset release IL9 to help $CD4^+$ T cell survival (Goswami & Kaplan, 2011; Pennock et al., 2013). Th17 and Th22 cells are the protectors in mucosal barriers and have the ability to produce IL-17 and IL-22, respectively. Th17 cells, depending on the disease context can however also be pathogenic. TGFβ and IL-6 are important cytokines for Th17 differentiation and these cells help fighting against bacterial and fungal infections (Yang et al., 2008; Zhu & Paul, 2008). Tfh cells are necessary for helping B cells during germinal center reactions and IL-6, IL-21 are essential for Tfh formation (Qin et al., 2018). Unlike other T cell subsets, Tregs have a suppressive activity and express the unique transcription factor FOXP3 (Fontenot et al., 2017). Tregs are capable of producing IL10 and TGFβ and suppress T cell proliferation and cytokine production from other Th cells (Harrison & Powrie, 2013; Russ et al., 2013). After pathogen clearance, memory T cell pools including central memory, effector memory and tissue resident memory T cells form. Depending on the type, memory T cells are able to access secondary lymphoid organs, can be found in peripheral circulation or stay in tissues under homeostasis and can react immediately to a pathogen re-encounter. These cells are more sensitive to antigen re-stimulation through the TCR receptor, which makes them quick responders to reinfection (Mueller et al., 2013). In addition to the conventional T cells, γδ T and NKT cells are also generated from the T cell lineage, and these have the unique ability to form a bridge between innate and adaptive immunity. They recognize antigens less specifically than conventional T cells however; they have rapid responses against pathogens (Mak et al., 2014).

## 1.4 Structure and function of the spleen

The spleen is the largest organ for filtering blood and is important for detecting blood borne pathogens. It has a unique architecture, which is necessary for function of innate and adaptive immune cells. Depending on the cell type, function and structure, the rodent spleen is divided into three parts: red pulp (RP), white pulp (WT) and marginal zone (MZ). Although the rodent splenic architecture is very well characterized, the anatomy of human spleens is known to be different. Nevertheless, a commonly observed difference of human spleen compared to rodent spleen is the presence of a perifollicular zone and the lack of a marginal sinus separating the MZ (Mebius & Kraal, 2005). In this thesis, the rodent splenic architecture and immune cell types therein will be

discussed further their structure is schematically depicted in **Figure 1-3**. One of the most important immune cells of the RP is the red pulp macrophage (RPM), which remove aged, infected, or dysfunctional red blood cells (RBCs) and recovers iron from them for systemic use (Kurotaki et al., 2015). The RP can harbor many innate immune cell types, including monocytes, neutrophils, NK cells and DCs however, in naïve state many of these populations are present only in very low numbers (Lewis et al., 2019).

The WP is mainly divided into B cell follicles and T cell zones. DCs are localized in between and can present antigens to help organize B cell follicles. The structure of the WP is preserved through chemokines that are released from fibroblasts and other cells in the surroundings (Zhao et al., 2015). Initiation of adaptive immunity generally occurs in the WP, where APCs enter the T cell zone thereby activating them. T cells then can migrate near the edge of the B cell follicles to induce B cell activation. B cells, T cells and DCs can migrate to RP or to MZ from the WP to exert their functions (Mebius & Kraal, 2005).

The MZ is at the interface of RP and WP and is a transit area for cells leaving the blood and entering the WP. It harbors marginal zone macrophages (MZMs), which forms the outer ring of the MZ and marginal zone metallophilic macrophages (MMMs) forming the inner ring. MZMs can recognize bacterial and viral pathogens by MARCO or SIGNR1 receptors and MMMs mediate pathogen recognition and elimination from circulation by MOMA-1 or SIGLEC receptors (Lewis et al., 2019). In addition, MMMs can interact with DCs to induce $CD8^+$ T-cell activation (Borges Da Silva et al., 2015). The MZ also contains innate-like B cells, namely MZB cells and DCs which quickly respond to blood borne pathogens and transport antigens to the WP for initiating adaptive immunity (Bronte & Pittet, 2013; Lewis et al., 2019). The composition and location of the immune cell subsets in the spleen is very critical for their function and any disturbances can lead to insufficient immune responses against pathogens.

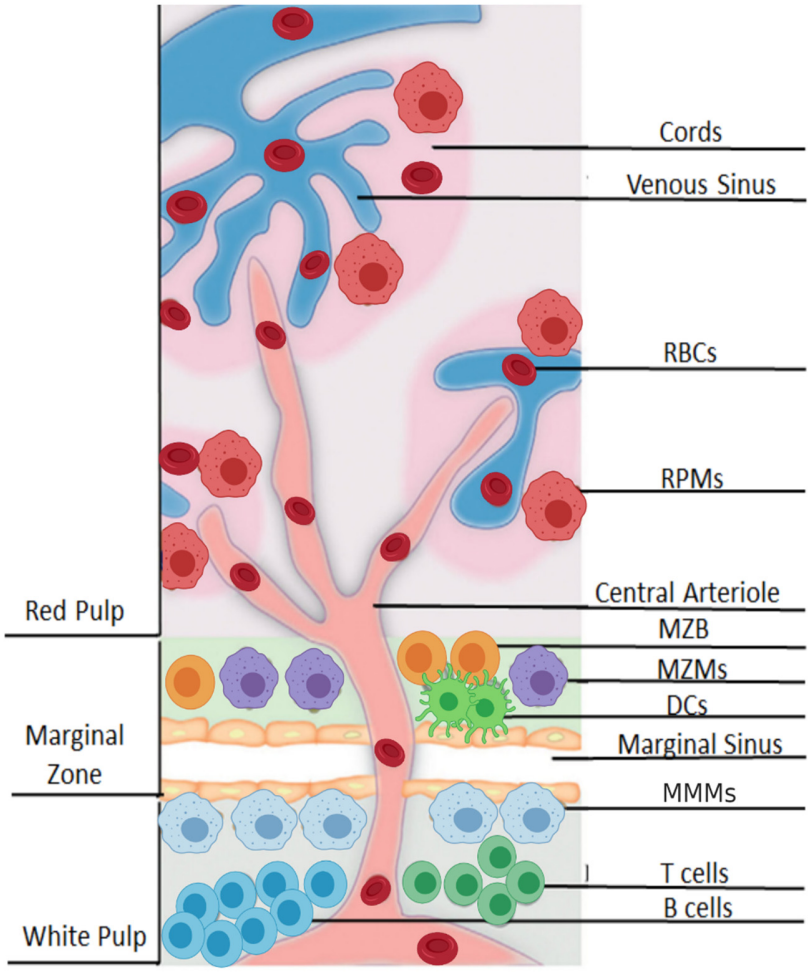


**Figure 1-3: Mouse splenic architecture**
The murine spleen is composed of the RP (red pulp), MZ (Marginal zone) and WP (White Pulp) all of which have a unique structure and composition of immune cells. The blood reaches the spleen at the MZ through the central arteriole and is distributed to different regions. The RP is rich in RPMs and they are required for phagocytosis of aged or infected RBCs. Lymphocytes are the major populations in the WP and are important for generating adaptive immunity. The MZ consist of macrophage types like MZMs at the outer layer and MMMs at the inner layer. Inner and outer layer of the MZ is separated by the marginal sinus. MZ also harbors MZB and DCs at the outer ring required for quick response to pathogens and transporting antigens to lymphocytes in WP. (Figure modified from Borges et al., 2015)

## 1.5 Structure and function of the gut associated lymphoid tissue

The gastrointestinal (GI) tract has a unique organization that forms a protective barrier between external environment and internal structures. Moreover, commensal bacteria (microbiota) in the GI tract provide additional protection against external threats. These bacteria also generate amino acids or vitamins, which are taken up and utilized by host cells. For maintaining homeostasis, a crosstalk among microbiota, epithelial cells and immune cells is essential. The gut associated lymphoid tissue (GALT) is part of the mucosa-associated lymphoid tissue (MALT), which is distributed along the intestinal tract and contains one of the largest lymphoid cell reservoirs. The GALT is composed of highly organized structures including Peyer`s patches (PPs), mesenteric lymph nodes (mLNs), isolated lymphoid follicles (ILFs), cryptopatches (CPs), fat-associated

lymphoid tissue and lamina propria (LP) (McGhee & Fujihashi, 2012). The general structure and composition of LP and PPs are represented in **Figure 1-4**. PPs contain special epithelial cells on their surface, namely follicle associated epithelial cells and microfold (M) cells (Fujimura, 1986). Many cells play a central role in regulating immunity in the gut. Once M cells transport antigens from lumen to DCs which in activates adaptive immune system (Jung et al., 2010). Activated B and T cells leave the PPs through lymphatics and reach MLNs. DCs can also take up antigens in the LP and travel to MLNs to activate naïve T lymphocytes there. From MLNs, lymphocytes travel through lymph and blood and finally reach the LP. In the LP, Th2 cells are critical for activating B cells. Upon activation, B cells become plasma cells and secrete IgA (Forchielli & Walker, 2005). IgA can block certain bacterial epitopes and prevent adhesion of microbiota with IECs (Gutzeit et al., 2014).

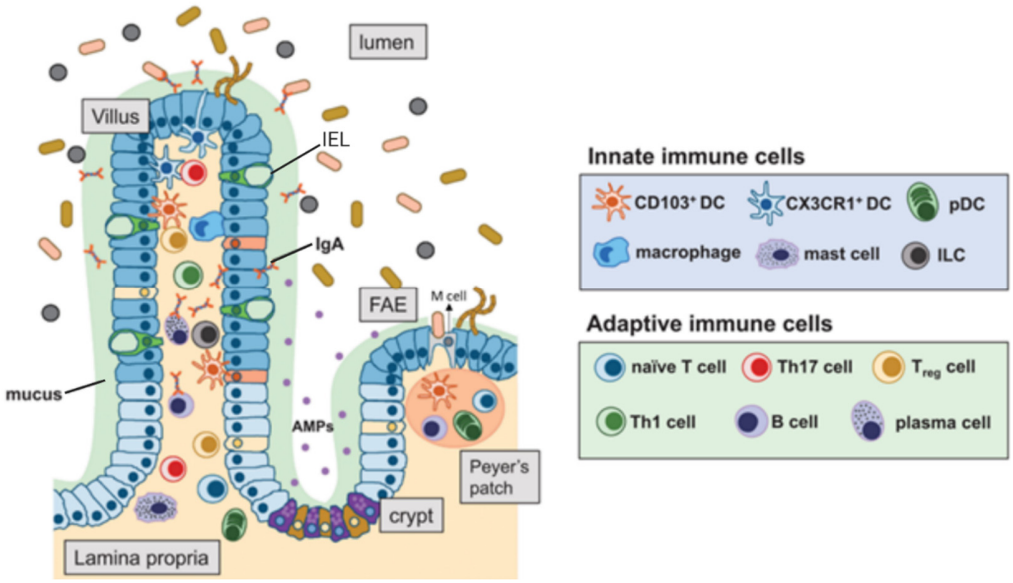


**Figure 1-4: Innate and adaptive immune cells of the small intestine.**
Innate and adaptive immune cells maintain the homeostasis in the gut and are important for controlling the outcome of infections. DCs, macrophages, mast cells and ILCs are the main innate immune cell types in the gut. Adaptive immune cells include helper and cytotoxic T cells as well as naïve or activated B cells. IELs are mainly composed of TCRγδ cells and reside in the epithelium. (Image adapted from Okumura et al., 2016)

Activated T cells produce large amounts of cytokines like IFNγ, IL-4 and IL-10 in response to a challenge. The LP also harbors other immune cell types such as mast cells, ILC and macrophages. The intestinal epithelium also contains intraepithelial lymphocytes (IELs) which are mainly

composed of TCRγδ cells but TCRαβ lineage cells also appear. Since majority of these cells express the CD8αα co-receptor on their surface, they have cytotoxic function and can kill infected epithelial cells. In addition, they produce cytokines and communicate with epithelial cells or other immune cell subsets (Cheroutre et al., 2011).

## 1.6 The Aryl hydrocarbon Receptor

In order to maintain homeostasis or to induce rapid responses upon external or internal changes in an organism, cells are constantly communicating with each other and with their surroundings. Cells have evolutionarily adapted multiple sensors to detect changes that occur in the cellular micromilieu and the environment. The Aryl hydrocarbon Receptor (AhR) is a sensor of environmental compounds and is a transcription factor (TF). The early studies of the AhR were conducted in the field of toxicology, which determined the reason for 2,3,7,8-tetrachlorodibenzo-p-dioxin (TCDD) induced chloracne outbreaks during the synthesis of herbicides. Mouse studies indicated binding of TCDD to the AhR and interactions with the Wnt/ b-catenin pathway and other TFs contributed to chloracne formation (Bock, 2016; Holsapple, 1991).

The AhR is a member of the family of basic helix-loop-helix (bHLH) containing TFs. bHLH containing TFs are found in organisms from yeast to humans, although their functions differ between species (S. Jones, 2004). They can sense environmental alterations, like circadian rhythm or oxygen gradients. The bHLH motif is involved in DNA binding and protein-protein interactions (Michael & Partch, 2013). In addition, the AhR contains two PER-ARNT-SIM (PAS) domains, PASA and PASB are used for heterodimerization with ARNT and in addition the PASB domain is also required for ligand binding (Soshilov & Denison, 2008). The Q-rich/PST domain of the AhR mediates ligand-induced nuclear transport and nucleoplasmic shuttling (Tkachenko et al., 2016). The functional domains of the AhR are depicted in **Figure 1-5**. Under steady state conditions, the AhR is inactive in the cytosol and bound to a chaperone complex. This molecular complex includes heat shock protein 90 (HSP90), AhR-interacting protein (AIP), p23 and Proto-oncogene tyrosine-protein kinase Src (SRC) (Petrulis & Perdew, 2002). AIP is essential to keep the AhR in a properly folded form in the cytosol to improve stability as well as ligand binding ability (A. Kazlauskas et al., 2000; Meyer et al., 2000). p23 is required for controlling cytoplasmic

localization of the AhR before ligand binding (Arunas Kazlauskas et al., 1999), and c-Src is important for AHR activation, once ligand bound (Enan & Matsumura, 1996).

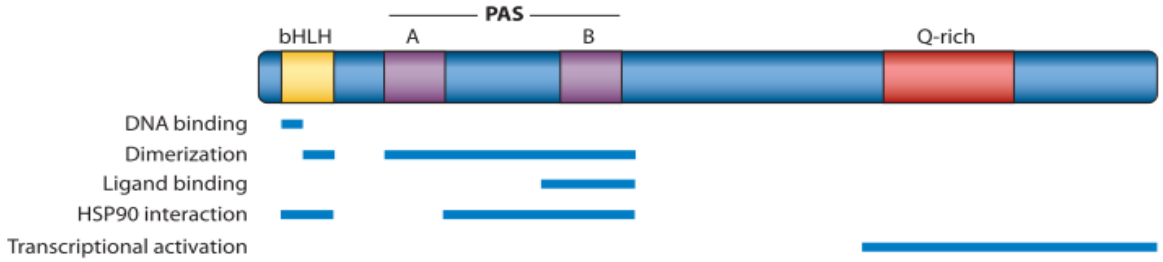


**Figure 1-5: Functional domains of Aryl hydrocarbon receptor.**
The AhR is a member of the basic helix-loop-helix/Per-Arnt-Sim (bHLH/PAS) containing transcription factor and has different functional domains. bHLH motif is important for DNA binding and protein-protein interactions, PAS domains are required for interactions with other PAS proteins and ligand binding (PASB), Q-rich domain is involved in transactivation. (Image taken from Stockinger et al., 2014)

### 1.6.1 AhR signaling pathway

The AhR is kept in an inactive state by the chaperone complex and is activated upon ligand binding. It is not clear yet, which co-chaperones stay in the cytosol but it is hypothesized that AIP may dissociate from the complex, leading to exposure of the nuclear localization and export signals in the cytosol (A. Kazlauskas et al., 2000). The ligand bound AhR then translocate into nucleus to exert its functions. Depending on its partners and binding to different consensus sequences, AhR signaling is classified into a canonical and a non-canonical pathway **(Figure 1-6)**.

**Canonical AhR signaling pathway:** Once in the nucleus, AhR binds to its partner ARNT (also known as HIF1β). Although AIP may dissociate from the AhR in the cytosol, some chaperones translocate to the nucleus with the AhR. Binding of the AhR to ARNT is required for release of the rest of the chaperone complex. The AhR-ARNT complex is then recruited to promoters containing xenobiotic response elements (XREs) and, in turn, initiates transcription of various genes. These genes include xenobiotic metabolizing mono-oxygenase of the cytochrome P450 family such as *Cyp1a1, Cyp1a2* and *Cyp1b1* (Nebert et al., 2000) and negative regulators of the AhR, such as the AhR-repressor (AhRR) (Mimura et al., 1999).

**Non-canonical AhR signaling pathways:** A crosstalk between the AhR and other signaling pathways defines the non-canonical pathway. The AhR can bind to c-MAF to promote differentiation of IL-27-induced T regulatory type 1 (Tr1) cells (Apetoh et al., 2010). Binding of the AhR to estrogen receptor (ER) leads to activation of transcription and estrogenic effects (Takahashi et al., 2003). Moreover, the AhR controls NF-κB dependent transcriptional regulation by interacting with RELA and RELB (Salisbury & Sulentic, 2015; Vogel et al., 2014). Possessing E3 ubiquitin protein ligase activity, the AhR targets certain proteins for degradation (Ohtake et al., 2007) and regulates chromatin remodeling by histone acetylation and methylation (Schnekenburger et al., 2007). The AhR also has an indirect influence on erythropoietin (EPO) expression (Asai et al., 2016) and hence RBC proliferation and maturation by competing with Hypoxia-inducible-factor 1α (HIF1α) for binding to ARNT.

**Regulation of AhR signaling pathway:** Since the AhR has diverse functions in cells, AhR signaling needs to be tightly controlled. The initial control is provided by the AhR chaperone complex, which allows the AhR to stay in the cytosol if it is not ligand bound. CYP1 family enzymes oxygenate AhR ligands leading to their metabolic clearance and detoxification thereby regulating AhR activity (Schmidt & Bradfield, 1996; Wincent et al., 2009). Ubiquitination and proteasome-mediated degradation of the AhR is another mechanism to control AhR activity (Ma & Baldwin, 2000). Competition of binding to ARNT with other molecules like HIF1α (Chan et al., 1999) or the AhRR also regulates AhR signaling. The function of the AhRR will be discussed in the next chapter in more detail.

### 1.6.2 AhR ligands

For many years, the AhR was studied in the context of detoxification of xenobiotic and exogenous chemicals but more recent studies have identified various dietary and endogenous compounds that influence AhR activity. Ligands coming from the diet, microbiota and host metabolism can serve as AhR agonists. Cruciferous vegetables like broccoli, sprouts and cabbage have various precursors for AhR ligands. These vegetables are rich in the glucosinolate glucobrassicin, which

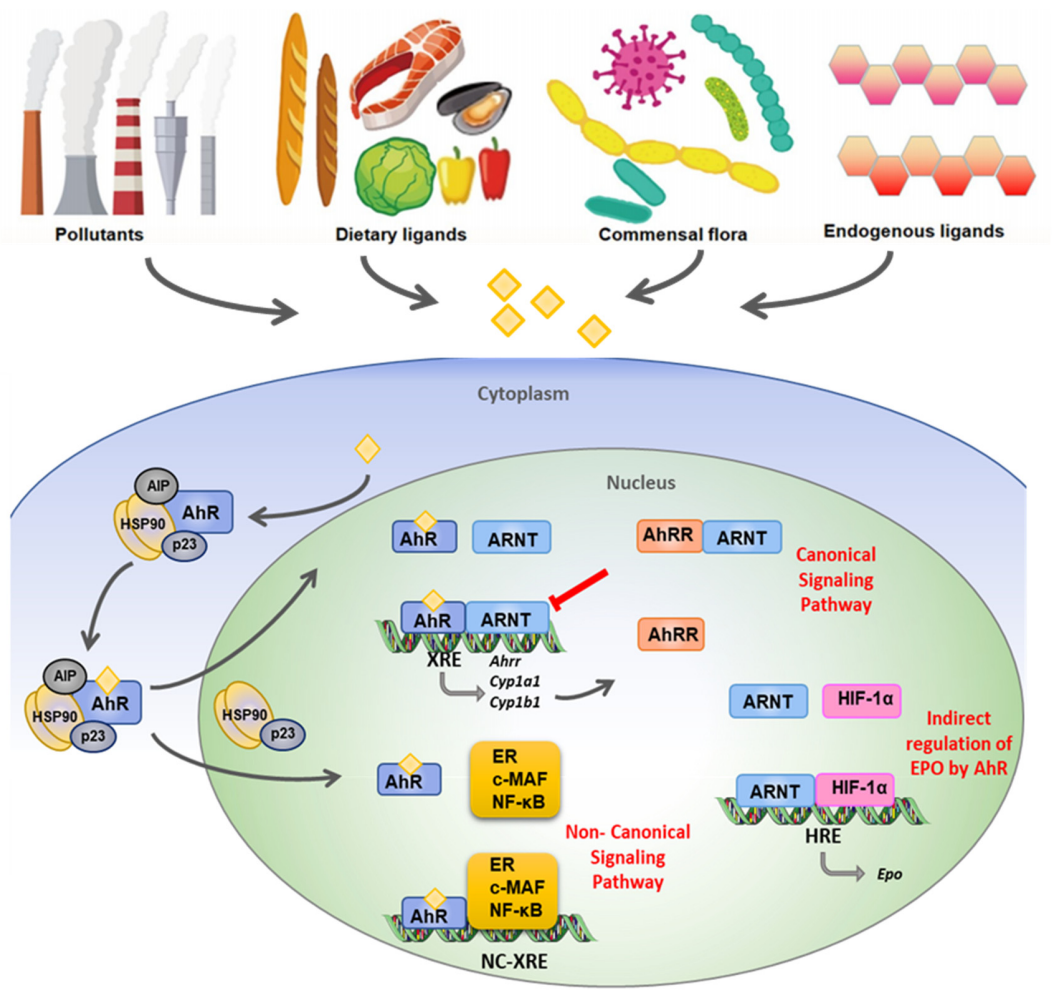


**Figure 1-6: AhR ligand and signaling pathway**.
Many molecules from external sources, commensal flora and endogenous sources can serve as AhR ligands. Under steady state conditions, the AhR is bound to its chaperone complex and is in the cytosol. Upon ligand binding, it is translocated into the nucleus and canonical or non-canonical signaling pathways are activated. In the canonical signaling pathway, the AhR binds to ARNT and regulates the expression of CYP1 family enzymes and the AhRR. The AhRR competes with AhR by binding to ARNT, thereby negatively regulates AhR signaling. In the non-canonical pathway, the AhR can bind to other transcription factors to regulate the expression of various genes. In addition, the AhR also have an indirect influence on EPO by competing with HIF1a for ARNT binding. (Image is modified from Zhao et al., 2019)

is converted to indole 3-carbinol (I3C) in the stomach under acidic conditions. I3C is further metabolized to the high-affinity AhR ligands indole-[3,2-b]-carbazole (ICZ) and 3,3-diindolymethane (DIM) (I. Chen et al., 1998; Y. H. Chen et al., 1995). Naturally occurring flavonoids from fruits and vegetables like quercetin are also known to activate the AhR (Ciolino et al., 1999). 6-formylindolo[3,2-b]carbazole (FICZ), a photoproduct of Tryptophan is also a high affinity AhR ligand (Rannug et al., 1987). Heme metabolites like bilirubin are another example

for AhR agonists (Sinal & Bend, 1997). In addition, the microbiota can serve as a source of AhR ligands. Probiotic bacteria, e.g. *Lactobacillus reuteri*, colonizes skin, GI tract and urinary tract and uses tryptophan as an energy source, leading to the production of indole-3-aldehyde, which is an AhR agonist (Zelante et al., 2013).

### 1.6.3 Function of the AhR in gut immunity

Depending on the tissue and cell type, AhR exerts diverse physiological functions. In the gut, AhR activity modulates the development, function, and maintenance of immune and non-immune cells. The AhR has been associated with intestinal pathologies such as intestinal inflammation, infection, and cancer. A study showed that the AhR is downregulated in intestinal tissue of patients suffering from Crohn`s disease compared to healthy controls (Monteleone et al., 2011). In line with this, AhR-deficient mice have a higher susceptibility to *Citrobacter rodentium* infection due to lack of IL-22 producing ILC in the intestinal lamina propria (Kiss et al., 2011). Furthermore, AhR signaling is necessary for survival of intestinal γδ T cells and TCRαβ CD8αα IELs (Y. Li et al., 2011). AhR regulates Treg and Th17 differentiation in mice in a ligand specific manner (Quintana et al., 2008). These studies indicated a role for AhR signaling in regulating intestinal homeostasis.

### 1.6.4 Function of the AhR in splenic immunity and extramedullary hematopoiesis

The spleen is a secondary lymphoid organ and functions as a filter for blood-borne pathogens. AhR tightly controls splenic architecture and the function of certain immune cells. For example, AhR-deficient mice have a smaller WP region, which is associated with a decreased number of T and B cells (Fernandez-Salguero et al., 1997). The AhR is expressed at high levels in MZ B cells and B1 B cells, and absence of the AhR in B cells reduces their proliferative capacity (Villa et al., 2017). Furthermore, absence of the AhR in splenic DC impairs IL-10 secretion and this reduction might induce a pro-inflammatory state (Nguyen et al., 2010).

The spleen is one of the major sites for extramedullary hematopoiesis (EH) (C. H. Kim, 2010). EH is defined by formation of blood cell components from hematopoietic stem cells (HSCs) external to bone marrow, for example, in spleen or liver. EH can occur during embryonic development, in hematological disorders or upon infection. The process of erythropoiesis starts from the HSCs, which differentiate first into early and late stages of erythrocyte precursor cells to

at last give rise to mature erythrocytes (Dzierzak & Philipsen, 2013). In the process of erythrocyte maturation, a pro-erythroblast can give rise to 2 basophilic, 4 polychromatic, 8 orthochromatic erythroblasts and 16 reticulocytes (Barminko et al., 2016). Hence, only a small quantity of precursors is enough to generate large numbers of mature RBCs. Erythropoiesis is regulated by growth factors including but not limited to erythropoietin (EPO), stem cell factor (SCF) and thrombopoietin (TPO) (V. K. Singh et al., 2014).

The AhR is known to be expressed by HSCs and mice exposed to TCDD displayed altered HSC differentiation by increasing the myeloid lineage at the expense of the lymphoid lineage. Furthermore, AhR activation reduced proliferation of HSC (K. P. Singh et al., 2009). In addition, AhR-deficient mice exhibited enlarged spleens with increased erythroid components and EH relative to naïve mice (Schmidt et al., 1996). This shows, that the AhR not only influences immune cell function but also HSCs homeostasis and EH in the spleen.

## 1.7 Aryl hydrocarbon receptor repressor

Although extensive studies have been performed to understand the role of the AhR in various tissues and cells, the AhRR functions are only recently being investigated. The AhRR is a negative regulator of AhR signaling and it is highly homologous to the AhR, containing a DNA-binding (bHLH) and a dimerization (PAS-A) domain (Mimura et al., 1999). However, the AhRR does not contain the PAS-B and Q-rich domains (Baba et al., 2001; Evans et al., 2008). Furthermore, it was shown that the AhRR does not bind to chaperones and is localized in the nucleus (Mimura et al., 1999). It is proposed that the AhRR dimerizes with ARNT and binds to XREs competing with AhR/ARNT heterodimer for binding to these sites and hence inhibiting target gene transcription (Mimura et al., 1999). In vitro studies also showed that the N-terminal part of the AhRR molecule is sufficient for trans-repression of AhR signaling; ARNT heterodimerization as well as direct binding to XREs is not required (Evans et al., 2008).

In addition to XREs, the *Ahrr* promotor contains binding sites for NF-κB and zinc-finger transcription factors of the Sp1 family (Baba et al., 2001). The AhRR is known to regulate tumor growth and inflammation. One study showed that the tumor suppressive function of the AhRR is mediated by its interaction with the non-canonical AhR pathway (Vogel et al., 2019). Furthermore,

AhRR downregulation in a human lung cancer cell line negatively regulated apoptotic signals and increased motility and invasion in vitro, showing that the AhRR might be an important tumor suppressor (Zudaire et al., 2008). Our group observed that AhRR expression is present mainly in immune cells of barrier organs, such as skin and gut (Brandstätter et al., 2016). Highest AhRR expression is present in immune cells of the small intestine, including $CD11c^+$ myeloid cells, T cells, ILC3 and IEL. In steady state and under inflammatory conditions, AhRR deficiency increases IL-1β production, demonstrating the importance of the AhRR in regulating intestinal immune cell functions (Brandstätter et al., 2016). These studies suggest that the AhRR regulates AhR signaling in a cell- and tissue-specific manner.

## 1.8 *Salmonella* infection

Genus *Salmonella* is a rod-shaped gram-negative bacterium belonging to the Enterobacteriaceae family and is one of the major sources of foodborne illnesses worldwide. *Salmonella* was first isolated from the intestine of pigs that had swine fever, by Theobald Smith and Dr. Daniel Elmer Salmon in 1855 (Eng et al., 2015). Initially, the Kauffmann and White scheme was used to identify the genus *Salmonella.* According to this scheme, serotypes are divided based on three antigenic determinants, somatic (O/LPS), capsular (K), and flagella (H) antigens and more than 2500 serotypes have been identified this way (Brenner et al., 2000). Later, the Center of Disease Control and Prevention (CDC) updated the nomenclature using World Health Organization (WHO) recommendations. By this system, *Salmonella* can be classified into two species; *Salmonella enterica* (*S. enterica*) and *Salmonella bongori (S. bongori)* (Andino & Hanning, 2015; Eng et al., 2015). Nowadays, the commonly used nomenclature is shortened. For example, *Salmonella enterica* subspecies *enterica* serovar Typhimurium is shortly written as *S*. Typhimurium (Brenner et al., 2000).

### 1.8.1 *Salmonella* characteristics and clinical manifestations

Depending on clinical patterns, the strains of *Salmonella* form two groups; typhoid *Salmonella* and non-typhoid *Salmonella* (NTS). *S*. Typhi and *S*. Paratyphi cause enteric (typhoid) fever and infect only humans and higher primates (Azmatullah et al., 2015; Eng et al., 2015). Symptoms of typhoid fever include headache, diarrhea/constipation, and abdominal pain. This follows increase in body temperature and patients may have an enlarged spleen (splenomegaly), myalgia or rose

spots on their chest (Kuvandik et al., 2009; Patel et al., 2010). If left untreated, the mortality rate is around 15 percent (Ohl & Miller, 2001). After the acute stage of infection, some people can become chronic carriers and bacteria can be isolated from stool long after initial infection. The infected feces can contaminate food and water sources, especially in endemic regions, leading to transmission of *Salmonella* to other individuals (Gal-Mor, 2019). NTS strains infect animals and are transferred to humans by consumption of infected animal products. NTS infections generally do not cause enteric fever. They have a shorter incubation period of only a few hours and last 10 days or less, mostly causing gastroenteritis in high income or developed countries. Symptoms may include vomiting, headache, nausea and diarrhea (Hohmann et al., 2006). In low-income regions like sub-Saharan Africa, invasive NTS (iNTS) disease is very common, which leads to bloodstream infections in adults and children. Common risk factors include HIV infection in adults, and malaria, HIV and malnutrition in children (Stanaway et al., 2019).

### 1.8.2 Epidemiology of *Salmonella* infections

A study from 2004 reported the incidence of enteric fever caused by *Salmonella* Typhi to be around 22 million cases and 200,000 deaths worldwide (Crump et al., 2004). While economically more stable countries like USA have less than 10 cases per 100,000, the highest incidence rate comes from underdeveloped countries like India and Pakistan with 214.2 cases per 100,000 people yearly (Mølbak et al., 2002; Ochiai et al., 2008). Many African countries have limited diagnostic resources, and hence it is hard to estimate cases there, therefore the incidence rates can be a lot higher than reported worldwide. In these endemic regions, the most affected individuals are infants and young children (Mweu & English, 2008). NTS lead to the most common *Salmonella* infections worldwide, 93.8 million cases are reported and 155,000 deaths occur annually (Majowicz et al., 2010). In undeveloped regions like Sub-Saharan Africa, iNTS is endemic (Galanis et al., 2006). Mortality rates of iNTS worldwide are shown in **Figure 1-7**.

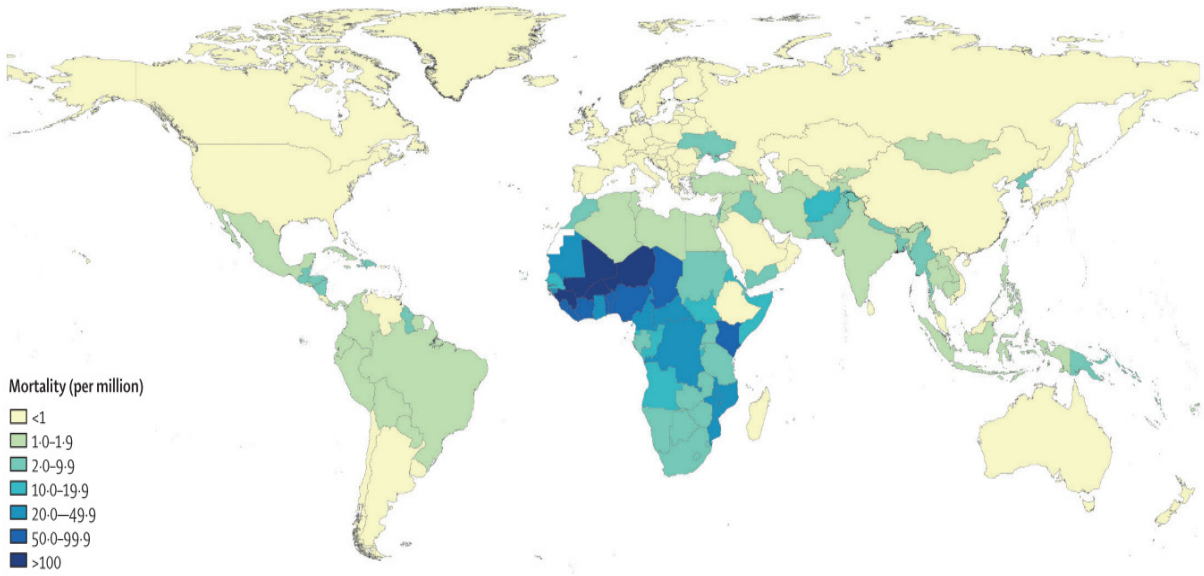


**Figure 1-7: Mortality rate of non-typhoidal *Salmonella* invasive disease (systematic analysis for the Global Burden of Disease Study 2017).**
Mortality rates worldwide are shown per million (Image is modified Stanaway et al., 2019)

### 1.8.3 Diagnosis, treatment, and preventive options for *Salmonella* infections

The most common diagnosis method for *Salmonella* is blood culture. The Widal test, which can be used to identify *Salmonella* Typhi detects antibodies against *Salmonella* O and H antigens in the serum of patients. However, this method does not really differentiate between different species. Testing *Salmonella* specific IgM and IgG antibodies by enzyme- linked immunosorbent assay (ELISA) is another method and is very sensitive (Adhikari et al., 2015). Another sensitive and specific method is the polymerase chain reaction method (PCR) that detects the *Salmonella* flagellin gene (fliC), polysaccharide capsule genes or virulence (vi) genes (tviA and tviB) (Pouzol et al., 2019).

Enteric fever needs to be treated, otherwise it can lead to death. Patients can be treated with antibiotics such as cefixime, chloramphenicol, amoxicillin, trimethoprim/sulfamethoxazole (TMP-SMX), azithromycin, aztreonam, cefotaxime or ceftriaxone (Gut et al., 2018). NTS in healthy individuals may not require any treatment, but complications can occur in infants and immunocompromised patients , therefore it is important to treat them with antibiotics such as ciprofloxacin, ceftriaxone and ampicillin (WHO, 2003). Since *Salmonella* Typhi and NTS

infections can be dehydrating, treatment also focuses on replacing fluids and electrolytes. Over the years, due to extensive or misuse of antibiotics, many bacteria have developed resistant strategies against these drugs and antimicrobial resistance (AMR) strains are formed (Medalla et al., 2017). AMR leads to serious public health concern and increase of costs for treating patients, therefore alternative methods are investigated currently.

Aside from providing access to clean water and food products, enteric fever vaccine strategies are studied to prevent *Salmonella* infections. Currently, there are two vaccines against *Salmonella* Typhi, inactivated and live typhoid vaccine. Inactivated typhoid vaccine can be administered intramuscularly and live typhoid vaccine is administered orally (Galen et al., 2016). However, there are several problems with these vaccines. On one hand, the availability, efficacy, and financial resources are limited and on the other hand, these vaccines are designed for *S.* Typhi and not for *S.* Paratyphi or for NTS strains. Moreover, children under the age of two cannot benefit from the vaccines. Therefore, there is a need for efficient and cost-effective vaccine development.

Another interesting option for prevention and treatment of *Salmonella* infections can be consumption of probiotics. Probiotics modulate the immune system, produce antibiotic molecules against pathogens or act directly on pathogens. For example, galactooligosaccharide, produced by the *Bifidobacterium bifidum* reduced the colonization and pathology associated with *S.* Typhimurium infection in a murine model system (Priyodip et al., 2017; Searle et al., 2009).

### 1.8.4 Studying *Salmonella* infections

Since available treatment and prevention strategies are not optimal for many of the *Salmonella* strains, new strategies need to be developed. Currently, many researchers in the *Salmonella* field are developing mouse models to further understand immune responses against *Salmonella* infections. Furthermore, many attenuated *Salmonella* strains are created to study specific innate and adaptive immune responses. Since *S.* Typhi is a strain restricted to humans, mice can be infected with *S.* Typhimurium, which is invasive in these animals.

Aside from this, human iNTS disease caused by *S.* Typhimurium can lead to a major health threat especially in immunocompromised patients and young children and hence needs to be treated. Many researchers are also focusing on understanding iNTS evasion systems and immune

responses in mice using *S*. Typhimurium (Stanaway et al., 2019). Although systemic infection with *S*. Typhimurium in mice depends on the genetic background of the mouse strains, many aspects of acute and chronic stages of infection can be explored. It is known that many of the commonly used mouse strains, including BALB/c or C57BL/6 mice, carry a single nucleotide polymorphism (SNP) in the natural resistance-associated protein 1 (Nramp1) which is important for regulating host resistance to infection. Mutant strains rapidly succumb to infections (Govoni et al., 1996; Hormaeche, 1979). In order to study long-term immune responses, as well as to create more efficient vaccines, attenuated *Salmonella* strains are employed. BRD509 is a commonly used attenuated strain, which has deletions in aroA and aroD genes, which leads to slower growth rate compared to wild-type strains (Dunstan et al., 1998). Another attenuated strain, TAS2010 that also has mutations in metabolic pathways is a promising vaccine strain tested in mice, conferring better protection to challenge with WT strains compared to BRD509 (Kupz et al., 2013).

### 1.8.5 *Salmonella* Typhimurium evasion mechanisms and generation of immune responses

*S.* Typhimurium has several virulence genes clustered together in the chromosome termed pathogenicity islands. While *Salmonella* pathogenicity island 1 (SPI-1) is important for intestinal epithelial cell invasion and induces inflammatory responses, SPI-2 is needed for intracellular replication of the bacteria and is important for systemic infection (Marcus et al., 2000). In addition, these islands also encode for a secretion system named type III secretion system (T3SS), which is needed for the delivery of bacterial virulence proteins into the cytoplasm of host cells (He, 1998). *S.* Typhimurium evasion mechanisms in the gut are depicted in **Figure 1-8**.

The natural route of *S.* Typhimurium infection is oral, and the first line of defense is the acidic pH of the stomach. However, many bacteria have developed an Acid Tolerance Response (ATR) and can survive this acidic environment (Foster, 1993). Upon reaching the intestine, *S.* Typhimurium can invade the host by crossing the epithelial lining of the gut, through specialized M cells in the follicle-associated epithelium (FAE) of PP or directly by DCs (B. D. Jones et al., 1994; Leoni Swart & Hensel, 2012) **(Figure 1-8)**. Thereafter, *S.* Typhimurium disseminates to draining lymph nodes, blood and finally to tissues, such as spleen and liver (Carter & Collins, 1974; McSorley, Asch, et al., 2002). Upon invasion of the bacteria, immigrating monocytes and neutrophils produce

TNF-α, IL-1 and nitric oxide to restrict bacterial growth (Rydström & Wick, 2007). Neutrophils and NK cells are some of the major sources of IFNγ, which regulates bacterial invasion during the early stage of infection (Kupz et al., 2013; Spees et al., 2014). DCs recognize bacterial LPS or flagellin, enhance their expression of MHCII, CD80, CD86, and CD40, and efficiently present antigens to CD4 T cells after migrating to LNs (McSorley, Ehst, et al., 2002; Salazar-Gonzalez et al., 2007). It was shown that the majority of *S.* Typhimurium found in tissues reside in macrophages. *S.* Typhimurium hides in *Salmonella*- containing vacuoles (SCV) in cells and can efficiently induce virulence gene expression. These phagocytic vacuoles contain cationic antimicrobial peptides (CAMPs) to control bacterial invasion, however, *S.* Typhimurium can activate signaling cascades to decrease effectiveness of CAMPs (Matamouros & Miller, 2015). In addition, SPI-1 genes encode T3SS which induce actin remodeling and contribute to host invasion (Cossart & Sansonetti, 2004).

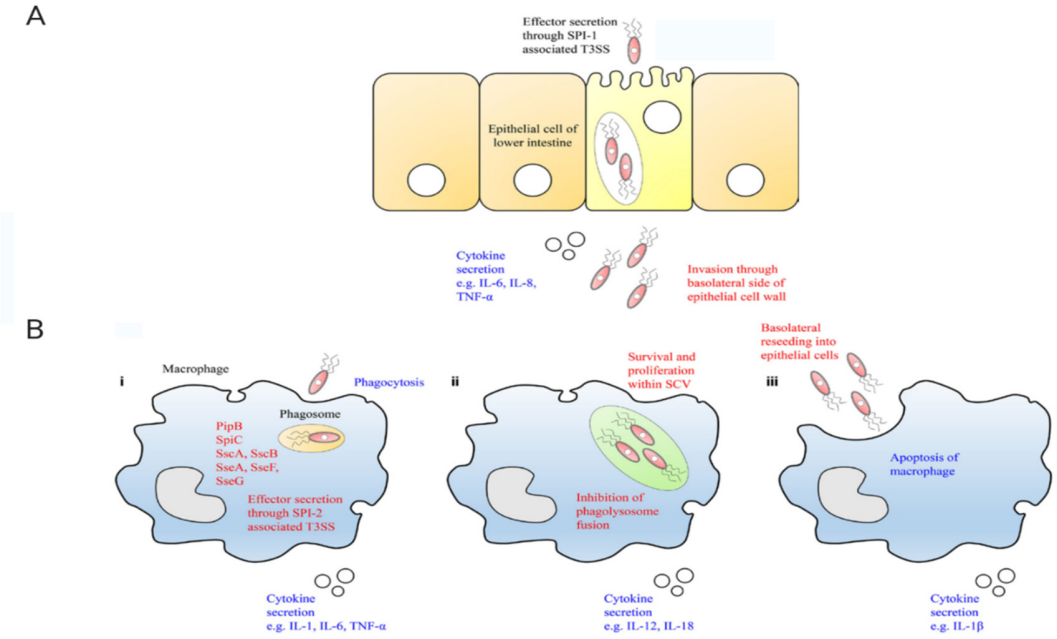


**Figure 1-8: *Salmonella* Typhimurium evasion mechanisms**
Upon oral infection, after passing the acidic conditions of the stomach, *S.* Typhimurium reaches the lumen of the small intestine and invades epithelial cells via effector secretion through SPI-1 associated T3SS (A). After crossing the epithelial barrier, bacteria are engulfed by macrophages and secrete effector proteins through the SPI-2 associated T3SS and prevent a fusion of phagosome and lysosome (B-i). *S.* Typhimurium proliferates within the SCV (B-ii) and finally will escape to reinvade epithelial or phagocytic cells (B-iii). (Image modified from Hurley et al., 2014)

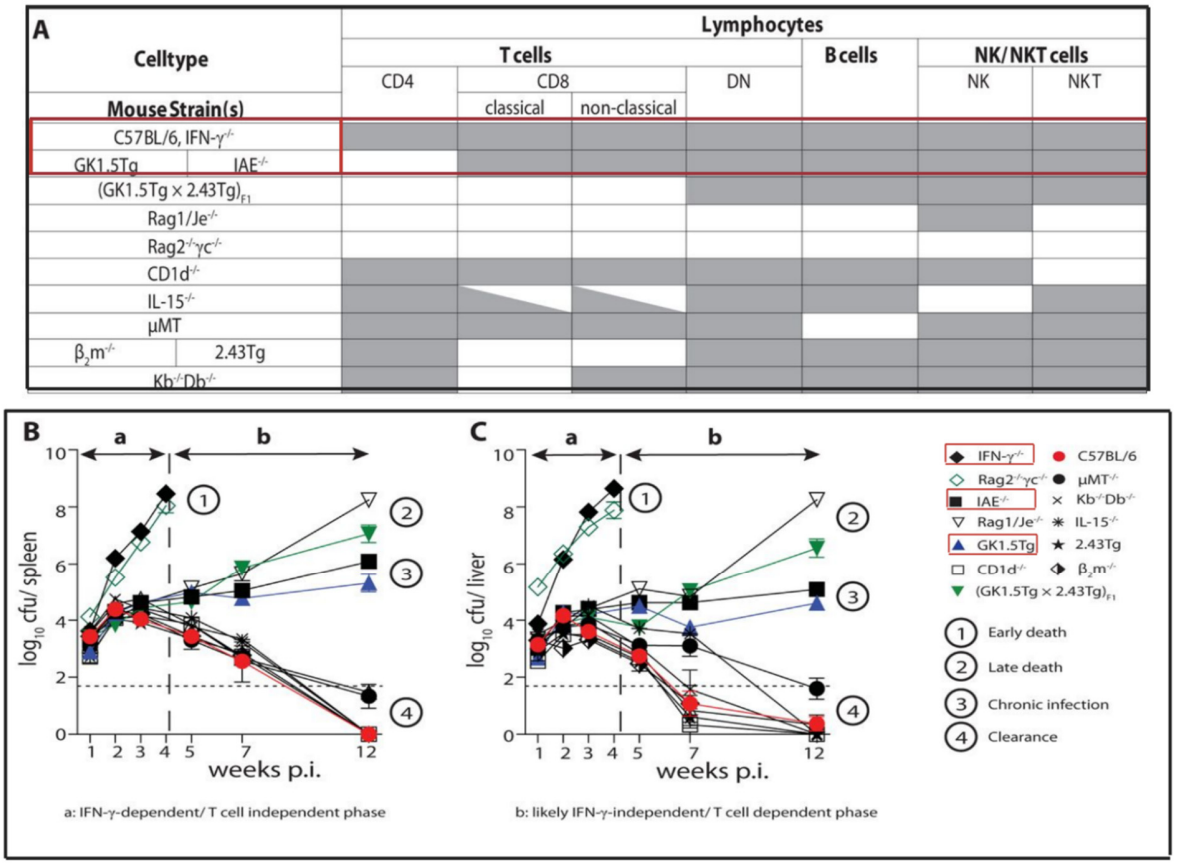


**Figure 1-9: Comprehensive study to show the requirement of IFNγ and different immune cell subsets for controlling *S.* Typhimurium infection**
White fields indicate absence; gray fields indicate the presence of the respective immune cell type (A). Different mouse models (with C57BL/6 background) including IFNγ-deficient (IFNγ$^{-/-}$) and CD4-deficient (GK1.5Tg, IAE$^{-/-}$) are infected with 200 CFU of attenuated BRD509 *Salmonella* intravenously, and at indicated weeks post infection, spleen (B) and liver (C) were collected and assessed for bacterial loads. BRD509 infection leads to two distinct phases, early control of infection and initiation of the "plateau phase" and final clearance. (Image is taken from Kupz et al., 2014)

The induction of humoral immunity against *Salmonella* infections is not very well studied. Although vaccinated people develop IgA and IgG against *S.* Typhi LPS, the function of these antibodies are not well understood (Wahid et al., 2012). Chronic carriers produce antibodies against the O- (LPS) and H-antigens (flagella) although they are not able to clear the infection (Sztein et al., 2014). One study showed that, B cells, which cannot produce antibodies, are important for regulating IFNγ production from T cells, indicating that B cells in addition to producing antibodies against the pathogen can also have alternative roles (Nanton et al., 2012).

Another study, however, showed that B cell-deficient mice cleared the infection similarly to naïve mice (Kupz et al., 2014).

The function of CD8 T cells in *S.* Typhimurium infection is also not very clear. The primary clearance of *S.* Typhimurium is probably not dependent on CD8 T cells as CD8-deficient mice do not have an increased bacterial burden compared to naïve mice (Kupz et al., 2014; Mcsorley, 2014). On the contrary, CD4 T cell function in *S.* Typhimurium infection is very well characterized. NTS strain can cause an iNTS in HIV infected people in Africa, and this might be due to strong reduction of CD4 T cells in these patients (Uche et al., 2017). One of the most important functions of CD4 T cells is to produce IFNγ, which is crucial for macrophage activation. Macrophage activation leads to expression of inducible nitric oxide synthase (iNOS) and production of nitric oxide (NO), thereby reducing growth and survival of *S.*Typhimurium (Blanchette et al., 2003). *S.* Typhimurium infection leads to CD4 T cell activation and induction of Th1 cells, which are the main producers of IFNγ. In line with this, in a study performed by Kupz et al, CD4-deficient mice showed an increased bacterial burden, which might be due to lack of IFNγ production by CD4 T cells, since also IFNγ-deficient mice possessed a very high susceptibility to *S.* Typhimurium infection (**Figure 1-9**) (Kupz et al., 2014). In addition, Th17 cells are also important for neutrophil recruitment to the gut early after infection, however, they are probably not needed for controlling systemic *Salmonella* infection (Raffatellu et al., 2008; Schulz et al., 2008). These findings indicate the need for further understanding of the influence of *S.* Typhimurium on innate and adaptive immunity.

## 1.9 *Toxoplasma gondii* infections

*Toxoplasma gondii* (*T.gondii*) is an obligate intracellular protozoan pathogen that has a worldwide distribution. It was first discovered in 1908 by Nicolle and Manceaux in a North African rodent (Weiss & Dubey, 2009). *T. gondii* is the only known species of the Toxoplasma genus and belongs to the phylum Apicomplexa (K. Kim & Weiss, 2004). It is estimated that approximately 30% of the world population is infected with *T.gondii,* however, some countries like Latin America and tropical Africa have higher prevalence than others. Humans most likely get infected by consumption of contaminated meat and water and although less likely, by contacting feline feces

(Robert-Gangneux & Dardé, 2012). When infected with *T.gondii*, immunocompetent patients can develop lymphadenopathy, fever, weakness and myalgia (Robert-Gangneux & Dardé, 2012). Immunocompromised patients might develop more severe symptoms including apathy, dementia, motor seizures, ataxia, hemiparesis and coma, and if left untreated, death may occur (Quan Liu et al., 2015; McAllister, 2005). During pregnancy, infected mothers can transfer the parasite to fetus and this can lead to abortion or severe neurological complications in the fetus (Wallon et al., 1999; H. Yamada et al., 2011). A reliable method to detect *T. gondii* in patients is to monitor the development of Toxoplasma-specific IgG antibodies (Bonyadi & Bastani, 2013). In the majority of cases, no treatment is necessary, however, pregnant, or immunosuppressed patients should be treated. Currently, pregnant women are treated with spiramycin during early pregnancy or with pyrimethamine, sulfadiazine and folinic acid at later stages of pregnancy, or if the infant has toxoplasmosis (H. Yamada et al., 2011). For immunocompromised patients, pyrimethamine and sulfadiazine seems to be the best treatment option so far (Konstantinovic et al., 2019). There are vaccines available for livestock and for domestic cats but no standardized human vaccine exists for *T. gondii* infection (Qi Liu et al., 2012; Ramakrishnan et al., 2019).

Genetic studies showed that *T. gondii* isolates can be divided into three major strain types, named 1, 2 and 3. The type 1 strain is highly virulent, type 2 is intermediate and type 3 shows the least virulence (Sibley et al., 2002; Sibley & Boothroyd, 1992). In Europe and North America type 1, in Africa both type 2 and 3 and in Asia, type 3 are the most frequently found strains (Robert-Gangneux & Dardé, 2012).

*T. gondii* can infect and replicate in any nucleated mammalian or avian cell. The life cycle of *T. gondii* consists of an asexual and sexual phase; depending on the host, different stages are observed **(Figure 1-10)**. Members of the family Felidae (domestic cats and their relatives) are the only definitive host of *T.gondii.* Upon shedding, oocysts sporulate in water, soil or plant material and hence become infective. Intermediate hosts such as rodents, birds and livestock can become infected upon consumption of infected material. In intermediate hosts, oocysts transform into tachyzoites. Tachyzoites are in a protective parasitophorous vacuole, have the fastest replicating life stage and are found in acute phase of toxoplasmosis. Tachyzoites differentiate to slower

replicating bradyzoites in neural and muscle tissue. These also replicate in a vacuole and form tissue cysts (Black & Boothroyd, 2000). These stages describe the asexual life cycle of *T.gondii.*

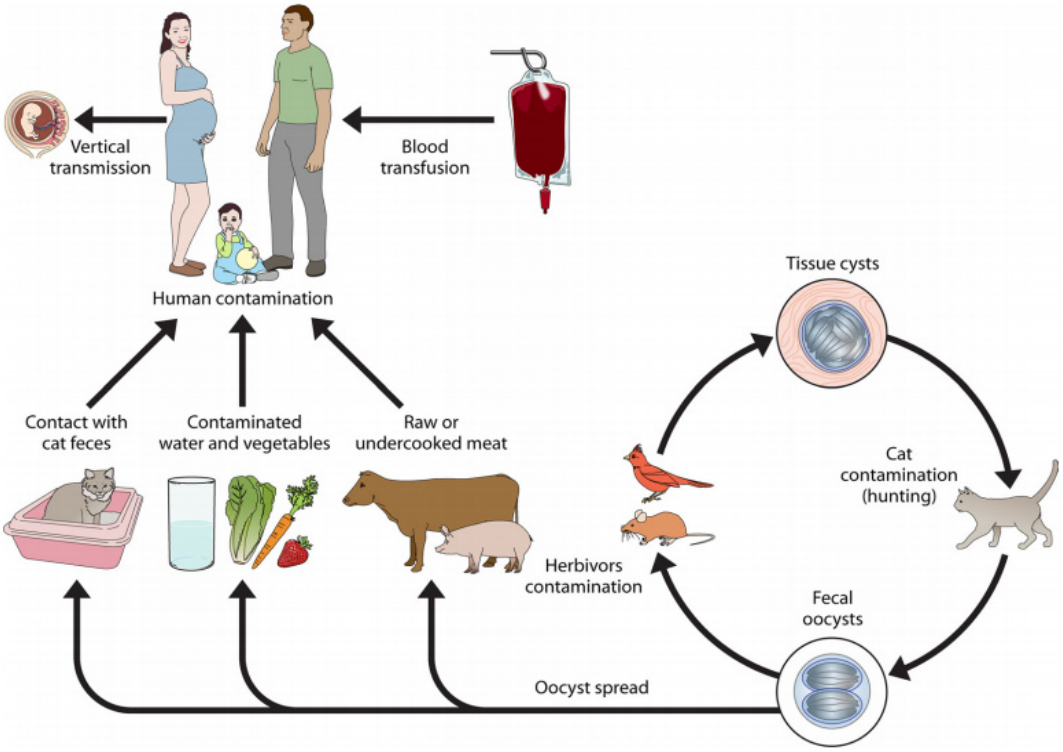


**Figure 1-10: Life Cycle of *Toxoplasma gondii***
The sexual reproduction of *T. gondii* occurs in intestine of cats, where oocysts are produced. These oocysts are found in cat feces and can spread to environment to infect livestock, soil, rodents, and birds. In intermediate hosts such as rodents or birds, oocysts transform into tachyzoites and later to bradyzoites containing tissue cysts and this process is referred as the asexual life cycle of *T.gondii*. Humans can get *T. gondii* infection from contact with cat feces, drinking or eating contaminated water/raw or undercooked meat, from blood transfusion or by vertical transmission. (Image is taken from Esch & Petersen et al., 2013)

Humans are also intermediate hosts and can be infected via eating infected livestock, consuming contaminated water, blood transfusion or transplacentally from mother to fetus. Cats are infected by consuming the intermediate hosts or directly by ingestion of sporulated oocysts. The parasite reaches to the small intestine and undergoes sexual development producing oocysts to complete its sexual life cycle (Dubey et al., 1997).

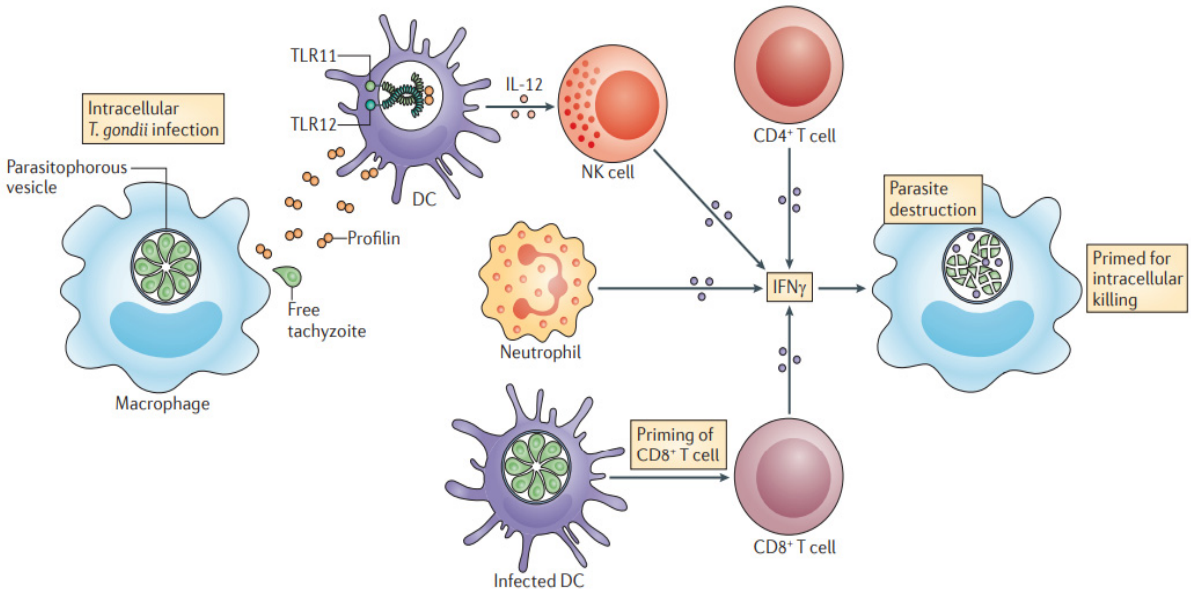


**Figure 1-11: Sources and function of IFNγ during *T. gondii* infection**
Profilin of tachyzoites is recognized by TLR11 and TLR12 on DC leading to IL-12 release by DC. IL-12 in turn activates T cells and NK cells which react by production of IFNγ. Other sources of IFNγ include neutrophils and ILCs. (Image is taken from Yarovinsky, 2014)

In order to study immunity against *T. gondii* infections, different strains and mouse models are used. Many studies use the type 2 strain ME49, which is relatively avirulent compared to other strains, e.g., the RH strain (type 1). Infected with ME49, BALB/c mice are more susceptible to infection, compared to C57BL/6 mice (Sibley & Boothroyd, 1992; Subauste & Remington, 2001). Other animal models are around which model toxoplasmosis. For example, experimental toxoplasmosis in cats has been studied to generate an efficient vaccine strategy (Darcy & Zenner, 1993). Furthermore, the intraperitoneal infection route is used in mice to study development of ocular toxoplasmosis in hamsters (Dukaczewska et al., 2015). Oral infection of C57BL/6 mice with *T.gondii*, however, triggers inflammatory responses in the ileum of the small intestine (ileitis) and this closely resembles human inflammatory bowel diseases (IBD), especially Crohn's disease (CD) (Egan et al., 2012). Therefore, this model is widely used to study immune responses related to CD.

In the ileitis model, *T. gondii* pass through the stomach acid and reach the intestine where many immune cells control parasite replication and growth. An IFNγ response is crucial in controlling *T. gondii* replication and many immune cells produce this cytokine in response to the parasite. For example, ILC1s produce IFNγ and TNF-α which contributes to the *T. gondii* response (Dunay & Diefenbach, 2018). Another study showed that AhR-deficient mice have less ILC3 and this leads to over activation of CD4 T cell responses during *T. gondii* infection (Wagage et al., 2015). IL-12 released from DCs lead to activation of NK cells, CD4 T cells, and cytotoxic CD8 T cells (C.-H. Liu et al., 2006; Sturge & Yarovinsky, 2014). Following IFNγ activation, infected cells induce reactive oxygen species (ROS) and indoleamine 2,3-dioxygenase (IDO), which contribute to parasite elimination (Pfefferkorn, 1984; Wilson et al., 1980). Moreover, in response to IFNγ, immunity-related GTPases (IRGs) are upregulated and recruited to the parasite-containing vacuoles, contributing to pathogen clearance (Etheridge et al., 2014). Taken together, these studies indicated that, IFNγ has a prominent function in the elimination of *T. gondii.*

# 2 Aims of the thesis

Since the physiological and immunoregulatory functions of the AhR have been initially discovered, immunologists have studied the AhR intensively. AhR signaling upregulates the AhRR, which in turn works in a negative feedback loop to regulate AhR activity (Mimura et al., 1999). Our group has generated a AhRR/eGFP-reporter mouse model and has shown that the AhRR is expressed mainly in the immune cells of barrier organs (Brandstätter et al., 2016). Furthermore, in a DSS-induced colitis model, the AhRR and the AhR were shown to work in concert to regulate intestinal damage, which indicated that the classical understanding of the antagonistic function of the AhRR on the AhR is dependent on the tissue and disease context (Brandstätter et al., 2016).

In order to define the function of the AhR/AhRR system further, our group also used an ileitis model induced by *T.gondii.* Using this model, it was shown that AhRR-deficiency leads to a higher disease susceptibility accompanied by severe intestinal damage (König, 2016). In the current thesis, the immune cells that contribute to *T. gondii* induced intestinal pathology in AhRR-deficient mice were investigated. Since IFNγ is highly upregulated during a *T. gondii* challenge (Scharton-Kersten et al., 1996) and excess IFNγ may indirectly influence tissue damage, this thesis focused on the impact of AhRR-deficiency on IFNγ producing T cells in the LP of the small intestine.

In addition, we used an *S.*Typhimurium infection model to understand the influence of the AhRR in immunoregulation in defense against bacterial infections. Using this model, we studied if the AhRR is required for the systemic response to *S.*Typhimurium infection.

Interestingly, only little is known about the function of the AhR upon *S.*Typhimurium infection. Thus, in the present thesis we also investigated the influence of AhR-deficiency on survival and bacterial loads in response to *S.* Typhimurium challenge. Moreover, the influence of AhR-deficiency on extramedullary erythropoiesis in the spleen as well as immunoregulation in the small intestine and spleen was explored.

Our group showed that AhRR-deficient mice displayed a disbalance in effector T cell differentiation in response to DSS-induced colitis (Brandstätter et al., 2016). Therefore, we used an *in vitro* cell culture model and mimicked physiological conditions to test if T cell intrinsic functions were responsible for these phenotypes.

# 3 Materials

## 3.1 Equipment

| Equipment | Article/Company | Company |
|---|---|---|
| Automatic tissue processor | Leica TP1020 (Leica Germany) | Microsystems, Wetzlar, Germany |
| Balances | 440-35A<br>ABJ-NM, EW-N, XS205 Dual Range | Kern & Sohn, Balingen, Germany<br>Mettler Toledo,Gißen,Germany |
| Beaker glass | 100ml | Simax Bohemia Cristal, Selb, Germany |
| Cell counting chamber | Neubauer improved | Labotec Göttingen, Germany |
| Centrifuges | 5415R, 5424R, 5810R ,5430R<br>Allegra X-15R | Eppendorf, Hamburg, Germany<br>Beckman Coulter, Pasadena, USA |
| Cryopreservation | 800 series-190 MVE | Thermo Scientific, Braunschweig |
| Cryostat | CM3050S | Leica, Wetzlar, Germany |
| ELISA washer | CAPP wash 12 | CAPP, Odense, Germany |
| Feeding needle | 18G, 2.25 mm tip,37mm | AgnTho, Lidingö, Schweden |
| Flow Cytometer | BD LSR II<br>BD FACSSymphony™ | BD Biosciences, Heidelberg, Germany |
| Freezer (-20°C) | Comfort<br>Bosch GSD12A20 | Liebherr, Biberach, Germany<br>Bosch, Gerlingen, Germany |
| Freezer (-80°C) | New Brunswick Ultra-Low Temperature Freezer | Eppendorf, Hamburg, Germany |
| Fridge (+4°C) | KTR16A21/02<br>MediLine LKUexv1610 | Bosch, Gerlingen, Germany<br>Liebherr, Biberach, Germany |
| Gel electrophoresis | PerfectBlue Gel System | Peqlab, Erlangen, Deutschland |
| Homogenizer | Stomacher® 80 Biomaster | Seward Limited, Worthing, UK |
| Hydrophobic barrier pen | ImmEdge pen | Vector Lab Inc., Burlingame, USA |

| | | |
|---|---|---|
| Ice machine | Scotsman Flockeneisbereiter AF200 | Hubbard Systems, Birmingham, USA |
| Incubator 37°C, 1% O2 | HERA cell 150 | Thermo Scientific, Braunschweig |
| Incubator 37°C, 5% O2 | CB 150 | Binder, Tuttlingen, Germany |
| Incubator shaker | Innova 44<br>S1500 | Eppendorf, Hamburg, Germany<br>Stuart, Staffordshire, UK |
| Laminar flowWorkbench | BDK Laminar Flow | BDK, Sonnenbühl, Genkingen, Germany |
| Magnet | Mojosort | Biolegend, San Diego, USA |
| Magnetic stirrer | IKA RCT basic | IKA-Werke GmbH & Co. KG, Staufen, Germany |
| Measuring cylinder | 250ml, 500ml, 1000ml, 2000m | VWR, Wayne, USA |
| Microscopes | BZ-9000<br>CKX41 | Keyence, Montabaur, Germany<br>Olympus, Hamburg, Germany |
| Microtome | Leica RM2255 | Leica Microsystems, Wetzlar, Germany |
| Microwave | NN-E235M | Panasonic, Osaka, Japan |
| Oven | EcoCell | MMM Medcenter, Munich,Germany |
| Pipette Controller, cordless | MATRIX CellMate II | Thermo Scientific, Waltham, USA |
| Pipettes | 10µl,20µl,200µl,1000µl,2.5µl ErgoOne<br>Multichannel DV8-10, DV12-50, DV8-300 | Eppendorf, Hamburg, Germany<br>StarLab, Hamburg, Germany<br>HTL Lab Solutions, Warszawa, Poland |
| Power supply | PowerPacTM | BioRad, Hercules, USA |
| Spectrophotometer (ELISA)<br>Spectrophotometer (Bacteria Culture) | EL800<br>Biophotometer | BioTek, Winooski, USA<br>Eppendorf, Hamburg, Germany |
| Thermal cycler | T100TM | BioRad, Hercules, USA |
| Threaded bottles | 100ml, 250ml, 500ml, 1000ml | Schott, Mainz, Germany |

| | | |
|---|---|---|
| Transport Box | Duraporter | Biozym, Oldendorf,Germany |
| Vortex shaker | Vortex Genie 2 | (Scientific Industries, New York, USA |
| Water Bath (Thermomix) | 1420 | B.Braun |

## 3.2 Consumables

| Item | Company |
|---|---|
| BD Plastipak 1ml Sub-Q | BD Medical, Le Pont de Claix Cedex, France |
| Cell strainer nylon (70µm, 100µm) | VWR, Radnor, USA |
| CellTrics® | Partec, Meckenheim, Germany |
| Cover slips | Roth, Karlsruhe, Germany |
| CryoPure Tube | Sarstedt, Nümbrecht |
| Culture plates (6-well/ 24-well/ 48-well/ 96-well, flat bottom) | Greiner, Frickenhausen, Germany |
| Disposable hypodermic needles, Sterican® | Braun, Melsungen |
| Disposal bags | Roth, Kalsruhe, Germany |
| ELISA plate (half-area, 96 K) | Greiner, Kremsmünster, Austria |
| Eppendorf Tubes® | Eppendorf, Hamburg, Germany |
| Filter tips | Sarstedt, Nümbrecht, Germany |
| Flow cytometry tubes | Sarstedt, Nümbrecht, Germany |
| Gloves | Semperit Technische Produkte GmbH, Austria |
| Low profile microtome blades | Leica, Nussloch |

| | |
|---|---|
| Measuring pipettes (5ml, 10ml, 25ml) | Greiner, Kremsmünster, Austria |
| Micro tube 1.1ml Z-Gel | Sarstedt, Nümbrecht, Germany |
| Microscope slides (Superfrost plus) | Thermo Scientific, Waltham, USA |
| Multiply®µStrip Pro mix.colour | Sarstedt, Nümbrecht, Germany |
| Parafilm® | American National Cam, Greenwich, USA |
| PCR tubes | Sarstedt, Nümbrecht, Germany |
| Petri dishes | Greiner, Kremsmünster, Austria |
| Precision wipes | Kimberly-Clark, Reigate, United Kingdom |
| Reaction tubes (15ml, 50ml) | Greiner, Frickenhausen, Germany |
| Reagent reservoirs | Thermo Scientific, Waltham, USA |
| Safe seal reaction tubes (0,5, 1.5ml, 2.0ml) | Sarstedt, Nümbrecht, Germany |
| Sterile applicators | Böttger, Bodenmais |
| Sterile filters (Filtopur S 0.45) | Braun, Melsungen, Germany |
| Stomacher® blender bags 80 ml | Seward Limited, Worthing, UK |
| Surgical disposable scalpel | Braun, Tuttlingen, Germany |
| Syringes Inject® (2ml, 5ml, 10ml, 20ml) | Braun, Melsungen, Germany |
| Syringes Inject-F Tuberkulin (1ml) | Braun, Melsungen, Germany |
| Tissue freezing medium | Leica, Nussloch, Germany |
| Tissue-Tek® Cryomold (15x15mm, 25x20mm) | Sakura Finetek, Torrance, USA |
| UVette® (220 nm – 1.600 nm) | Eppendorf, Hamburg, Germany |

| | |
|---|---|
| Weighing pans | Roth, Karlsruhe, Germany |

## 3.3 Chemicals & Reagents

| Chemical/ reagent | Company |
|---|---|
| 100bp DNA Ladder | New England BioLabs, Ipswich, USA |
| 10x TAE buffer | Invitrogen, Carlsbad, USA |
| 2-mercaptoethanol | Sigma-Aldrich, Steinheim, Germany |
| 2-Propanol >99.5% | Roth, Karlsruhe, Germany |
| Acetic acid 100% | Roth, Karlsruhe, Germany |
| Acetone | VWR, Darmstadt, Germany |
| Albumin Bovine Fraction V | SERVA Electrophoresis GmBH, Heidelberg, Germany |
| Ampuwa | Fresenius Kabi, Bad Homburg, Germany |
| Bacto™ Agar | BD Bioscience, Franklin Lakes, USA |
| Brefeldin A solution (1000x) | eBioscience, San Diego, USA |
| CountBright™ absolute counting beads | Life technologies, Carlsbad, USA |
| DABCO | Sigma-Aldrich, Steinheim, Germany |
| DAPI | Sigma-Aldrich, Steinheim, Germany |
| Dithiothreitol (DTT) Molecular Grade | Promega, Fitchburg, USA |
| DNase/RNase-Free Water | Zymo Research, Irvine, USA |

| | |
|---|---|
| Dulbecco's PBS | Sigma-Aldrich, Steinheim, Germany |
| Entellan | Merck, Darmstadt, Germany |
| Eosin Y solution (alcoholic) | Sigma-Aldrich, Munich,Germany |
| Ethanol 70% (methylated) | Roth, Karlsruhe, Germany |
| Ethanol absolute for molecular biology | ApliChem, Darmstadt, Germany |
| Ethanol Rotipuran >99.8% | Roth, Karlsruhe, Germany |
| Ethylenediaminetetraacetic acid (EDTA) | Sigma-Aldrich, St. Louis, USA |
| Euparal | Roth, Karlsruhe |
| FACS Clean Solution | BD Bioscience, Franklin Lakes, USA |
| FACS Rinse Solution | BD Bioscience, Franklin Lakes, USA |
| Fetal Bovine Serum | ThermoFischer, Waltham, USA |
| Ficoll-Paque™ PLUS (density 1.077 g/ml) | GE Healthcare, Freiburg, Germany |
| FICZ | Abcam, Cambridge, UK |
| Fixable Viability Dye eFluor 450/ 780 | eBioscience, San Diego, USA |
| Glycerol | Roth, Karlsruhe, Germany |
| Goat serum | Sigma-Aldrich, St. Louis, USA |
| Hank's Balanced Salt Solution (HBSS) (10x) | Gibco by Life Technologies, Carlsbad, USA |
| Hemalum solution (Mayer's) | Merck, Darmstadt, Germany |
| HEPES | Sigma-Aldrich, St. Louis, USA |

| | |
|---|---|
| Hydrochloric acid 37% | Roth, Karlsruhe, Germany |
| IMDM medium Gibco™ | Life Technologies, Carlsbad, USA |
| Ionomycin | Sigma-Aldrich, St. Louis, USA |
| LB Broth, high salt | Sigma-Aldrich, St. Louis, USA |
| L-Glutamine | Gibco by Life Technologies, Carlsbad, USA |
| L-Lysine HCl | Sigma-Aldrich, St. Louis, USA |
| Mowiol | Sigma-Aldrich, St. Louis, USA |
| OneComp/ UltraComp ebeads | eBioscience, San Diego, USA |
| Paraformaldehyde (PFA) | Merck, Darmstadt, Germany |
| Penicillin-Streptomycin | Gibco by Life Technologies, Carlsbad, USA |
| peqGOLD Universal Agarose | Peqlab, Erlangen, Germany |
| Phorbol myristate acetate (PMA) | Sigma-Aldrich, St. Louis, USA |
| Phosphate Buffered Saline Dulbecco | Merck, Darmstadt, Germany |
| RBC Lysis Buffer (10X) | BioLegend, San Diego, USA |
| Retinoic acid | Sigma-Aldrich, Munich,Germany |
| RPMI 1640 | ThermoFisher, Waltham, USA |
| Saponin | Sigma-Aldrich, St. Louis, USA |
| Sodium hydroxide solution | Roth, Karlsruhe, Germany |
| Sodium Periodate | Sigma-Aldrich, St. Louis, USA |
| Sodium pyruvate (100 mM) | Invitrogen, Carlsbad, USA |

| | |
|---|---|
| Sorenson`s Salt | Sigma-Aldrich, St. Louis, USA |
| Streptomycin sulfate | Roth, Karlsruhe, Germany |
| Sucrose | Sigma-Aldrich, St. Louis, USA |
| Sulfonic acid (H2SO4), 25% | Roth, Karlsruhe,Germany |
| Sulfuric acid ($H_2SO_4$) | Roth, Karlsruhe, Germany |
| SYBR® DNA Gel Stain | Invitrogen, Carlsbad, USA |
| Tissue Freezing Medium | Leica Biosystems, Nussloch, Germany |
| Tris Buffered Saline | Merck, Darmstadt, Germany |
| Triton x100 | Roth, Karlsruhe,Germany |
| TruStain fcX™ (anti-mouse CD16/32) (Clone: 93) | BioLegend, San Diego, USA |
| Trypan Blue | Sigma-Aldrich, St. Louis, USA |
| Tween-20 | Roth, Karlsruhe, Germany |
| XLD agar | Sigma-Aldrich, St. Louis, USA |
| Xylol | Roth, Karlsruhe, Germany |

## 3.4 Solutions & Buffers

| Solution/buffer | Content |
|---|---|
| Complete IMDM medium | 10% FCS<br>1% L-glutamine<br>1% Penicillin (10000U/ml)<br>/Streptomycin (100000 U/ml)<br>β-mercaptoethanol |

| | |
|---|---|
| Complete RPMI 1640 medium | 10% FCS<br>1% L-glutamine<br>1% Penicillin (10000U/ml)<br>/Streptomycin (100000 U/ml)<br>β-mercaptoethanol |
| EDTA (0.5M) | 186.g EDTA approx. 20g<br>NaOH 1000ml $H_2O$<br>(pH 7.8-8.0) |
| ELISA stopping solution | 25% $H_2SO_4$ in $H_2O$ |
| ELISA wash buffer | 0.05% Tween-20 in PBS |
| FACS buffer | PBS<br>0.5% BSA<br>2mM EDTA |
| Histology blocking buffer | PBS<br>0,3 %Triton X 100<br>1% BSA<br>5% goat serum |
| Intestinal digestion solution I | 5mM DTT in HBSS<br>2% FCS<br>Penicillin: 100U/ml<br>Streptomycin: 100µg/ml |
| Intestinal digestion solution II | HBSS<br>5mM EDTA<br>2% FCS<br>Penicillin: 100U/ml<br>Streptomycin: 100µg/ml |
| Intestinal digestion solution III | HBSS<br>10mM HEPES<br>Penicillin: 100U/ml<br>Streptomycin: 100µg/ml |
| Lysis buffer (tail lysis) | A. dest<br>5 mM EDTA, pH 8,0<br>0,2 % SDS<br>200 mM NaCl<br>0,1 mg/ml Proteinase K |
| PERM buffer | PBS<br>0.5% Saponin<br>0.5% BSA |

| | |
|---|---|
| PLP solution | Total volume 200 ml<br>75mM L-Lysine HCl<br>10mM Sorenson`s Salt<br>1,25% PFA<br>10mM Sodium Periodate<br>pH 7,2 |

## 3.5 Enzymes

| Enzyme | Company |
|---|---|
| DNase I | Roche, Basel, Switzerland |
| Horseradish Peroxidase | Sigma-Aldrich, St. Louis, USA |
| Liberase™ | Roche, Basel, Switzerland |
| Proteinase K | Sigma-Aldrich, St. Louis, USA |
| DNA Polymerase (OneTaq) | N.E. Biolabs, Frankfurt,Germany |

## 3.6 Cytokines

| Description | Source | Company |
|---|---|---|
| Recombinant Human TGF-β1 | HEK293 cells | Immunotools, Friesoythe,Germany |
| Recombinant Murine IL-12 (p70) | CHO cells | PeproTech, Hamburg,Germany |
| Recombinant Murine IL-2 | *E. coli* | PeproTech, Hamburg,Germany |
| Recombinant Murine IL-6 | *E. coli* | PeproTech, Hamburg,Germany |

## 3.7 Kits

| Name | Company |
|---|---|
| Elisa kits IFNγ , IL-17, TGFβ | R&D Systems, Mineapolis, USA |
| Foxp3 / Transcription Factor Staining Kit | eBioscience, Frankfurt, Germany |
| Legendplex™ Mouse HSC Erythroid Panel | Biolegend, Fell, Germany |
| LIVE/DEAD® Fixable Violet Dead Cell Stain Kit, for 405 nm excitation | Life Technologies, Carlsbad, USA |
| Mojosort™ mouse CD4 naïve T cell isolation kit | Biolegend, Fell, Germany |

## 3.8 Antibodies

### 3.8.1 FACS Antibodies

| Antigen | Dilution | Clone | Conjugate | Company |
|---|---|---|---|---|
| B220 | 1:200 | RA3-6B2 | APC, FITC | BioLegend |
| CD11b | 1:200 | M1/70 | BUV395, BV605 | BioLegend |
| CD25 | 1:200 | PC61 | PE-Cy7 | BioLegend |
| CD28 | 1µg/ml | 37.51 | LEAF™ Purified | BioLegend |
| CD3ε | 1:200 | 145-2C11 | BV605 | BioLegend |
| CD3ε | 3µg/ml | 145-2C11 | Leaf purified | BioLegend |
| CD4 | 1:200, 1:500 | RM4-5 | APC-Cy7, PE-T.red | BioLegend |
| CD44 | 1:200 | IM7 | PE | BioLegend |
| CD45 | 1:200 | 30-F11 | BV510, PE-Cy7 | BioLegend |
| CD62L | 1:200 | MEL-14 | APC | BioLegend |

| | | | | |
|---|---|---|---|---|
| CD69 | 1:200 | H1.2F3 | FITC | BioLegend |
| CD71 | 1:200 | RI7217 | BV421 | BioLegend |
| CD8α | 1:200 | 53-6.7 | PerCp, PE-Cy7,PE | BioLegend |
| F4/80 | 1:200 | BM8 | PE | ebioscience |
| FoxP3 | 1:100 | FJK-16s | PE | ebioscience |
| GFP, rabbit, IgG Fraction | 1:1000 | Polyclonal | Purified | Life Technologies |
| Goat anti-rabbit IgG (H+L) | 1:500 | Polyclonal | AF488 | Life Technologies |
| IFNγ | 1:100 | XMG1.2 | APC, PE | BioLegend |
| IFNγ | 10µg/ml | R4-6A2 | LEAF™ Purified | BioLegend |
| IL-17A | 1:100 | eBio17B7 | PE | BioLegend |
| IL-4 | 10µg/ml | 11B11 | LEAF™ Purified | BioLegend |
| Ki67 | 1:200 | 16A8 | APC | BioLegend |
| Ter119 | 1:200 | TER-119 | APC-Cy7 | BioLegend |
| TruStain fcX™ (CD16/32) | 1:200 | 93 | Purified | BioLegend |

### 3.8.2 Histology Antibodies

| Antigen | Dilution | Clone | Conjugate | Company |
|---|---|---|---|---|
| B220 | 1:100 | RA3-6B2 | Purified | ebioscience |
| TCRβ | 1:100 | H57-597 | Biotin | BD bioscience |
| Rat IgG | 1:300 | Polyclonal | AF647 | Biolegend |
| Streptavidin | 1:300 | | AF594 | Invitrogen |

## 3.9 Microorganisms

| Microorganism | Strain | Source |
|---|---|---|
| *Toxoplasma gondii* | ME 49 | Prof. Dr. Klaus Pfeffer, Düsseldorf, Germany |
| *Salmonella* Typhimurium | TAS2010 | Prof.Dr. Richard Strugnell, Melbourne, Australia |

## 3.10 Software

| Software | Company |
|---|---|
| Argus X1 | Biostep GmbH, Jahnsdorf |
| Biorender | BioRender, Toronto, Canada |
| BZ-II Analyzer,Viewer | Keyence, Montabaur, Germany |
| FACS Diva | BD, Franklin Lakes, USA |
| Fiji (Image J) | Open-source scientific analysis program |
| FlowJo 9.9.7/10.4.1 | TreeStar, Inc., Ashland, USA |
| GraphPad Prism 6 | GraphPad, La Jolla, USA |
| Inkscape 0.92.4 | Harrington, B. et al, Inkscape |
| Legendplex™ Analysis | Biolegend,USA |
| Mendeley Software | Elsevier, Amsterdam, Netherlands |
| Microsoft Office | Microsoft, Redmond, USA |

# 4 Methods

## 4.1 Animals for research and housing conditions

CD1 female mice were purchased from Charles River Laboratories. $AhR^{-/-}$, $AhRR^{E/E}$ and control mice (WT-C57BL/6J, $AhRR^{+/+}$ or $AhR^{+/+}$) were bred at the Genome Resource Centre (GRC) of the Life and Medical Sciences (LIMES) Institute, Bonn. $AhR^{-/-}$ mice were generated in the lab of Chris Bradfield and provided by Charlotte Esser, IUF, Düsseldorf (Schmidt et al., 1996). $AhRR^{E/E}$ is a mouse line expressing eGFP under the control of the *ahrr* promoter instead of functional AhRR and was described previously (Brandstätter et al., 2016). All mice were bred under specific pathogen free (SPF) conditions in cages, which were individually ventilated. Food and water source was available *ad libitum*. All experiments were performed in accordance with institutional, state, and federal guidelines and with permission number 81-02.04.2018.A094 of the state government of North Rhine-Westphalia, Germany.

## 4.2 Genotyping of animals used in research

The genotype of each mouse was determined using tail or ear biopsies. Biopsies were lysed at 56 $^{o}$C O/N in 500µl lysis buffer containing proteinase K. Following, the samples were centrifuged at 16000 G for 10 minutes and supernatant was collected in a new tube. Next, 500µl isopropanol was added to the samples and centrifuged at the same speed. Supernatant was discarded and the pellet was dissolved in 300µl 70% EtOH and centrifuged at 16000 G for 5 min. The pellet was air-dried and was dissolved in 100µl $dH_2O$. The samples were then prepared for PCR using protocols in depicted in **Table 4-1**. The product was loaded on a 2% TAE agarose gel supplemented with Sybersafe and sizes were determined using a 100 bp DNA ladder.

**Table 4-1:** PCR reaction setup (left) and PCR cycle protocol (right) with expected band sizes

| Reaction setup | | Cycle Protocol | | | | |
|---|---|---|---|---|---|---|
| **Reagent** | **1 PCR react.** | | **AhR** | **Time** | **AhRR** | **Time** |
| OneTaq Master Mix | 12,5 µl | Gene/Allele | $AhR^{+/+}$ $AhR^{-/-}$ | | $AhRR^{+/+}$ $AhRR^{E/E}$ | |
| dH2O | 9,5 µl | Band Size | 800 bp 900 bp | | 450 bp 800 bp | |
| Primer 1 (Forward) | 0,5 µl | Denaturing | 94ºC | 30 sec | 94ºC | 1 min |
| Primer 2 (Reverse) | 0,5 µl | Melting | 94 ºC | 20 sec | 94ºC | 30 sec |
| Primer 3( eGFP-AhRR or F-ex2-AhR) | 0,5 µl | Annealing | 57 ºC | 20 sec | 55 ºC | 1 min |
| DNA | 1,5 µl | Elongation | 68 ºC | 1.20 min | 68 ºC | 1 min |
| **Total** | **25µl** | End | 68 ºC | 5min | 68 ºC | 5 min |

## 4.3 Cell isolation from organs

### 4.3.1 Single cell isolation from spleen

Spleens harvested from animals were kept in ice-cold PBS. A 100µm strainer was attached to a 50ml Falcon tube and was moistened with 1ml PBS. Using forceps, spleens were transferred to the strainer and with the help of a syringe were meshed gently. 20ml PBS were added on top of the tissue and pressed through the strainer. The cell suspension was centrifuged at 250 G for 5 min at 4ºC. The supernatant was discarded; the cell pellet was resuspended in 3ml RBC lysis buffer and incubated for 10 min at RT for erythrocyte lysis. The reaction was stopped with 25 ml ice cold PBS, the cell suspension was passed through a 70µm cell strainer and was centrifuged at 250 G

for 5 min at 4ºC. Supernatant was discarded, the pellet was resuspended in 1ml PBS and cell numbers were determined using a counting chamber.

### 4.3.2 Isolation of naïve CD4$^+$T cells from spleen

Naïve CD4$^+$ T cells were isolated from splenocytes using the Mojosort$^{TM}$ mouse CD4 naïve T cell isolation Kit from Biolegend according to the manufacturer´s guidelines. A small aliquot of the cells was spared to check the purity and stained for naïve CD4$^+$ T cell surface markers including antibodies against TCRβ (BUV737), CD4 (APC-Cy7), CD8 (PerCp), CD44 (PE), CD62L (APC), CD25 (PE-Cy7) and Live/Dead marker. Dead cells were excluded and naïve CD4$^+$ T cells were identified as TCRβ$^+$CD4$^+$CD8$^-$CD44$^{lo}$CD62L$^{hi}$CD25$^-$. The rest of the cells was used for the T cell differentiation assay.

### 4.3.3 Lamina Propria isolation from ileum

The small intestine was harvested together with cecum for orientation and kept on ice-cold PBS. The distal region of the small intestine (ileum) was separated from the rest of the small intestine and cecum using surgical scissors and aligned on a tissue paper. Fat was removed using forceps and the intestinal content was washed away with PBS using gavage needles. Then, PPs were removed using surgical scissors and the ileum was cut open first longitudinally and later into 3 cm pieces. The tissue was then transferred to Falcon tubes containing 20ml of solution I and was washed at 37ºC in a shaking incubator with 140 rpm for 20 minutes for mucosal removal. The content was filtered using a 100µm strainer and tissue pieces were transferred to new 50ml Falcon tubes containing 15 ml of solution II. The tissue was later washed at 37ºC in a shaking incubator with 140 rpm for 15 minutes. This step was repeated two more times and between the steps, new solution II was added. Then, tissues were transferred to a new tube containing 10 ml solution III. After 10 min washing with 10ml of solution III, FCS and EDTA was removed and tissues were transferred to a 6 well plate and minced using scissors. 7 ml solution III was added per well and basement membrane digestion was achieved by adding Liberase and DNAse. Plates were incubated for 45min at 37ºC in a shaking incubator at 60 rpm. Next, the tissue was passed through a 70µm cell strainer and Falcon tubes were filled up with ice-cold PBS. The suspension was centrifuged at 400g for 10 min at 4ºC. The pellet was stained for surface and intracellular markers and analyzed by FACS.

## 4.4 Flow cytometry

### 4.4.1 Staining of cell surface antigens

Preferred numbers of cells were centrifuged at 220 G for 5 minutes at 4ºC. The supernatant was discarded, and cells were resuspended in 50µl PBS containing a mixture of fluorophore-coupled antibodies directed against the desired antigens and Fc Block™. Moreover, within the mixture of antibodies specific for surface markers, the LIVE/DEAD® fixable dead cell stain kit was used labeling dead cells at a concentration 1:1000. The cells were then incubated at 4ºC in the dark for 30 minutes, washed with 300µl ice-cold PBS and centrifuged at 220 G for 5 minutes. The pellet was resuspended in 200µl FACS buffer and cells were analyzed by FACS or processed further for intracellular staining.

### 4.4.2 Fixation of cells for intracellular staining

After surface staining, cells were washed once with PBS and were fixed with 2% paraformaldehyde (PFA) for 20 min, RT at dark. Later, cells were washed with 200µl PBS and resuspended in 200µl FACS buffer. Fixation of Tregs was done using eBioscience™ Foxp3 / transcription factor staining buffer set according to the manufacturer's instructions.

### 4.4.3 Intracellular staining

For intracellular cytokine staining, fixed cells were washed and resuspended in 50µl PERM buffer containing fluorophore-coupled antibodies directed against intracellular antigens. The cells were then incubated O/N at 4°C. PERM buffer of eBioscience™ Foxp3 / transcription factor staining buffer set was used for incubating anti-FOXP3 antibody O/N. In addition, when necessary, anti-GFP antibody was added to intracellular cytokines/TFs mix. The next day, cells were washed with 200µl PERM buffer and centrifuged at 250 G for 5 min. If anti-GFP was used, then cells were resuspended in 50µl PERM buffer containing a fluorophore-coupled secondary antibody directed against the species of the primary anti-GFP antibody and incubated 45 minutes at 4°C. Next, cells were washed in FACS buffer and resuspended in 200µl FACS buffer for FACS analysis.

## 4.5 Histology

### 4.5.1 Paraffin sections

Ileum or spleen samples were transferred to 6 well plates containing 4% PFA and fixed O/N at 4°C. Following day, fixed tissue samples were relocated to cassettes and transferred to a Leica Benchtop Tissue Processor. In the tissue processor, samples go through a series of alcohol concentrations for dehydration and are prepared for paraffin embedding (70% EtOH x2, 80% EtOH x2, 95% EtOH x2, 100% EtOH x2, xylol x3 and paraffin, 1 hour each). Following, samples were cut into 3 equal pieces and were embedded into paraffin blocks and cooled down. Solid paraffin blocks were stored at RT. Samples were later cut into 7µm sections using a Leica microtome and were transferred first into a water bath at 45°C, and then were placed on glass slides. Samples were dried in a heating cabinet up to a day and were stored at RT until further processing.

### 4.5.2 Cryosections

After harvesting, spleens were fixed in fresh PLP solution containing Lysine HCl, Sodium periodate and 1,25 % PFA, O/N at 4°C. Then, organs were dehydrated in 20% sucrose in PBS O/N at 4°C. The samples were embedded in Tissue-Tek® on dry ice and were stored at -80°C. Using a Leica cryostat, 7µm sections were obtained, sections were fixed in ice cold acetone for 10 min and were dried shortly. Samples were stored at -80°C until further use.

### 4.5.3 Hematoxylin and eosin (H&E) staining

To define tissue morphology, H&E staining was used. Paraffin sections were first treated with xylol, alcohol and water to remove the paraffin from the tissue. Then, Hematoxylin staining was performed. Hematoxylin is a positively charged molecule and hence binds to negatively charged molecules like DNA and RNA. Therefore, it is used to stain nuclei with a dark violet color. Eosin Y stains the proteins in cytoplasm in pink color. At the end of the staining, the slides were mounted in Entellan, dried O/N and stored at RT until further analysis. The detailed H&E protocol is listed in **Table 4-2**.

**Table 4-2:** Hematoxylin and eosin (H&E) staining protocol

| Treatment | Time |
|---|---|
| Xylol | 10 min |
| Xylol | 10 min |
| 100% Ethanol | 5 min |
| 100% Ethanol | 5 min |
| 95% Ethanol | 2 min |
| 70% Ethanol | 2 min |
| Aqua dest. | 1 min |
| Mayer's hemalum solution | 5 min |
| 1% Hydrochloric acid in 70% Ethanol | 10 sec |
| Tap water | 5 min |
| Eosin Y solution | 4 min |
| Tap water | 10 dips |
| 95% Ethanol | 5 min |
| 100% Ethanol | 5 min |
| 100% Ethanol | 5 min |
| Xylol | 5 min |
| Xylol | 5 min |

### 4.5.4 Immunofluorescence staining

Frozen sections were air dried for 15 minutes at RT and were encircled with ImmEdge Pen to create a hydrophobic barrier around the samples. Next, samples were placed in a humidified chamber, rehydrated in PBS for 10 min and later permeabilized using PERM buffer containing 0,3% Triton X and 1%BSA for another 10 min. In order to prevent unspecific binding, a blocking buffer containing 5% normal goat serum in PERM buffer was added to the sections and incubated 2 hr at RT. Next, sections were stained with primary antibodies in PERM buffer and incubated O/N in a humidified chamber at 4°C. Next day, samples were washed with PBS (x3) for 5 min,

secondary antibodies were added in PBS and were incubated for 2 hr at RT. Later, nuclei were stained with 4',6-diamidino-2-phenylindole (DAPI) diluted 1:5,000 in PBS for 5 minutes at RT and rinsed with PBS (3x 5min) followed by mounting with Mowiol / DAPCO. Afterwards, slides were dried O/N and later stored at 4°C in the dark.

### 4.5.5 Microscopy

Images from H&E and immunofluorescent stained sections were taken using a Keyence BZ-9000 microscope. Images were further analyzed with the BZ-II Viewer and Analyzer or Fiji (ImageJ) software. H&E stained ileal sections were evaluated for possible necrotic and fibrotic regions, inflammatory cell infiltration and changes in the villous structure. Immunofluorescently labeled spleen sections were used for analysis of $B220^+$ B cell cluster sizes and $TCR\beta^+$ T cells distribution within spleen using Fiji.

## 4.6 Determination of cell numbers

The cell numbers were generally determined using a hemocytometer. The cells were diluted 1:10 with Trypan blue, loaded on the hemocytometer, and later counted using a microscope. Dead cells were stained dark blue and were excluded from counting. Live (uncolored) cells were counted in 2 large squares of the hemocytometer and the average was calculated. Later, total cell number /ml was calculated using the formula:

$$\text{Cell count (cells/ml)} = \frac{\text{Number of live cells}}{\text{Number of large squares}} \times \text{Dilution factor} \times 10^4$$

Alternatively, absolute cell numbers were determined using FACS. To do this, samples were diluted in 200µl FACS buffer or PBS and 20µl of Precision count beads™ were added. The cells were incubated for 10 minutes and later analyzed using FACS. Beads form a distinct population and were gated. Later, absolute numbers were determined using the formula below:

$$\text{Absolute cell count (cell/µl)} = \frac{\text{Cell count} \times \text{Beads volume}}{\text{Beads Count} \times \text{Cell volume}} \times \text{Bead concentration}$$

## 4.7 Serum preparation

Blood was collected in Micro tubes 1.1ml serum gel with clotting activator using the submandibular bleeding method and centrifuged at 16000 G for 5 minutes at RT. The serum was transferred to a new tube and was stored at -20°C until analysis by ELISA.

## 4.8 Enzyme-linked Immunosorbent Assay (ELISA)

Secreted cytokines in serum or cell culture supernatants were measured using ELISA kits obtained from R&D systems according to the manufacturer's instructions. Briefly, capture antibodies were coated on 96 well plates by incubation in PBS at RT, O/N. Following day, the plates were washed with ELISA wash buffer and incubated with blocking buffer (1% BSA in PBS) for 1 hour at RT. Serial dilutions from the protein standards were prepared and used for quantifying concentration of antigens in samples. After washing away the blocking buffer, samples and standards were added to the plates and were incubated 2 hours at RT. After washing the plates, Streptavidin-coupled Horseradish Peroxidase in reagent diluent was incubated for 20 minutes at RT. Another washing step was performed and then plates were incubated with TMB PLUS2 for 10 minutes. The reaction was stopped with ELISA stop solution, which turns the solution from blue to yellow. Absorption was then measured using a microtiter plate reader at 450nm/630nm.

## 4.9 Legendplex$^{TM}$ multi-analyte flow assay kit (HSC-Erythroid Panel)

This kit is a bead-based multiplex assay, which has a similar principal as sandwich immunoassays and permits spontaneous quantification of various targets. The HSC-Erythroid panel allows detection of TPO, IL-6, GM-CSF, TGFβ, SCF, EPO and CXCL12 in serum using two sets of beads. Each bead set has a unique size and internal fluorescence intensity which can be identified in a flow cytometer. The smaller bead A detects TPO (A7), IL-6 (A8), GM-CSF (A9) and the larger bead B detects TGFβ (B3), SCF (B6), EPO (B7) and CXCL12 (B9). The experimental protocol is as follows: first, a mixture of beads was prepared in a volume of 25µl. Then, samples were diluted in 25µl assay buffer to obtain a volume of 50µl and then 25µl of vortexed mixed beads were added to each well. Serial dilutions (1:4) of standards were prepared and diluted in Matrix A and with addition of 25µl mixed beads such that a final volume of 75µl was reached. The plates were sealed and incubated at 120 G on a plate shaker for 2 hours at RT. The plate was

centrifuged at 120 G for 5 minutes and the supernatant was discarded followed by washing the beads with 200µl wash buffer. Later, 25µl of detection antibodies were added to each well and incubated at 800 rpm for 1 hour at RT on a plate shaker. Following this, 25µl of SA-PE was added to each well and incubated for 30 min at RT. After washing the cells with wash buffer, the final volume was adjusted to 150µl with wash buffer. The samples were analyzed using FACS.

## 4.10 T cell differentiation

A day before the start of the differentiation, flat bottom 96 well plates were coated with anti-CD3 (3µg/ml) in 200µl PBS. At the day of differentiation, naïve T cells were seeded in 96 well plates at a concentration of $2x10^5$ cells/well in 200µl IMDM complete medium. Depending on the helper T cell type, different cytokine and antibody mixes were added in IMDM complete medium. All conditions included soluble anti-CD28 (1µg/ml) and IL-2 (5ng/ml). The cells were cultured either in normoxia (21% $O_2$), 5% $CO_2$ or in hypoxia (21% $O_2$), 5% $CO_2$ for 4 days. Naïve $CD4^+$ T cells were differentiated to Th1, Th17 and Tregs and undifferentiated T cells (Th0) were used as controls. Different cytokine and antibody mixes for different helper T cell subsets are depicted in **Table 4-3**.

**Table 4-3** : Additives for differentiation of naïve T cells to different helper T cell subsets

| **Helper T cell Subset** | **Cytokine Name** | **Cytokine Concent. /well** | **Antibody Name** | **Antibody Concent. /well** |
|---|---|---|---|---|
| Th0 | | | a-IFNγ<br>a-IL-4 | 10µg/ml |
| Th1 | IL12 | 20ng/ml | a-IL-4 | 10µg/ml |
| Th17 | IL-6<br>TGFβ<br>FICZ | 100ng/ml<br>5ng/ml<br>300nM | a-IFNγ<br>a-IL-4 | 10µg/ml |

| | | | | |
|---|---|---|---|---|
| Treg | TGFβ<br>Retinoic Acid | 5ng/ml<br>2,5ng/ml | a-IFNγ<br>a-IL-4 | 10µg/ml |

### 4.10.1 Validation of T cell differentiation

Differentiation of naïve T cells to different helper T cell subsets were validated measuring secreted IFNγ for Th1, IL-17 for Th17 and TGFβ for Tregs using ELISA. Furthermore, extra-, and intracellular cytokine staining were used to validate differentiation by FACS. For this purpose, Th0, Th1 and Th17 cells were re-stimulated in complete IMDM medium and then the cells were stained for surface antibodies against CD4 (APC-Cy7), CD8 (PerCp) and Live/Dead marker. Later, cells were fixed and permeabilized to allow O/N staining with intracellular antibodies against IFNγ (PE) and IL-17 (PE). Moreover, the proliferation rate was determined using an antibody against Ki67 (APC). In vitro differentiated Tregs do not require re-stimulation with PMA and ionomycin for FOXP3 detection. Hence, after differentiation, Tregs were stained with surface markers first, then fixed and permeabilized using FOXP3 Transcription Factor Staining Buffer Kit from eBioscience for FOXP3 (PE) staining. Next, the cells were washed in FACS buffer and analyzed by FACS.

## 4.11 *Toxoplasma gondii* infection model

### 4.11.1 Parasite passaging

CD1 mice are resistant to health impairments caused by *Toxoplasma gondii* and hence were used to propagate the parasite. For this purpose, CD1 female mice were used and infected i.p. with 20 lysed ME49 cysts. 3-4 weeks post infection, the parasite can be isolate from the brain in cyst form. To achieve this, harvested brains were washed in PBS in 50 ml Falcon tubes and then moved to another tube with 25 ml PBS to flush off the remaining blood. Later, brains were transferred to small petri dishes and roughly cut into small pieces. Next, 4 ml PBS was added and using different size of needles, the tissue was homogenized (starting with G18 then G20, G22 and lastly G23) The suspension was centrifuged 5 min at 50 G, RT and the supernatant was discarded. The pellet was then resuspended in 15 ml PBS, underplayed with 10 ml Ficoll-Paque™ PLUS (density 1.077

g/ml) and centrifuged 25 min at 700 G with moderate acceleration (from 7 to 9) and no brake. Later, the supernatant was discarded, and the pellet washed in 50ml PBS followed by centrifugation for 15 min, 450 G, RT. After discarding the supernatant, the pellet was resuspended in 500µl PBS and cysts were counted using 10µl of the suspension. 40 cysts were taken and lysed to release bradyzoites using Trypsin/EDTA. The reaction was stopped with 500µl FCS, 2ml PBS was added and the suspension was centrifuged for 15 min, 360 G at RT. The pellet was resuspended in 400µl PBS. Each CD1 mouse (total 2) was infected with 20 cysts in 200 µl PBS using the i.p route.

### 4.11.2 Oral infection

For oral infection, 25 cysts were dissolved in 200µl PBS. Mice were stabilized with one hand and the cyst containing solution was slowly administered orally using a 1ml syringe with a gavage needle. WT and AhRR-deficient mice were infected with cysts and analyzed 6 days post infection.

### 4.11.3 Clinical Score

**Table 4-4** was used for assessment of clinical scores of *T. gondii* infected mice. Mice were checked every day and weight as well as clinical scores were noted. Mice reaching a high stress level (>=10) were taken out of the experiment. At the end, all mice were anaesthetized and were killed by cervical dislocation.

**Table 4-4 :** *T. gondii* (also *S.*Typhimurium) infection clinical score assessment

| **1. General Conditions** | **Points** |
|---|---|
| Normal appearance, coat adjoining, clean | 0 |
| Maintenance deficit, fur ruffled | 1 |
| Increasing care deficit: pus around eyes and anus | 2 |
| Major care deficient: moist body openings | 4 |
| **2. Spontaneous behavior** | |
| Normal behavior: mouse explores cage | 0 |
| Minor deviations from the normal behavior: mouse sits predominantly in one place | 1 |
| Stronger deviation from normal behavior: increasing lethargy, mouse avoids movements, whole body movement after slight touch still present | 4 |
| Strong deviation from normal behavior: mouse does not move by itself despite slight touch | 10 |

| 3.Posture | |
|---|---|
| Normal posture | 0 |
| Little hunchback, swaying gait | 2 |
| Strong hunchback | 4 |
| **4. Weight** | |
| Normal weight (up to 5% weight reduction) | 0 |
| Weight loss> 5% | 1 |
| Weight loss> 10% | 3 |
| Weight loss> 15% | 5 |
| Weight loss> 20% | 10 |

| Rating | Points | Action taken |
|---|---|---|
| No stress | 0 | |
| Low stress | 1-3 | |
| Moderate stress | 4-9 | Animal keeper notifies experimenter; Food is placed on the cage floor |
| High Stress | >= 10 | Animal is immediately killed without pain |

### 4.11.4 Analysis of *Toxoplasma gondii infected mice*

At the end of the infection, blood was collected, and animals were sacrificed. Serum isolated from blood was used for IFNγ detection by ELISA. Furthermore, ileum was used for detection of IFNγ producing T cells and AhRR expressing T cells. For this purpose, LP cells from ileum was isolated and stained with surface markers including antibodies against TCRβ (BUV737), CD4 (PE-T.red) and with Live/Dead marker. After washing, the cells were fixed with 2% PFA and were permeabilized for intracellular staining with antibodies against IFNγ (APC). To detect eGFP expression, cells were incubated O/N with anti-GFP and then stained with fluorophore-coupled secondary antibody (AF488) for 45 min at 4°C.

## 4.12 *Salmonella* Typhimurium infection model

### 4.12.1 Growth and storage of *S.* Typhimurium

S. Typhimurium (TAS2010) was grown overnight at 37 °C in a shaking incubator in 10ml Luria-Bertani broth (LB broth) or on LB agar plates supplemented with 50µg/ml streptomycin.

Following day, the culture was transferred to a canonical glass beaker, supplemented with 90 ml fresh LB broth & streptomycin (50µg/ml) and incubated 4 hours in a shaking incubator. Using 1ml from the culture, the optical density at 600nm was measured to detect bacterial concentration. Then, the culture was centrifuged at 1530 G for 10 min at 4ºC and washed 2x with 50ml PBS. $5x10^7$ bacteria were mixed with 500µl LB/glycerol mix at a 1:1 ratio and was stored in cryotubes at -80ºC. The rest of the culture was used for oral infection of mice.

### 4.12.2 Oral infection

For oral infection of WT, AhR- and AhRR-deficient mice, $2,5x10^9$ TAS2010 per animal in LB broth/10 % sodium bicarbonate solution at a 1:1 ratio was prepared. Mice were stabilized and 200µl LB broth/Sodium bicarbonate containing inoculum was slowly administered using a 1ml syringe with a feeding gavage needle. For determining the time course of infection, mice were sacrificed at 1-, 2-, 3- or 4-weeks post infection. Otherwise, animals were sacrificed at 2- or 5-weeks post infection.

### 4.12.3 Clinical Score

**Table 4-4** was used for clinical assessment of *S.* Typhimurium infected mice. Animals were checked 3 times a week in the first two weeks and once a week after that. If an animal reached a medium stress level, animal caretakers were notified, food was placed on the cage and animal was checked every 8 hours until taken out of the experiment by reaching high stress level or until decreasing their stress level.

### 4.12.4 Analysis of *S.* Typhimurium infected mice

At the end of the infection, blood was collected, and animals were sacrificed. Serum isolated from blood was used for IFNγ detection by ELISA or for erythroid markers using Legendplex™ mouse HSC Erythroid panel from Biolegend. Spleen and liver were harvested, and their weights were measured using a sensitive scale. Spleen and liver from selected animals were used for detecting bacterial loads (CFUs). The spleens from the rest of the animals were divided into two based on their weights. One half was used for histology analysis and the other half was used for analysis of spleen cells via FACS. Harvested ilea from selected animals/genotypes were used for histology analysis and the rest were used for isolation of LP cells and FACS analysis.

#### 4.12.4.1 Bacterial counts

Spleen and liver were homogenized in 5ml (spleen) or 10ml (liver) PBS for 15 min using Stomacher® 80 homogenizer. 200µl from each sample was taken and serial dilutions (1:10) were prepared ($10^{-1}$, $10^{-2}$, $10^{-3}$, $10^{-4}$). From each dilution, 50µl was plated on XLD plates containing 50µg/ml streptomycin. Plates were incubated for 24 hours at 37 ºC. Following day, the bacterial colonies appeared in black and bacterial loads per organ (CFU/organ) were calculated.

#### 4.12.4.2 FACS analysis of spleen and LP

LP cells from ileum of WT, AhR- or AhRR-deficient mice were isolated and stained with surface markers including, antibodies against CD45 (BV510), CD4 (PE-T.red), CD8 (PE-Cy7) and with Live/Dead marker. After washing, the cells were fixed with 2% PFA and were permeabilized for intracellular staining by antibody against IFNγ (APC). In addition, to detect eGFP expression in AhRR-deficient mice, cells were incubated O/N with anti-GFP and were then stained with fluorophore-coupled secondary antibody (AF488) for 45 min at 4ºC.

After single cell isolation from spleen, the total cell number was determined using trypan blue staining. For Panel I (myeloid cells &RBCs) and Panel II (T cells), RBC lysis was not performed during single cell isolation and only surface staining was performed. However, RBC lysis was done when detecting IFNγ expressing T cells in spleen (Panel III-intracellular). Panels used for detecting different cell subsets are depicted in **Table 4-5**.

**Table 4-5**: Panels used for detecting surface and intracellular cell markers in spleen

| PANEL I Myeloid & RBC | | |
|---|---|---|
| 1 | Cd11b | BUV395 |
| 2 | F4/80 | PE |
| 3 | TCRβ | BUV737 |
| 4 | CD45 | PE-Cy7 |
| 5 | L/D | BV510 |
| 6 | B220 | APC |
| 7 | Ter119 | APC-Cy7 |
| 8 | CD71 | BV421 |
| | | |
| | | |

| PANEL II T cell | | |
|---|---|---|
| 1 | TCRβ | BUV737 |
| 2 | CD45 | PE-Cy7 |
| 3 | CD4 | PE-Tred |
| 4 | CD8 | BUV805 |
| 5 | CD69 | FITC |
| 6 | B220 | APC |
| 7 | L/D | BV510 |
| 8 | Ter119 | APC-Cy7 |
| 9 | CD71 | BV421 |
| 10 | Cd11b | BV605 |

| PANEL III T cell & Intracellular | | |
|---|---|---|
| 1 | TCRβ | BUV737 |
| 2 | CD45 | PE-Cy7 |
| 3 | CD4 | PE-Tred |
| 4 | CD8 | PE |
| 5 | L/D | BV510 |
| 6 | IFNγ | APC |
| 7 | B220 | FITC |
| 8 | Ter119 | APC-Cy7 |
| 9 | CD71 | BV421 |
| | | |

#### 4.12.4.3 Histological analysis of ileum and spleen

Ileum and spleen from WT, AhR- and AhRR- deficient mice were stained using H&E staining for morphological analysis. Ileums were evaluated for possible necrotic and fibrotic regions, inflammatory cell infiltration and changes in the villous structure after TAS2010 infection. Spleens were evaluated for possible distortions in WP and MZ structures upon TAS2010 infection. IF staining was used to further investigate the structural differences observed in AhR-deficient mice. For this purpose, B220 marker was used to identify B cells and B cluster areas were measured. Moreover, TCRβ identified T cell clusters and possible T cell re-localization from WP region to RP region was evaluated.

## 4.13 Statistical analysis

All statistical analyses were performed using GraphPad prism. For statistical analysis of two independent groups, unpaired students t-test was used. Statistical analysis of three or more independent groups were calculated using one-way ANOVA. In the case of survival studies, significance was calculated using Log-rank (Mantel-Cox) test. All data are represented as mean plus standard error of the mean (SEM) unless stated otherwise in the figure legend. Significant differences were depicted as *$p < 0.05$; **$p < 0.01$; ***$p < 0.001$; ****$p < 0.0001$.

# 5 Results

## 5.1 Correlation of IFNγ production with *Toxoplasma gondii* induced intestinal tissue damage in AhRR-deficient mice

Previously, it was shown by our group that the AhRR is mainly expressed in immune cells of barrier organs, like skin and gut and the function of the AhRR was therefore studied in the context of inflammation within these sites. In this thesis, we studied functions of the AhRR upon *T. gondii* infection using AhRR-deficient ($AhRR^{E/E}$) mice. Oral infection of mice with *T. gondii* leads to ileitis (inflammation of ileum part of the small intestine) and resembles human inflammatory bowel disease (Egan et al., 2012).

The protocol to orally infect mice with *T.gondii* was established by Dr. Jessica König. In her thesis, she showed that AhRR-deficient mice were more susceptible to *T. gondii* infection compared to WT mice. Furthermore, morphological analysis of the small intestine indicated more tissue damage in the ileum of AhRR-deficient mice relative to WT mice (König, 2016). Since excess IFNγ production may correlate with local tissue injury, we examined the IFNγ-producing T cells in the ileal LP.

Initially, AhRR-deficient and WT mice were orally infected with 50 *T. gondii* cysts and organs were analyzed 8 days post infection. However, we observed an increased virulence of *T. gondii* compared to the initial analysis done by Dr. Jessica König. Therefore, the following experiments were analyzed 6 days post infection.

### 5.1.1 Systemic IFNγ levels remain similar in WT and AhRR-deficient mice after *T. gondii* infection

Although an excess of IFNγ could correlate with tissue damage, a sufficient IFNγ release is critical for host survival during *T. gondii* infections, since IFNγ-deficient mice showed extreme susceptibility to the parasite (Scharton-Kersten et al., 1996). Therefore, initially, the systemic IFNγ response to oral *T. gondii* infection was analyzed. Although *T. gondii* infection increased serum IFNγ levels, WT and AhRR-deficient mice induced systemic IFNγ levels similarly upon *T. gondii* infection **(Figure 5-1)**.

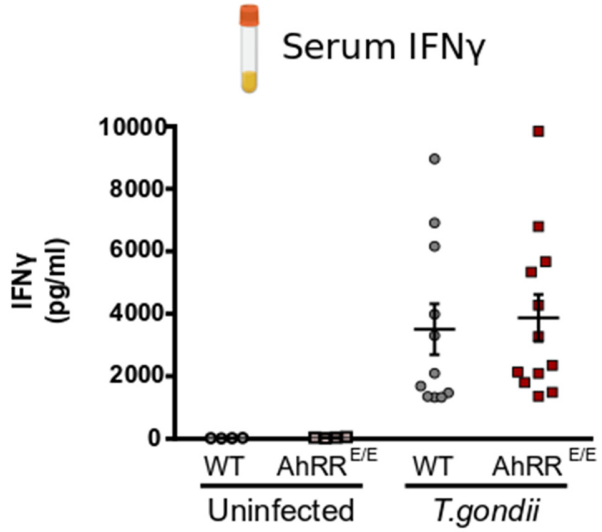


**Figure 5-1: *T. gondii* induces production of IFNγ similarly in WT and AhRR-deficient mice**
Blood was taken from WT and AhRR-deficient animals at the end of the experiment and the serum was isolated. IFNγ levels were measured using ELISA. Data are pooled from three independent experiments (n=4-12 mice). Results are shown as mean +/– SEM and no significance could be detected between genotypes upon *T. gondii* infection

### 5.1.2 Quantification of IFNγ- and AhRR-expressing T cells in the LP upon *T. gondii* infection

We next tested whether the increased susceptibility of AhRR-deficient mice to *T. gondii* infection is due to an increase in local IFNγ production in the gut. For this purpose, we analyzed IFNγ producing T cells in the ileum. To detect IFNγ $^{+}$CD4$^{+}$ (Th1) and IFNγ $^{+}$CD8$^{+}$ (Tc1) T cells in the ileum, lymphocytes were isolated from *T. gondii* infected LP and analyzed by FACS. Prior to analysis, the isolated lymphocytes were stimulated with PMA/ionomycin in the presence of Brefeldin A and later fixed in 2% PFA for intracellular staining. The gating strategy for FACS analysis is depicted in **Figure 5-2 A**. In naïve AhRR-deficient mice, a slight but not significant increase in the frequency of CD4$^{+}$ T cells was observed relative to WT mice. Upon *T. gondii* infection, the CD4$^{+}$ T cell frequency was similar in WT and AhRR-deficient mice, which was approximately 58-68 % **(Figure 5-2 B)**. While the proportion of CD8$^{+}$ T cells were around 18 % in WT and 16% in AhRR-deficient mice in naïve mice, *T. gondii* infection slightly increased the frequency of CD8$^{+}$ T cells in both WT and AhRR-deficient mice to around 26% **(Figure 5-2 D).**

Examination of IFNγ levels in CD4$^{+}$ and CD8$^{+}$ T cells revealed that roughly 10% and 6% of IFNγ$^{+}$CD4$^{+}$ T cells were present in naïve WT and AhRR-deficient mice, respectively. Although *T. gondii* infection increased the frequency of IFNγ$^{+}$CD4$^{+}$ and IFNg$^{+}$CD8$^{+}$ T cells in both WT and AhRR-deficient mice, this increase was significant only in AhRR-deficient mice. In addition,

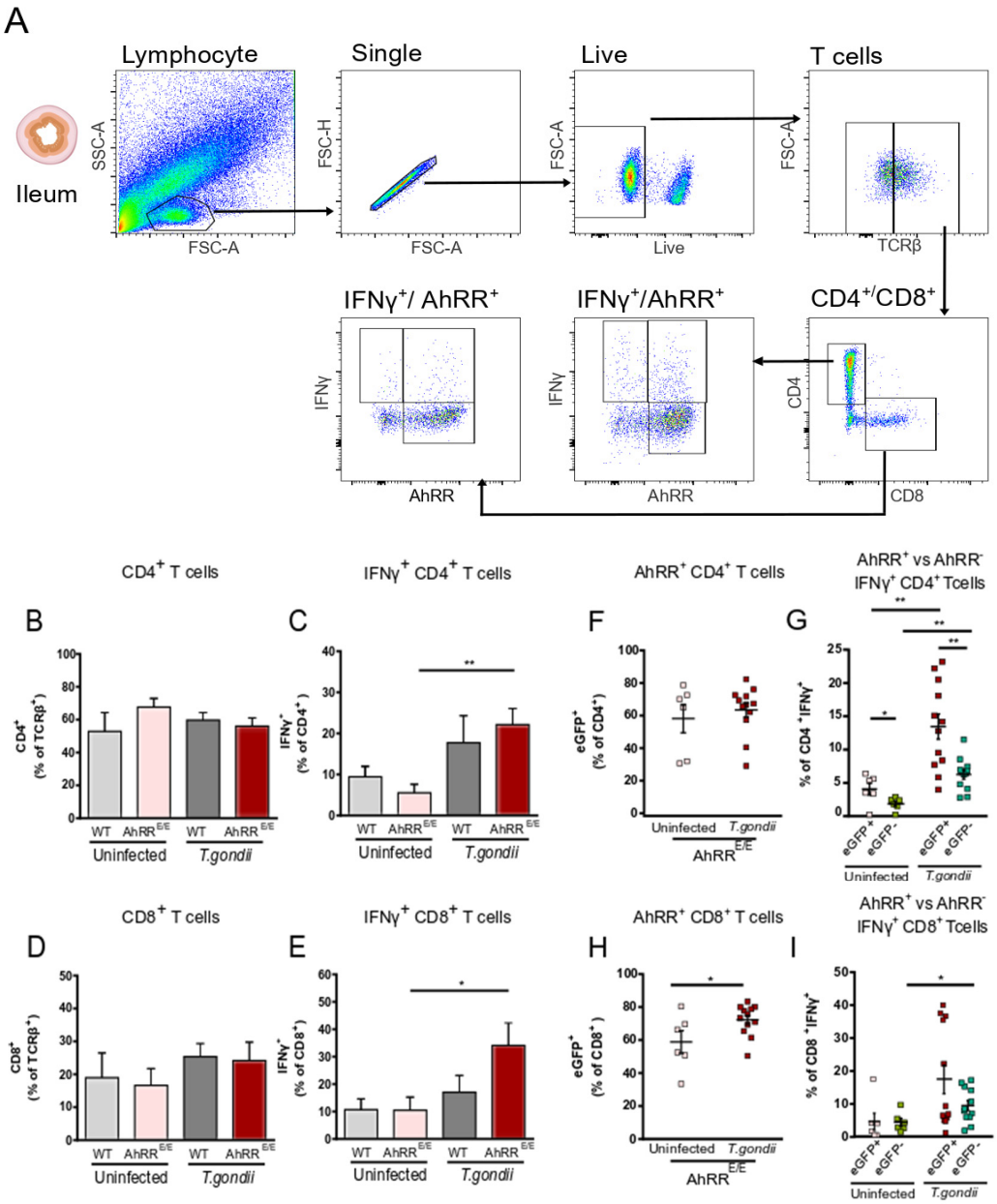


**Figure 5-2: Analysis of IFNγ and AhRR expressing T cells in LP upon *T. gondii* infection**
WT and AhRR-deficient mice were infected with *T. gondii* and the ileum was collected 6 days post infection. The LP cells were isolated, stained for T cells and intracellular IFNγ, and analyzed by FACS. The cells were gated for single cells, live cells, and conventional T cells. Then $CD4^+$ and $CD8^+$ T cell populations were determined. This was followed by gating of $IFN\gamma^+$ and AhRR/$eGFP^+$ populations among $CD4^+$ and $CD8^+$cells (A). The frequency of $CD4^+$ cells among all conventional T cells (B), and $IFN\gamma^+$ $CD4^+$ T cells (C). The frequency of $CD8^+$ cells among all conventional T cells (D), and $IFN\gamma^+$ $CD8^+$ T cells (E). The frequency of AhRR/eGFP expressing cells of all $CD4^+$ (F) and $CD8^+$ (H) T cells. The frequency of AhRR/$eGFP^+$ vs AhRR/$eGFP^-$ $IFN\gamma^+$ $CD4^+$ T cells (G) and $IFN\gamma^+$ $CD8^+$ T cells (I). Data are pooled from three independent experiments (n=5-12 mice). Results are shown as mean +/– SEM and significance was determined by one-way ANOVA corrected for multiple comparisons by the Bonferroni's method or by unpaired students t-test (F, H) (****$p<0.0001$, *** $p<0.001$, ** $p<0.01$, *$p<0.05$).

AhRR-deficient mice slightly but not significantly enhanced the frequency of IFNγ$^+$CD4$^+$ and IFNg$^+$CD8$^+$ T cells compared to WT mice upon *T. gondii* infection (**Figure 5-2 C, E)**.

Using AhRR/eGFP mouse model, we next assessed the AhRR expression in CD4$^+$ and CD8$^+$ T cells after *T. gondii* infection. Although *T. gondii* infection did not influence the frequency of AhRR/eGFP expressing CD4$^+$ T cells, AhRR/eGFP expressing CD4$^+$ T cells produced significantly more IFNγ compared to AhRR/eGFP$^-$ CD4$^+$ T cells **(Figure 5-2 F, G)**. Moreover, the frequency of AhRR/eGFP expressing CD8$^+$ T cells was significantly enhanced after *T. gondii* infection and here, AhRR/eGFP expressing CD8$^+$ T cells had slightly higher IFNγ levels compared to AhRR$^-$ CD8$^+$T cells **(Figure 5-2 H, I)**.

These data suggest that, an increased fraction of IFNγ$^+$CD4$^+$ and IFNγ$^+$ CD8$^+$ T cells might contribute to increased ileal tissue damage observed in AhRR-deficient mice upon *T. gondii* infection. Interestingly, AhRR/eGFP expressing T cells seem to produce more IFNγ compared to AhRR/ eGFP$^-$ T cells.

## 5.2 Function of the AhRR in the defense against *Salmonella* Typhimurium infection

In addition to the parasitic infection model with *T.gondii*, we also used a *S.* Typhimurium infection model to study the function of the AhRR under the inflammatory conditions. Since many mice succumb to the infection after inoculation with highly virulent *S.* Typhimurium WT strains like SL1344 (Wei et al., 2019), it is very difficult to study the long-term immune responses. However, attenuated *S.* Typhimurium strains can be used to overcome this problem. Therefore, we used an attenuated *S.* Typhimurium strain, TAS2010. Initially, a time course experiment was conducted in orally infected WT mice to find the optimal time point for detailed analysis of the infection. Afterwards, WT and AhRR-deficient mice were infected with TAS2010 and blood, ileum as well as spleen and liver were analyzed.

### 5.2.1 Determining the time course of TAS2010 infection in mice

In this study, oral route was used to mimic the natural course of infection. Since TAS2010 strain is cleared by C57Bl/6 mice 5-6 weeks post infection, CFUs (bacterial loads) were monitored

weekly up to 4 weeks to determine the course of infection. WT mice were orally infected with 2,5x10$^9$ bacteria, and serum IFNγ levels as well as CFUs in spleen and liver were assessed at 1-, 2-, 3- and 4-week post TAS2010 infection.

Oral TAS2010 infection of WT mice resulted in the highest serum IFNγ levels in the first and second week, while lower levels were detected at 3 weeks post infection. Although a slight increase in IFNγ levels were observed 4 weeks post infection, this was still less than in the first and second week **(Figure 5-3 A)**. TAS2010 was detected in spleen already after week 1 and the bacterial numbers increased until week 3 **(Figure 5-3 B)**. In liver, TAS2010 was present at 1 week post infection and the bacterial numbers increased in the second week. From the third week onward CFUs decreased compared to 2 weeks post infection **(Figure 5-3 C)**. These data suggested that the peak of infection was reached around 2 weeks post inoculation, hence this time point was chosen for further analysis.

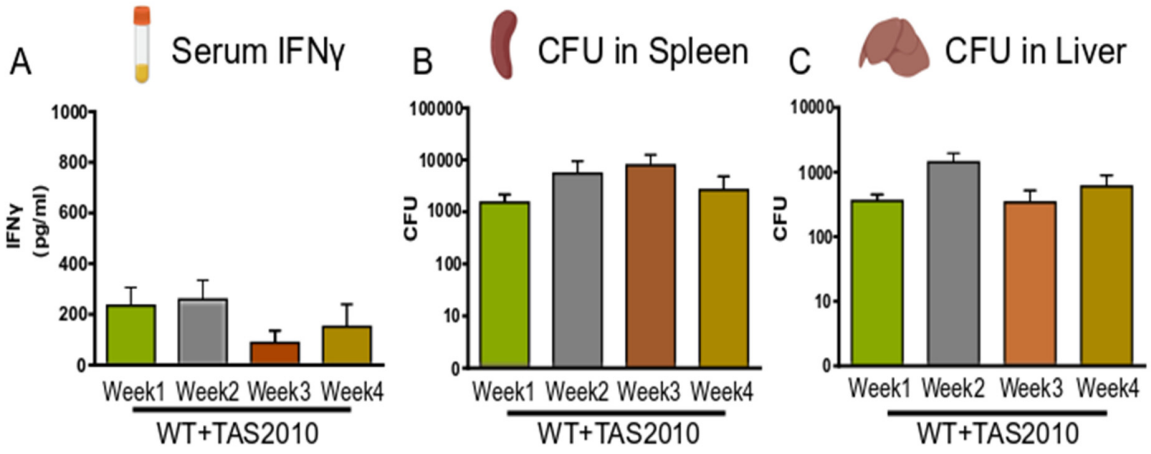


**Figure 5-3: Evaluation of the time course of TAS2010 infection in WT mice**
WT mice were infected with 2,5x10$^9$ TAS2010 and analyzed 1-, 2-, 3- and 4-weeks post infection for serum IFNγ levels (A) and bacterial loads (CFUs) in the spleen (B) and the liver (C). Data were pooled from one to three experiments (n=4-24 mice). Results are shown as mean +/– SEM and significance was determined by one-way ANOVA corrected for multiple comparisons by the Bonferroni's method. No significant difference between the different groups detected in this experiment.

### 5.2.2 AhRR does not have an influence on serum IFNγ levels or bacterial counts in spleen and liver after *S.* Typhimurium infection

After the establishment of the infection procedure, AhRR-deficient and WT mice were infected with TAS2010 and bacterial loads in spleen and liver as well as serum IFNγ levels were analyzed 2 weeks post infection. TAS2010 infected AhRR-deficient and WT mice had similar numbers of bacteria in spleen **(Figure 5-4 A)**. Although AhRR-deficient mice had slightly lower bacterial counts in liver compared to WT mice, the difference was not significant **(Figure 5-4 B)**. Analysis of serum IFNγ levels also showed no difference between AhRR-deficient and WT mice **(Figure 5-4 C)**.

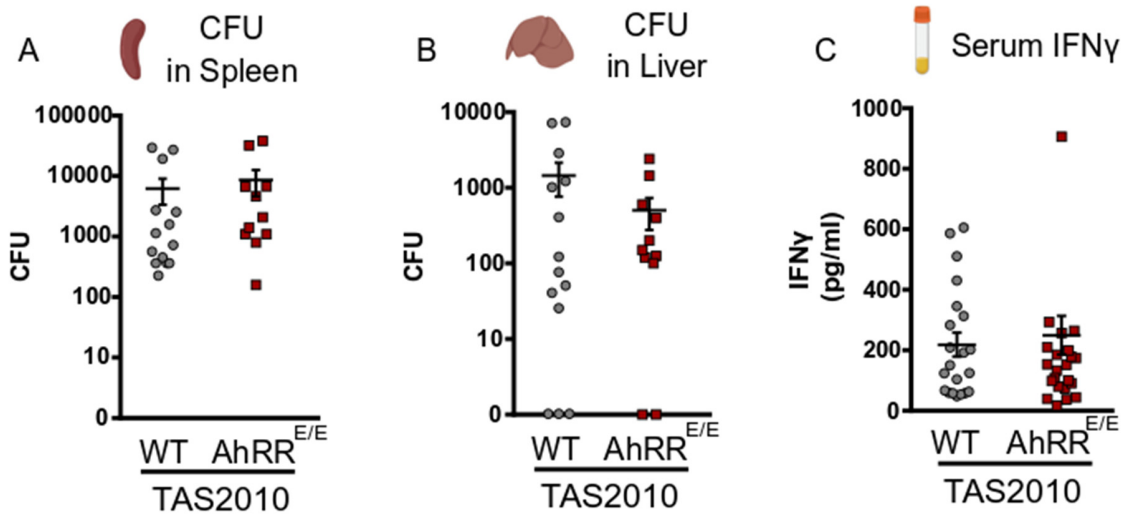


**Figure 5-4: AhRR-deficient mice have similar serum IFNγ levels and bacterial numbers in spleen and liver after TAS2010 infection**
WT and AhRR-deficient mice were infected with 2, $5x10^9$ TAS2010 and analyzed 2 week post infection for bacterial loads (CFUs) in spleen (A) and liver (B) and serum IFNγ levels (C). Data were pooled from three independent experiments (n=11-24 mice). Results are shown as mean +/– SEM and significance was determined by unpaired students t-test. No significant difference between the different groups detected in this experiment.

### 5.2.3 TAS2010 infection induced slightly stronger splenomegaly in AhRR-deficient mice

Since systemic *S.* Typhimurium infection with an attenuated strain induces splenomegaly in WT mice (Jackson et al., 2010), we next checked if the AhRR might have an influence on *Salmonell*a-induced splenomegaly. Although, AhRR-deficient mice had slightly larger spleens following

TAS010 infection compared to the WT mice, the difference was not significant **(Figure 5-5 A)**. While livers of naïve AhRR-deficient mice were already slightly larger compared to those of WT mice, after TAS2010 infection livers of both, WT and AhRR-deficient mice were enlarged, but showed similar weights **(Figure 5-5 B)**.

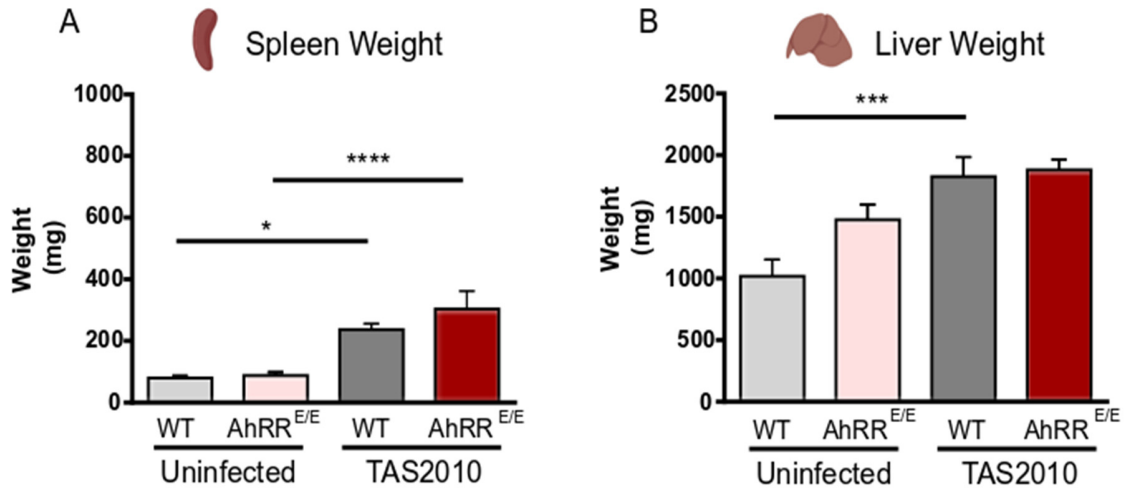


**Figure 5-5: Spleen and liver weights of WT and AhRR-deficient mice after TAS2010 infection**
AhRR-deficient and WT mice were infected with 2,5x$10^9$ TAS2010 for 2 weeks. Spleen (A) and liver (B) were assessed for alterations in weight. Data were pooled from three independent experiments (n=10-11 mice) for spleen and from one experiment (n=5 mice) for liver. Results are shown as mean +/– SEM and significance was determined by one-way ANOVA corrected for multiple comparisons by the Bonferroni's method (****p<0.0001, *** p<0.001, ** p<0.01, *p<0.05).

### 5.2.4 AhRR-deficient mice displayed increased tissue damage in the ileum compared to WT mice after TAS2010 infection

*S.* Typhimurium infection induces intestinal inflammation mainly in the ileum therefore we next questioned whether TAS2010 infection also leads to enhanced ileal tissue damage in AhRR-deficient mice as already observed for the *T. gondii* infection. The ileum of infected WT and AhRR-deficient mice were fixed with 4% PFA and embedded in paraffin. Later, the tissue morphology was analyzed by H&E staining. Tissues were evaluated for possible necrotic and fibrotic regions, inflammatory cell infiltration and changes in the villous structure. TAS2010 infection induced inflammatory cell infiltration in WT and AhRR-deficient mice as indicated by

the **blue arrow** in **Figure 5-6**. Moreover, the ileum of AhRR-deficient mice displayed villous blunting or distortion **(Figure 5-6-black arrow)**. This could hint to a more severe tissue destruction in AhRR-deficient mice compared to WT mice upon TAS2010 infection.

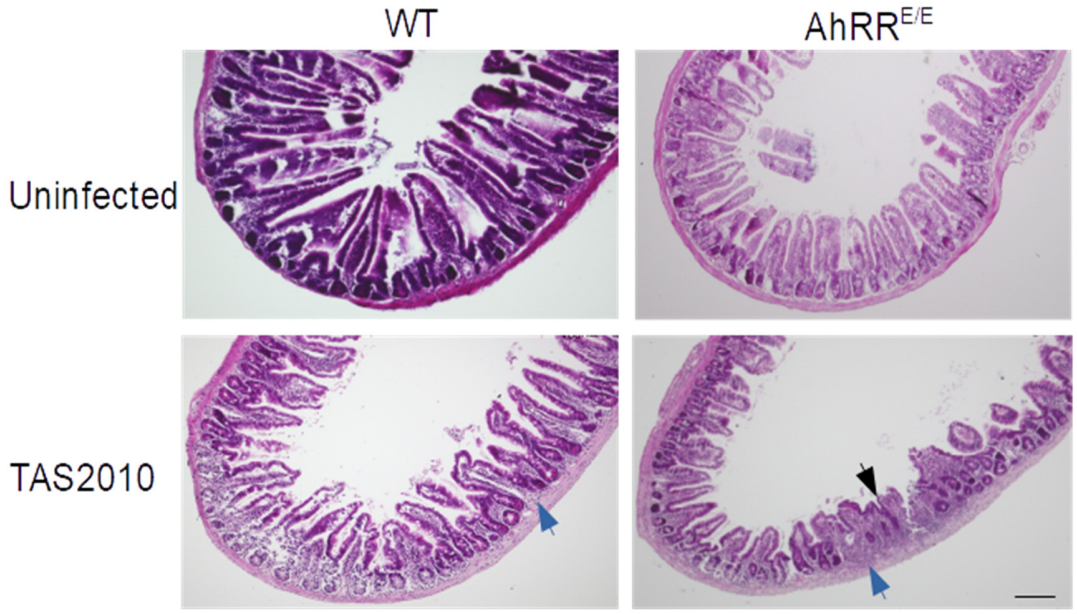


**Figure 5-6: AhRR-deficient mice show elevated ileal tissue damage upon TAS2010 infection**
The ileum samples were collected from uninfected and TAS2010 infected WT and AhRR-deficient mice and embedded in paraffin. Representative ileum sections were stained with H&E for morphological analysis. Data are representative of n=4-5 mice, 1-2 ileal sections per mice. Blue arrow indicates inflammatory cell infiltration and black arrow shows disrupted villous structure. Scale bar: 100µm

### 5.2.5 Analysis of IFNγ- and AhRR-expressing T cells in the LP after TAS2010 infection

We next tested whether the ileal damage of TAS2010 infected mice also correlated with increased IFNγ expression in LP T cells. The gating strategy used for the FACS analysis is depicted in **Figure 5-7 A**. We observed a moderately increased frequency of $CD4^+$ and $CD8^+$ T cells in AhRR-deficient mice in the naïve state relative to WT mice, although, $CD4^+$ and $CD8^+$ T cells were present at similar frequencies in WT and AhRR-deficient mice upon TAS2010 infection **(Figure 5-7 B, D)**. While in both, WT and AhRR-deficient mice, the frequency of $IFN\gamma^+CD4^+$ T cells clearly increased after TAS2010 infection, this increase was significantly higher in AhRR-deficient mice **(Figure 5-7 C).** TAS2010 infection did not influence the ratio of $IFN\gamma^+CD8^+$ T cells in WT mice, but a moderate increase was seen in AhRR-deficient mice (**Figure 5-7 E**).

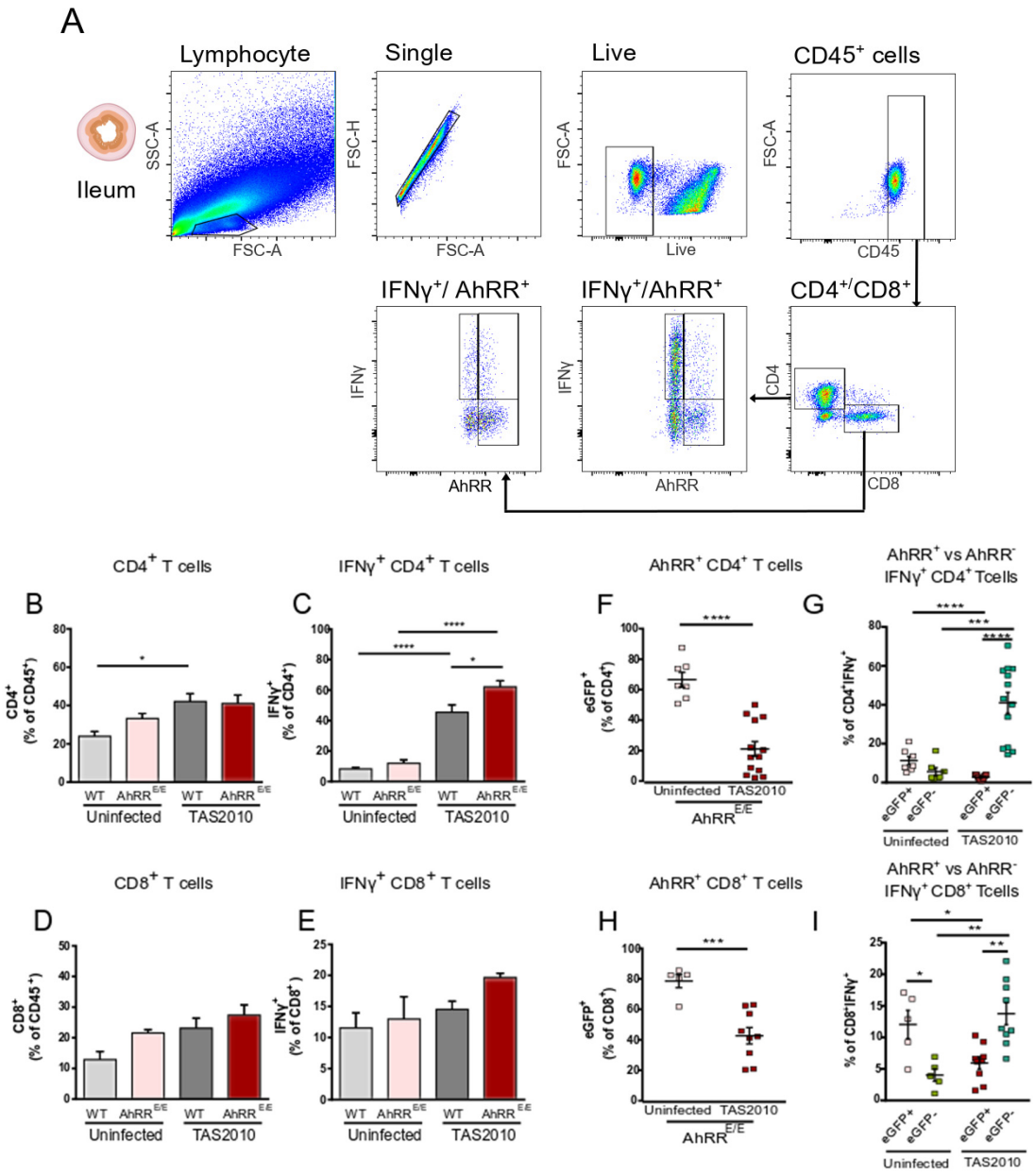


**Figure 5-7: Frequency of IFNγ- and AhRR-expressing T cells in the LP upon TAS2010 infection**
WT and AhRR-deficient mice were infected with TAS2010 and the ileum was collected 2 weeks post infection. LP cells were isolated, stained for T cells and intracellular IFNγ, and analyzed by FACS. The cells were gated for single cells, live cells, $CD45^+$ cells. Then $CD4^+$ and $CD8^+$ T cell populations were determined. This was followed by gating $IFN\gamma^+$ and $AhRR^+$ populations among $CD4^+$ and $CD8^+$cells (A). The frequency of $CD4^+$ cells among all $CD45^+$ cells (B), and $IFN\gamma^+$ $CD4^+$ T cells (Th1) (C). The frequency of $CD8^+$ cells among all $CD45^+$ cells (D), and $IFN\gamma^+$ $CD8^+$ T cells (Tc1) (E); the frequency of AhRR expression in all $CD4^+$ (F) and $CD8^+$ (H) T cells; the frequency of $AhRR/eGFP^+$ vs $AhRR/eGFP^-$ $IFN\gamma^+$ $CD4^+$ T cells (G) and $IFN\gamma^+$ $CD8^+$ T cells (I). Data were pooled from three independent experiments (n=4-13 mice). Results are shown as mean +/– SEM and significance was determined by one-way ANOVA corrected for multiple comparisons by the Bonferroni's method or by unpaired students t-test (F, H) (****$p<0.0001$, *** $p<0.001$, ** $p<0.01$, *$p<0.05$)

Interestingly, the frequency of AhRR/eGFP expressing $CD4^+$ and AhRR/eGFP $^+$ $CD8^+$ T cells were decreased from 65% and 80% to 20% and 40 % , respectively, after TAS2010 infection (**Figure 5-7 F, H**). Moreover, IFNγ was mainly produced by AhRR/eGFP $^-$$CD4^+$ T cells and AhRR/eGFP $^-$$CD8^+$T cells after TAS2010 infection (**Figure 5-7 G, I**).

In summary, these data indicate that the presence of the AhRR does not influence bacterial clearance or systemic IFNγ levels but might to some extent restrict IFNγ production in LP T cells as well as ileal tissue damage upon TAS2010 infection.

## 5.3 Role of the AhR in defense against *Salmonella* Typhimurium infection

Up to now, little is known about the function of the AhR during *S.* Typhimurium infection. Although the focus of this thesis was initially on the characterization of the role of the AhRR in immune responses to infection, we decided to also analyze whether the AhR itself influences host defense and host immunity in *S.* Typhimurium infections.

### 5.3.1 AhR-deficient mice display elevated bacterial counts in liver and spleen and strongly increased serum IFNγ levels after TAS2010 infection

Since TAS2010 infection peaks after 2 weeks, AhR-deficient mice and WT mice were initially infected for 2 weeks and analyzed thereafter. All 17 WT mice and 16 out of 18 AhR-deficient mice survived the infection (data not shown). Spleen and liver were collected, and the bacterial counts were determined to check the severity of infection. Moreover, serum was collected for detection of systemic IFNγ levels. Compared to WT mice, AhR-deficient mice had significantly increased bacterial counts in spleen and liver **(Figure 5-8 A, B)**. Furthermore, it was shown that the systemic IFNγ levels in *S.* Typhimurium infected mice correlate with disease severity (Kupz et al., 2014). In line, we observed 10-fold increased serum levels of IFNγ in infected AhR-deficient mice compared to WT mice **(Figure 5-8 C).** These data suggest that unlike AhRR-deficient mice, AhR-deficient mice are profoundly susceptible to TAS2010 infection.

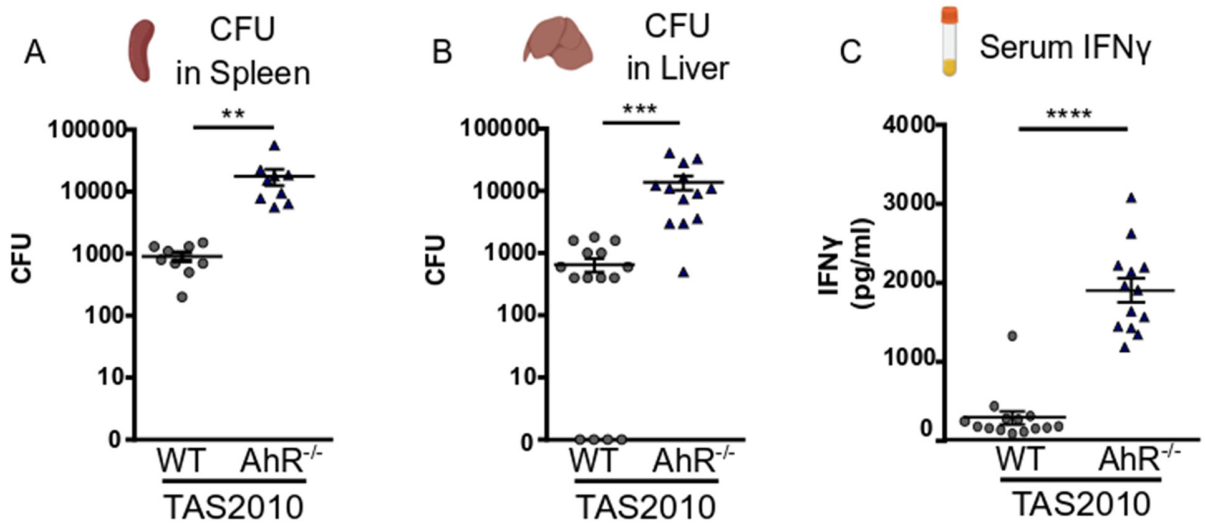


**Figure 5-8: AhR-deficient mice show enhanced serum IFNγ levels and bacterial counts after TAS2010 infection**
WT and AhR-deficient mice were infected with 2, $5x10^9$ TAS2010 and analyzed 2 weeks post infection for bacterial loads (CFUs) in spleen (A) and liver (B) and serum IFNγ levels (C). Data were pooled from three independent experiments (n=7-14 mice). Results are shown as mean +/– SEM and significance was determined by unpaired students t-test (****p<0.0001, *** p<0.001, ** p<0.01, *p<0.05).

### 5.3.2 TAS2010 infection enhances splenomegaly and increases liver weight in AhR-deficient mice

In line with the experiments shown in **Figure 5-5**, spleens of TAS2010-infected WT mice were about 3-fold heavier than spleens of naïve WT mice, weigh around 270 mg on average. AhR-deficient mice had slightly enlarged spleens, already in the naive state. After TAS2010 infection, spleens of AhR-deficient mice weighted around 700 mg **(Figure 5-9 A).** This represents a 6-fold increase compared to naïve AhR-deficient mice and nearly a 3-fold increase compared to TAS2010-infected WT mice. Furthermore, as AhR-deficient mice show an abnormal liver development (Lahvis et al., 2000) and in line with the literature, we found that these mice have smaller livers compared to WT mice in naïve state. TAS2010 infection increases liver weight of AhR-deficient mice, however, these infected livers were still significantly smaller than those of WT mice **(Figure 5-9 B)**.

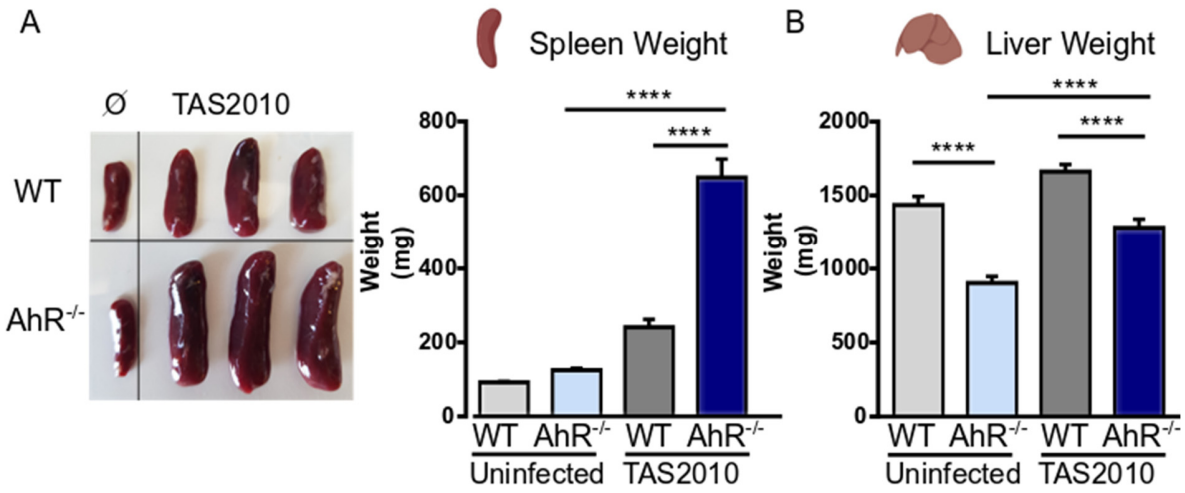


**Figure 5-9: AhR-deficient mice have enhanced splenomegaly and increased liver weight upon TAS2010 infection**
AhR-deficient and WT mice were infected with TAS2010 for 2 weeks then spleen (A) and liver (B) were assessed for weight changes. Data were pooled from three (spleen) and two (liver) independent experiments (n=6-8 mice). Results are shown as mean +/– SEM and significance was determined by one-way ANOVA corrected for multiple comparisons by the Bonferroni's method (****p<0.0001, *** p<0.001, ** p<0.01, *p<0.05).

## 5.3.3 Analysis of ileum morphology and IFNγ producing T cells in the LP of AhR-deficient mice after TAS2010 infection

### 5.3.3.1 Increased ileal tissue damage in AhR-deficient mice upon TAS2010 infection

AhR-deficient mice might show stronger pathology in the ileum like seen in AhRR-deficient mice after TAS2010 infection. To test this, ileum sections of WT and AhR-deficient mice infected for 2 weeks with TAS2010 were prepared and the tissue morphology was analyzed with H&E staining. Tissues were evaluated for possible necrotic and fibrotic regions, inflammatory cell infiltration and changes in the villous structure. As shown above, TAS2010 infection induced inflammatory cell infiltration in WT mice **(blue arrow in Figure 5-10)**. Some of the animals showed more severe tissue damage like increased villous damage compared to infected WT animals **(Figure 5-10)**, conversely others appeared to have a normal tissue morphology. These data might indicate a possible increase in tissue damage in AhR-deficient mice, however, this was not as apparent as detected in *S.* Typhimurium infected AhRR-deficient mice.

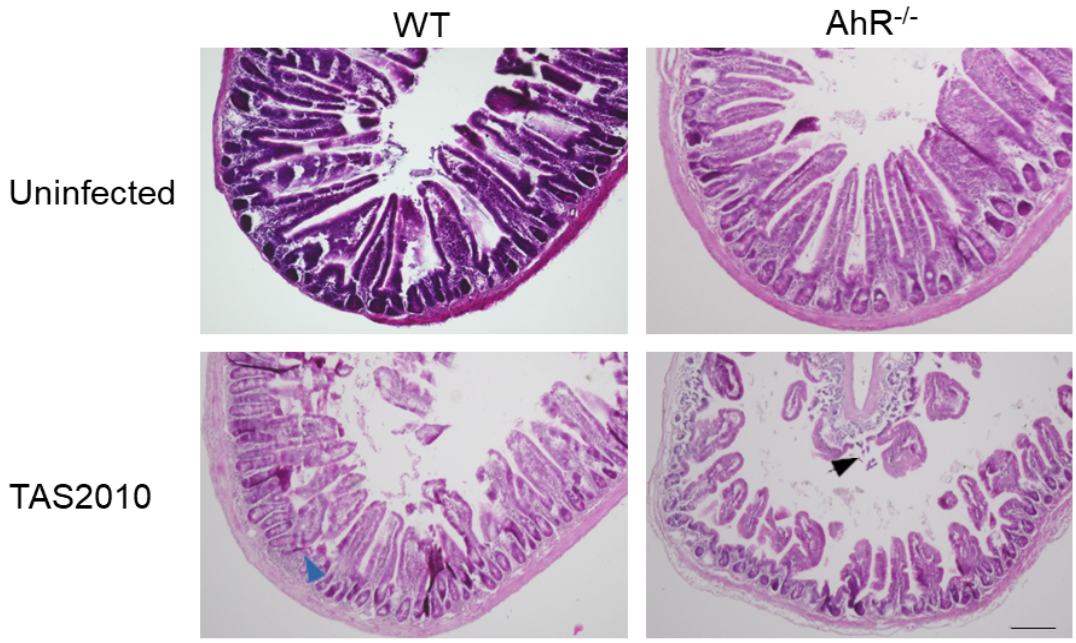


**Figure 5-10: Histological analysis of ileum samples from WT and AhR-deficient mice after TAS2010 infection**
Ileum samples were collected from uninfected and TAS2010 infected WT and AhR-deficient mice and embedded in paraffin. Representative ileum sections were stained with H&E for morphological analysis. Data are representative of n=4 mice, 1-2 ileal sections per mice. Blue arrow indicates inflammatory cell infiltration and black arrow shows disrupted villous structure. Scale bar: 100µm

### 5.3.3.2 The frequency of LP IFNγ$^+$CD4$^+$ T cells increased similarly in WT and AhR-deficient mice after TAS2010 infection

Next, T cell abundance in ileal LP of AhR-deficient mice after TAS2010 infection was determined. The LP cells were isolated as described above, the gating strategy is depicted in **Figure 5-11 A**. TAS2010 infection increased the frequency of CD4$^+$ T only slightly in WT mice **(Figure 5-11 B, D)** and somewhat more in AhR-deficient mice **(Figure 5-11 B).** However, the frequency of IFNγ$^+$CD4$^+$ T cells increased significantly in both WT and AhR-deficient mice after TAS2010 infection with no apparent difference between the different genotypes **(Figure 5-11 C)**. Although there was also a slight increase in the frequency of IFN-γ$^+$CD8$^+$ T in AhR-deficient mice compared to WT mice after TAS2010 infection, the difference was not significant **(Figure 5-11 E)**.

In summary, there was only a moderate increase in the frequency of IFNγ$^+$CD8$^+$ T cells in AhR-deficient mice, which might contribute to the slightly increased ileal tissue damage but is unlikely to account for the stronger susceptibility of these mice to TAS2010 infection.

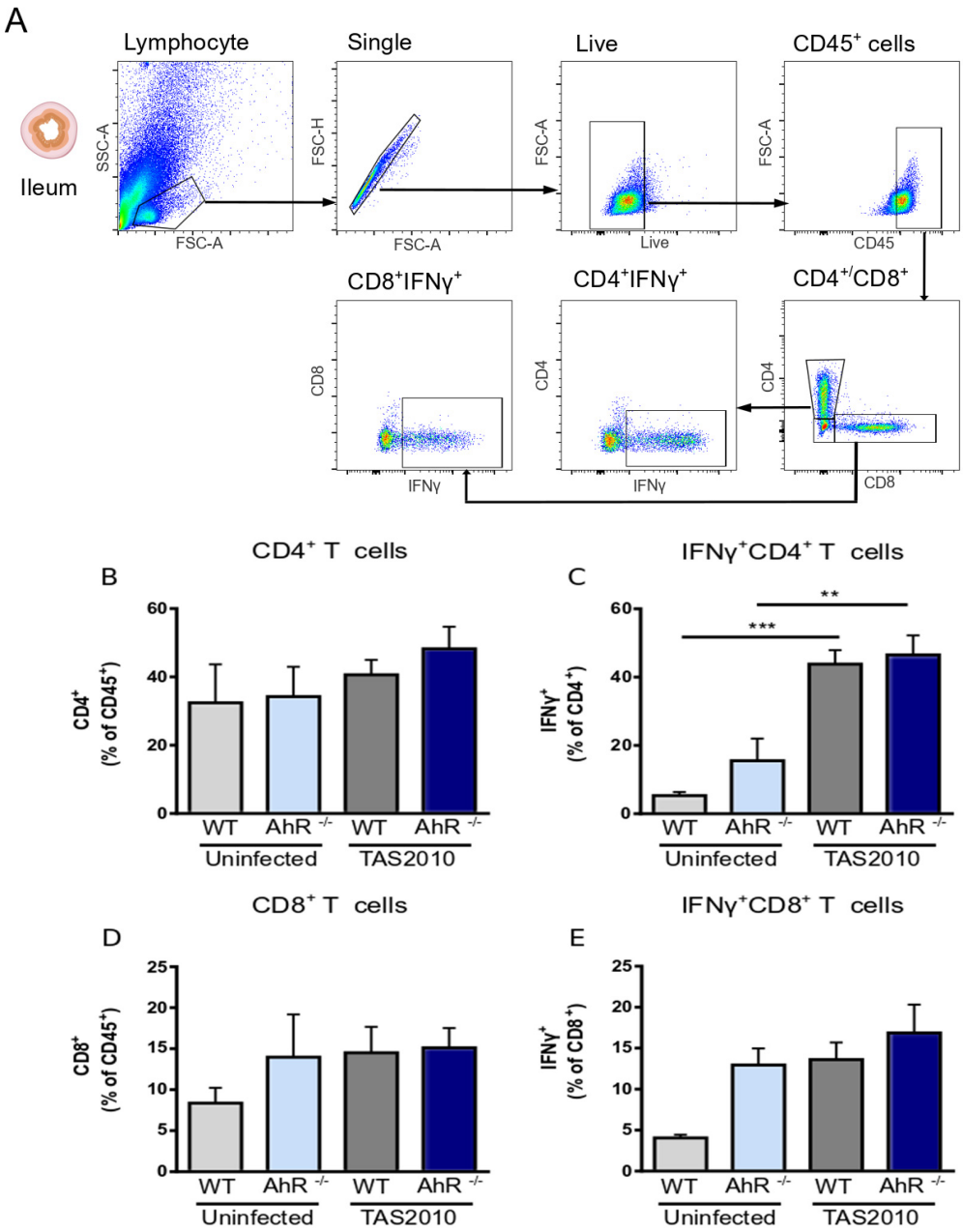


**Figure 5-11: The frequency of IFNγ$^+$ T cells in the LP of WT and AhR- deficient mice after TAS2010 infection**

WT and AhR-deficient mice were infected with TAS2010 and the ileum was collected two weeks post infection. The LP cells were isolated and gated for single cells, live cells, CD45$^+$ cells. Then, CD4$^+$ and CD8$^+$ T cell populations were determined. This was followed by gating IFNγ$^+$ populations among CD4$^+$ and CD8$^+$cells (A). The frequency of CD4$^+$ cells among all CD45$^+$ cells (B), and IFNγ$^+$ CD4$^+$ T cells (Th1 cells) (C). The frequency of CD8$^+$ cells among all CD45$^+$ cells (D), and IFNγ$^+$ CD8$^+$ T cells (Tc1) (E). Data were pooled from two independent experiments (n=4-10 mice). Results are shown as mean +/– SEM and significance was determined by one-way ANOVA corrected for multiple comparisons by the Bonferroni's method (****p<0.0001, *** p<0.001, ** p<0.01, *p<0.05)

### 5.3.4 Contribution of different cell types to enhanced splenomegaly in AhR-deficient mice

We showed that AhR-deficient mice had a significantly enhanced splenomegaly compared to WT mice after TAS2010 infection. Since *S.* Typhimurium infection is known to increase cellularity in the spleen (L. X. Li et al., 2016), we suspected that the enhanced spleen weight result from increased cell numbers in AhR-deficient mice. To test this hypothesis, single cell suspensions from spleens of WT and AhR-deficient mice were prepared and total cell numbers were calculated using a Neubauer chamber. Naïve AhR-deficient mice had already slightly higher cell counts in spleen compared to WT mice, which is in line with the increased spleen weight. As expected, after TAS2010 infection, AhR-deficient mice showed significantly higher splenic cell numbers compared to WT mice **(Figure 5-12)**.

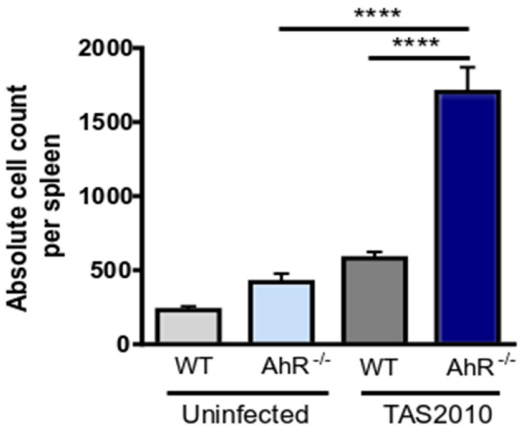


**Figure 5-12: Enhanced splenomegaly observed in AhR-deficient mice after TAS2010 infection is due to an increase in splenic cell counts**
WT and AhR-deficient mice were infected with TAS2010 and the spleens were collected two weeks post infection. Splenic cells were counted using a Neubauer chamber. (n=3-4 mice). Results are shown as mean +/– SEM and significance was determined by one-way ANOVA corrected for multiple comparisons by the Bonferroni's method (****p<0.0001, *** p<0.001, ** p<0.01, *p<0.05)

#### 5.3.4.1 Analysis of immune cell populations in spleens of AhR-deficient mice

The increase of splenic cell numbers during *S.* Typhimurium infections is known to be in part due to infiltration and expansion of phagocytes and lymphocytes (Ganesh et al., 2014; Srinivasan et al., 2004). Therefore, we next assessed the frequencies and cell numbers of $CD11b^+F4/80^+$ macrophages, B cells, $CD4^+$ and $CD8^+$ T cells in WT and AhR-deficient mice upon infection. Spleen cells were isolated and FACS analysis was performed to identify different immune cell populations. The gating strategy is shown in **Figure 5-13 A.** The frequency of $CD11b^+F4/80^+$ macrophages in WT mice and AhR-deficient mice was around 2% and 3%, respectively. Thus,

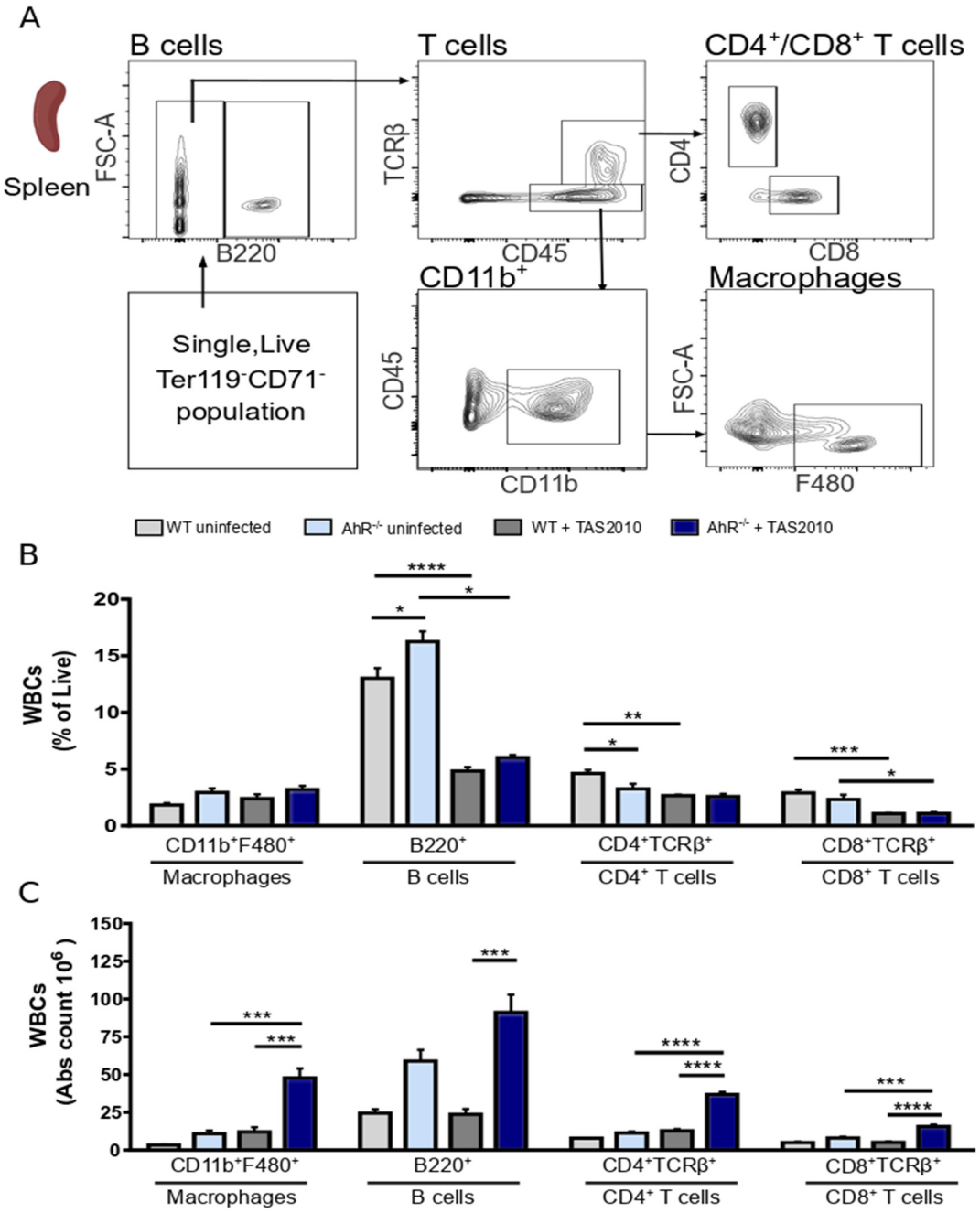


**Figure 5-13: Analysis of immune cell populations in spleen of AhR-deficient and WT mice upon TAS2010 infection**

WT and AhR-deficient mice were infected with TAS2010 and spleen was collected two weeks post infection for immune cell analysis. $CD11b^+F480^+$ macrophages, $B220^+$ B cells and $CD4^+$ and $CD8^+$T cells were depicted (A). The frequency (B) and absolute numbers (C) of indicated immune cell subsets were shown. (n=3-4 mice). Results are shown as mean +/– SEM and significance was determined by one-way ANOVA corrected for multiple comparisons by the Bonferroni's method (****p<0.0001, *** p<0.001, ** p<0.01, *p<0.05)

TAS2010 infection did not have a major influence on the frequency of $CD11b^+F4/80^+$ macrophages in WT and AhR-deficient mice. In contrast, the frequency of $B220^+$ B cells was decreased in both WT and AhR-deficient mice after TAS2010 infection. In addition, AhR-deficient mice had a lower frequency of $CD4^+$ and $CD8^+$ T cells compared to WT mice already in the naïve state. Infection with TAS2010 decreased $CD4^+$ and $CD8^+$ T cells frequencies in WT and AhR-deficient mice similarly **(Figure 5-13 B).** In line with the overall increased spleen cell numbers and spleen weight, $CD11b^+F4/80^+$ macrophages, B cells as well as $CD4^+$ and $CD8^+$ T cells numbers were significantly enhanced in AhR-deficient mice compared to WT mice after TAS2010 infection **(Figure 5-13 C)**.

### 5.3.4.2 Analysis of splenic red blood cell populations in AhR deficient mice

Although, we have shown that the increased cellularity is in line with increased immune cell numbers in the spleen, these numbers do not add up to the total cell numbers after TAS2010 infection. Moreover, the relative decrease in the frequency of these immune cells suggested an increase of other cell types in AhR-deficient mice. It is known that in response to *S.* Typhimurium infection, major splenic extramedullary erythropoiesis can occur, accompanied by immature RBC expansion (Jackson et al., 2010). Therefore, we quantified the immature and mature RBC populations using FACS and analyzed the contribution of each population to the increased cellularity observed in AhR-deficient mice upon TAS2010 infection. By using CD71 and Ter119 markers on the RBC cell surface, we identified four different RBC groups: immature $Ter119^{med}CD71^{hi}$ pro-erythroblasts, $Ter119^{hi}CD71^{hi}$ basophilic & polychromatic erythroblasts, $Ter119^{hi}CD71^{med}$ basophilic erythrocytes & reticulocytes and mature $Ter119^{hi}CD71^{low}$ Erythrocytes. The gating strategy is depicted in **Figure 5-14 A**. We observed low frequencies of $Ter119^{med}CD71^{hi}$ cells in WT mice under steady state conditions. The frequencies of $Ter119^{hi}CD71^{hi}$ and $Ter119^{hi}CD71^{med}$ cells were slightly higher, whereas the $Ter119^{hi}CD71^{low}$ cells accounted for the highest proportion of RBCs, contributing to 60 % of all living cells in naïve WT mice. Interestingly, AhR-deficient mice had slightly enhanced frequencies of $Ter119^{med}CD71^{hi}$, $Ter119^{hi}CD71^{hi}$ and $Ter119^{hi}CD71^{med}$ cells compared to WT mice already in naïve state. Although TAS2010 infection increased the frequency of all immature RBC populations in both WT and AhR-deficient mice, the frequencies of $Ter119^{med}CD7^{hi}$ and $Ter119^{hi}CD71^{med}$ cells in AhR-deficient mice were significantly higher than those of WT mice.

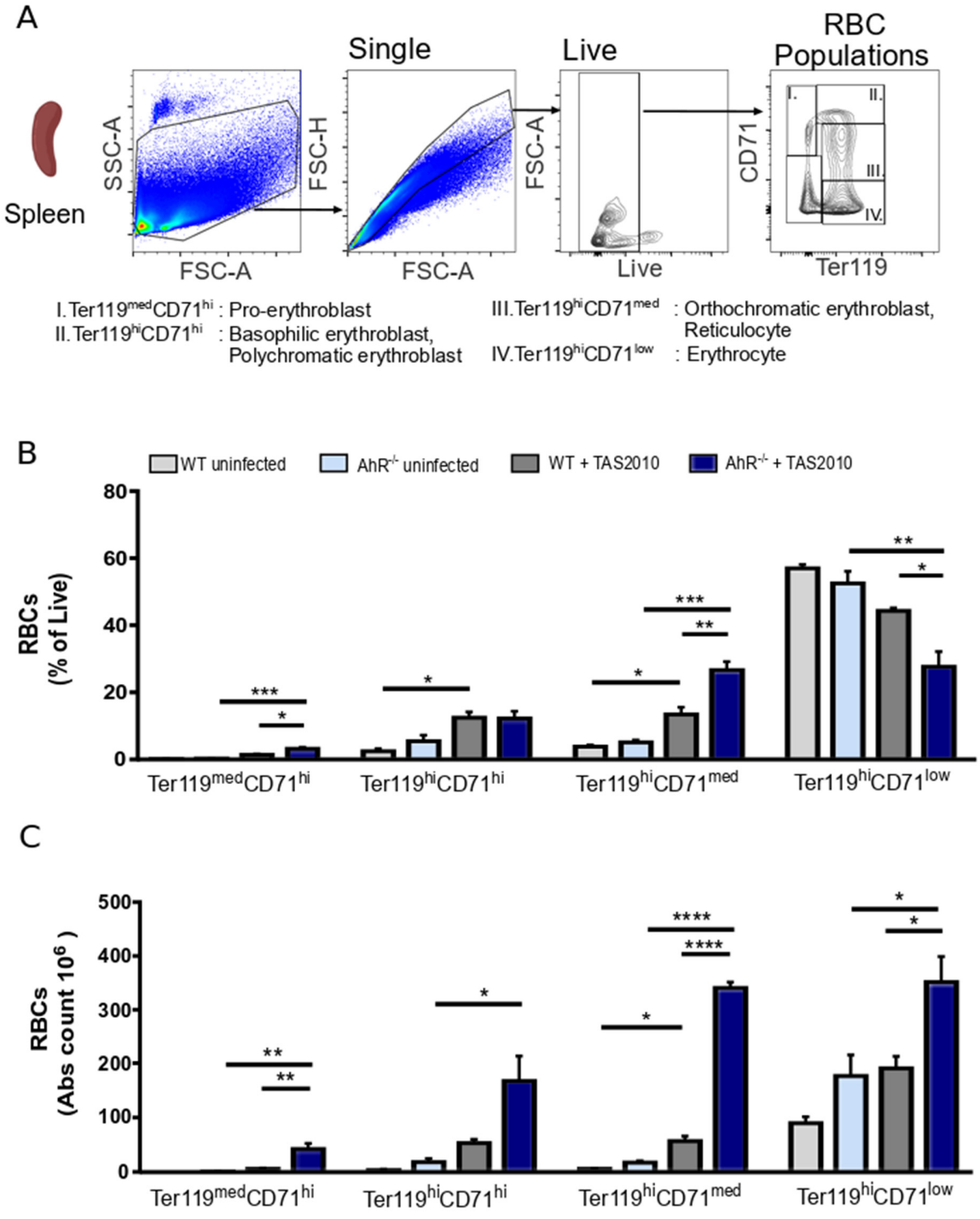
A
Spleen
SSC-A
FSC-A
FSC-H
FSC-A
Single
FSC-A
Live
Live
CD71
Ter119
RBC Populations
I.
II.
III.
IV.
I. Ter119med CD71hi : Pro-erythroblast
II. Ter119hi CD71hi : Basophilic erythroblast, Polychromatic erythroblast
III. Ter119hi CD71med : Orthochromatic erythroblast, Reticulocyte
IV. Ter119hi CD71low : Erythrocyte
B
WT uninfected
AhR-/- uninfected
WT + TAS2010
AhR-/- + TAS2010
RBCs (% of Live)
Ter119medCD71hi
Ter119hiCD71hi
Ter119hiCD71med
Ter119hiCD71low
C
RBCs (Abs count 10^6)
Ter119medCD71hi
Ter119hiCD71hi
Ter119hiCD71med
Ter119hiCD71low

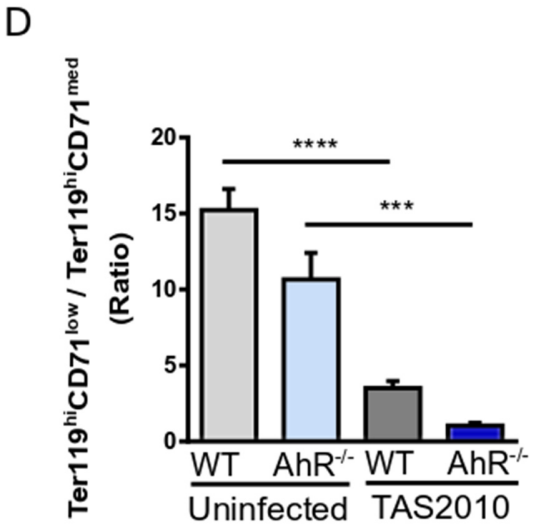


**Figure 5-14: Analysis of RBCs in the spleen of AhR-deficient and WT mice upon TAS2010 infection**
WT and AhR-deficient mice were infected with TAS2010 and spleens were collected two weeks post infection for RBC analysis. CD71 and Ter119 markers were used to identify immature and mature RBCs. $Ter119^{med}CD71^{hi}$ pro-erythroblasts (I), $Ter119^{hi}CD71^{hi}$ basophilic & polychromatic erythroblasts (II), $Ter119^{hi}CD71^{med}$ orthochromatic erythroblasts & reticulocytes (III) and mature $Ter119^{hi}CD71^{low}$ erythrocytes (IV) are depicted (A). The frequencies (B) and absolute numbers (C) of the indicated RBC subsets shown. (n=3-4 mice). The ratio of $Ter119^{hi}CD71^{low}$ to Ter119hiCD71$^{med}$ RBCs were indicated (D). Results are shown as mean +/– SEM and significance was determined by one-way ANOVA corrected for multiple comparisons by the Bonferroni's method (****p<0.0001, *** p<0.001, ** p<0.01, *p<0.05)

Moreover, AhR-deficient mice possessed a significantly lower frequency of $Ter119^{hi}CD71^{low}$ mature RBCs relative to WT mice upon TAS2010 infection **(Figure 5-14 B)**. In line with their increased frequency, the absolute numbers of $Ter119^{med}CD71^{hi}$ and $Ter119^{hi}CD71^{med}$ cells were also significantly higher in AhR-deficient mice compared to WT mice. Moreover, $Ter119^{hi}CD71^{hi}$ and $Ter119^{hi}CD71^{low}$ cells were also significantly increased in absolute terms **(Figure 5-14 C).** In the naïve state, the ratio of $Ter119^{hi}CD71^{low}$ cells to $Ter119^{hi}CD71^{med}$ cells in WT mice was 15, and upon TAS2010 infection, this ratio dropped to 4 **(Figure 5-14 D)**, indicating certain RBC maturation defect related to the infection. Interestingly, AhR-deficient mice had nearly similar $Ter119^{hi}CD71^{low}$ and $Ter119^{hi}CD71^{med}$ RBC counts after TAS2010 infection. Hence, the ratio of $Ter119^{hi}CD71^{low}$ cells to $Ter119^{hi}CD71^{med}$ cells was around 1 **(Figure 5-14 D)**. These data indicated a more pronounced RBC maturation defect in AhR-deficient mice compared to WT mice upon infection. In summary, the enhanced splenomegaly and increased cellularity observed in AhR-deficient mice after TAS2010 infection is partially due to an increase in immune cell numbers, but the major reason is the increase in the abundance of RBCs.

### 5.3.5 Increased frequency of splenic $IFN\gamma^+CD4^+$ and $IFN\gamma^+CD8^+$ T cells in AhR-deficient mice after TAS2010 infection

Since IFNγ enhances the immune defense against *Salmonella* Typhimurium infection, we next looked at the frequency of $IFN\gamma^+CD4^+$ and $IFN\gamma^+CD8^+$ T cells in spleen with FACS using the

gating strategy shown in **Figure 5-15**. In the naïve state, AhR-deficient mice had a slightly increased frequency of IFNγ$^+$CD4$^+$ and IFNγ$^+$CD8$^+$ T cells. Upon TAS2010 infection, however, the frequencies of IFNγ$^+$CD4$^+$ and IFNγ$^+$CD8$^+$ T cells were significantly enhanced in AhR-deficient mice relative to WT mice **(Figure 5-15 B, C)**.

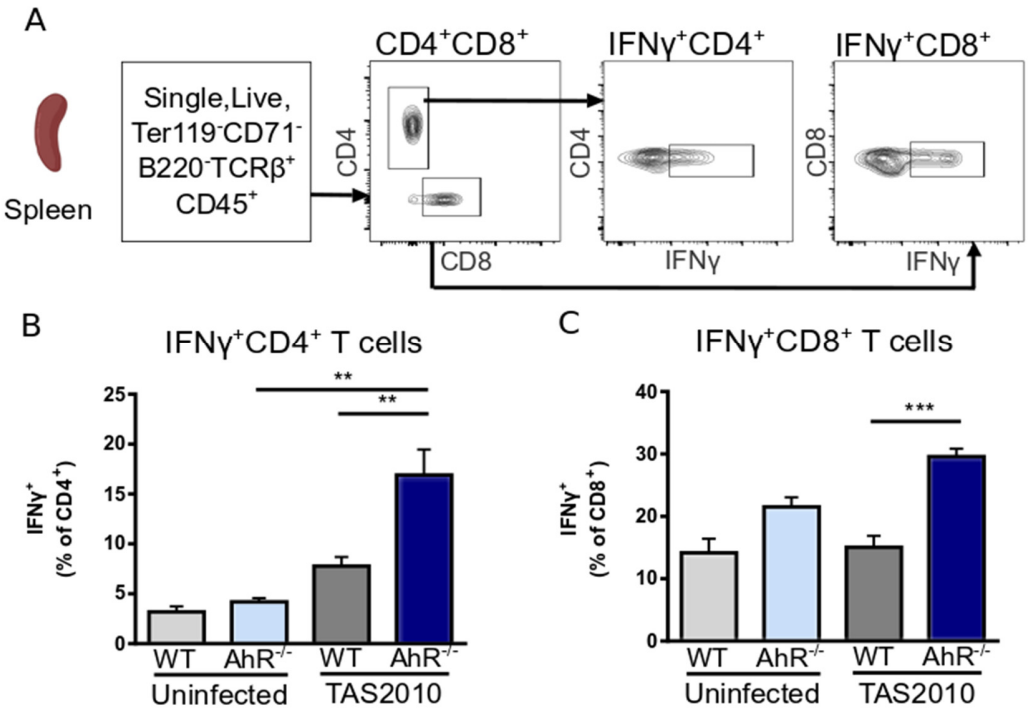


**Figure 5-15: AhR-deficient mice display an increased frequency of IFNγ$^+$ T cells upon TAS2010 infection**
WT and AhR-deficient mice were infected with TAS2010 and spleens were collected two weeks post infection. The splenic cells were first gated for single cells, live cells, and conventional T cells. Then CD4$^+$ and CD8$^+$ T cell populations were determined. This was followed by gating IFNγ$^+$ populations among CD4$^+$ and CD8$^+$cells (A). Frequency of IFNγ$^+$ CD4$^+$ T cells (B) and frequency of IFNγ$^+$ CD8$^+$ T cells (C) (n=3-4 mice). Results are shown as mean +/– SEM and significance was determined by one-way ANOVA corrected for multiple comparisons by the Bonferroni's method (****p<0.0001, *** p<0.001, ** p<0.01, *p<0.05)

## 5.3.6 Strong upregulation of CD69 expression on T cells and CD11b$^+$ myeloid cells in AhR-deficient mice upon TAS2010 infection

CD69 is an early activation marker and is known to be expressed by activated T lymphocytes as well as myeloid cell (Cibrián & Sánchez-Madrid, 2017). This marker is also known to be upregulated upon *S.* Typhimurium infection (Yrlid et al., 2001). Therefore, the frequency of CD69 expressing CD4$^+$ and CD8$^+$ T cells and myeloid CD11b$^+$ cells were analyzed as depicted in **Figure**

**5-16.** In line with the literature, TAS2010 infection increased the frequency of $CD4^+CD69^+$ and $CD69^+CD8^+$ T cells as well as $CD69^+CD11b^+$ myeloid cells in WT mice **(Figure 5-16 B, C)**. Interestingly, AhR-deficient mice had an even higher frequency of $CD69^+$ cells, in particular the frequency of $CD69^+CD8^+$ T cells and $CD69^+CD11b^+$ myeloid cells were significantly enhanced in AhR-deficient mice relative to WT mice upon infection **(Figure 5-16 B, C, D)**.

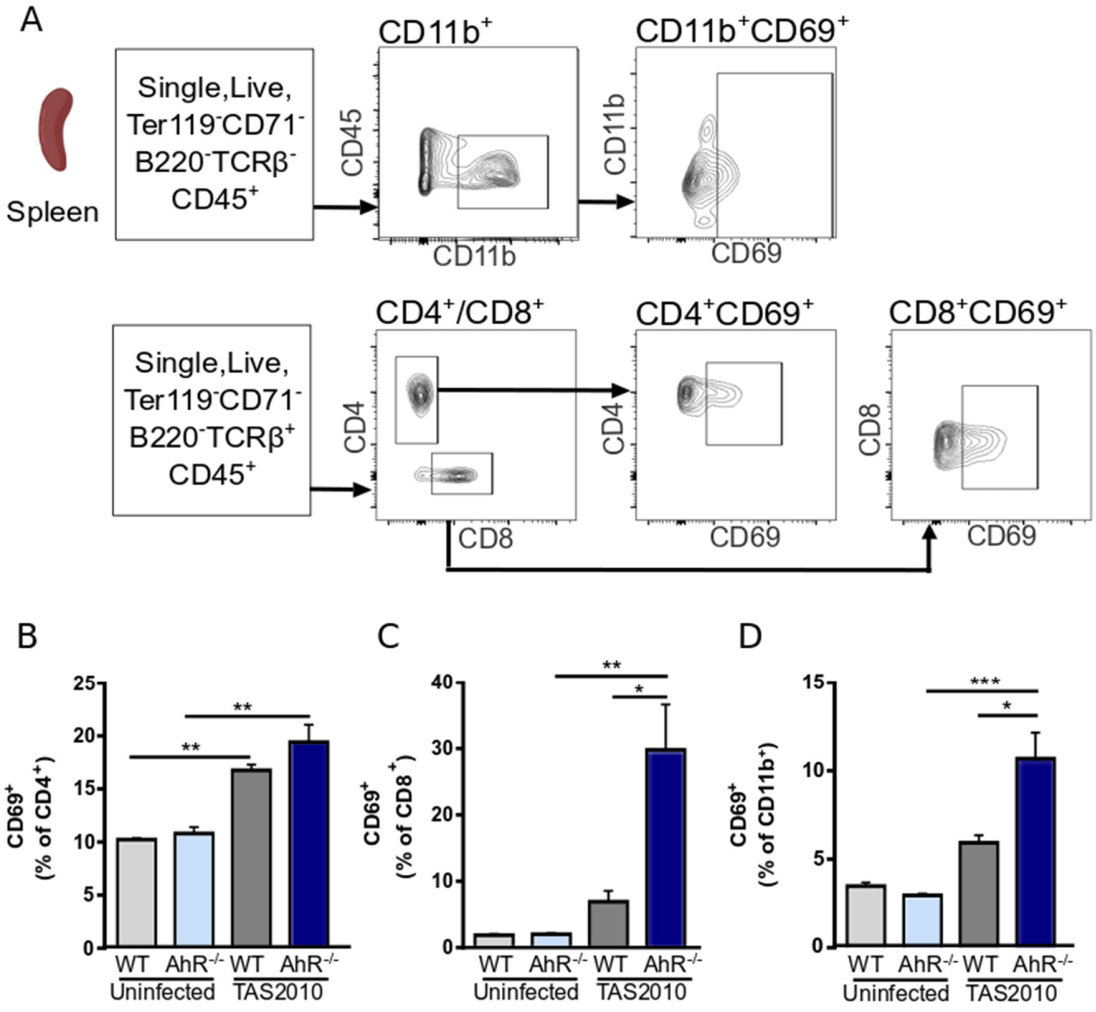


**Figure 5-16: The frequency of CD69 expressing T cells and $CD11b^+$ myeloid cells are increased in AhR-deficient mice in response to TAS2010 infection**
WT and AhR-deficient mice were infected with TAS2010 and spleens were collected two weeks post infection. Splenic cells were gated for single cells, live cells, and then for $CD4^+$ and $CD8^+$ T cells, or for CD11b+ cells. This was followed by gating $CD69^+$ populations among T cells or $CD11b^+$ cells (A). The frequency $CD69^+$ $CD4^+$ T cells (B) the frequency of $CD69^+$ $CD8^+$ T cells (C) and the frequency of $CD69^+$ $CD11b^+$cells (C). (n=3-4 mice). Results are shown as mean +/– SEM and significance was determined by one-way ANOVA corrected for multiple comparisons by the Bonferroni's method (****p<0.0001, *** p<0.001, ** p<0.01, *p<0.05)

### 5.3.7 Destruction of the splenic architecture in AhR-deficient mice upon TAS2010 infection

In order to see whether infection with the attenuated strain TAS2010 also have an influence on the splenic architecture of WT and AhR-deficient mice, H&E staining was performed. Using this staining method, the red pulp was stained in dark pink, the white pulp in purple and the marginal zone in a light pink color. We observed that WT mice had intact white pulp regions, which are surrounded by the intact marginal zones under steady state conditions. However, these structures were not as clearly distinguishable in AhR-deficient mice compared to WT mice in the naïve state, since most of the light pink marginal zone region was lost, and the WP region appeared to be disrupted. Upon infection, WT mice had only a slightly altered splenic architecture, which was characterized by smaller WP/MZ areas and occasionally disrupted borders between WP and RP. In contrast, the splenic architecture was strongly altered in AhR-deficient mice as the borders between WP and RP could no longer be defined and areas of WP were much smaller(**Figure 5-17**).

Next, we wanted to assess the distribution of different immune cell types within the spleen including the altered WP region in AhR-deficient mice. The WP is mainly composed of B and T cells. For this reason, the immunofluorescence staining of $B220^+$cells (B cells) and $TCR\beta^+$ cells (T cells) were analyzed. Spleens from WT mice showed large B cell follicles (cyan) which surround the T cell zones (red), forming an intact WP region in the naïve state. Surprisingly, AhR-deficient mice showed significantly smaller B cell follicles already in the naïve state, but these smaller B cell follicles also surrounding the T cell zones as seen in the WT background **(Figure 5-18 A).** TAS2010 infection had an influence on B cell follicle sizes, since WT mice possessed smaller B follicles compared to the naïve state. Interestingly, AhR-deficient mice had even smaller B cell follicles compared to WT mice after TAS2010 infection **(Figure 5-18 A, B)**. Furthermore, some of the T cell zones were still intact in the WT mice and were surrounded by B cell follicles, while T cells were also dislocated into the RP region upon infection. In contrast, in AhR-deficient mice, there were no visible T cell zones anymore, and these cells were distributed all over the spleen after TAS2010 infection **(Figure 5-18 A)**. These data clearly indicate that AhR-deficient mice have an altered splenic architecture already in naïve state and that TAS2010 infection leads to further disruption of the WP region, a process that was clearly different from WT mice.

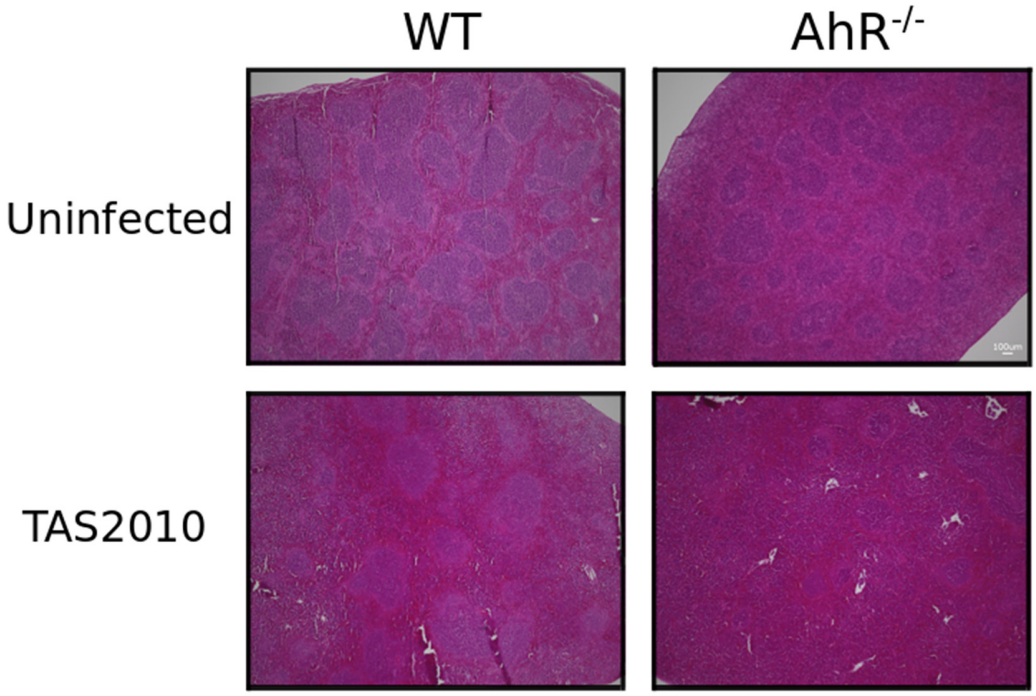


**Figure 5-17: Histological analysis of spleen sections of WT and AhR-deficient mice by H&E staining after TAS2010 infection**
Spleens were collected from uninfected and TAS2010 infected WT and AhR-deficient mice and embedded in paraffin. Representative spleen sections were stained with H&E for morphological analysis. Scale bar: 100µm

In summary, these data indicate that the severity of TAS2010 infection is much stronger in the absence of AhR expression compared to the WT background. Thus, AhR-deficient mice showed more tissue damage in the ileum and significantly enhanced splenomegaly relative to WT mice after TAS2010 infection. While an increase in immune cell numbers was partially responsible for the enhanced splenomegaly observed in AhR-deficient mice, the main reason for the splenomegaly appears to be an increase in immature RBC numbers, 2 weeks post infection. Moreover, AhR-deficient mice most likely have a defect in the RBC maturation process after TAS2010 infection. Furthermore, histological analysis of infected spleens from AhR-deficient mice demonstrated disruptions in the splenic architecture in the WP region, as indicated by smaller B follicles and loss of T cell zones. In addition, splenic T cells and myeloid cells of infected AhR-deficient mice were hyperactivated, based on increased CD69 expression as well as enhanced frequencies of IFNγ producing T cells compared to WT mice.

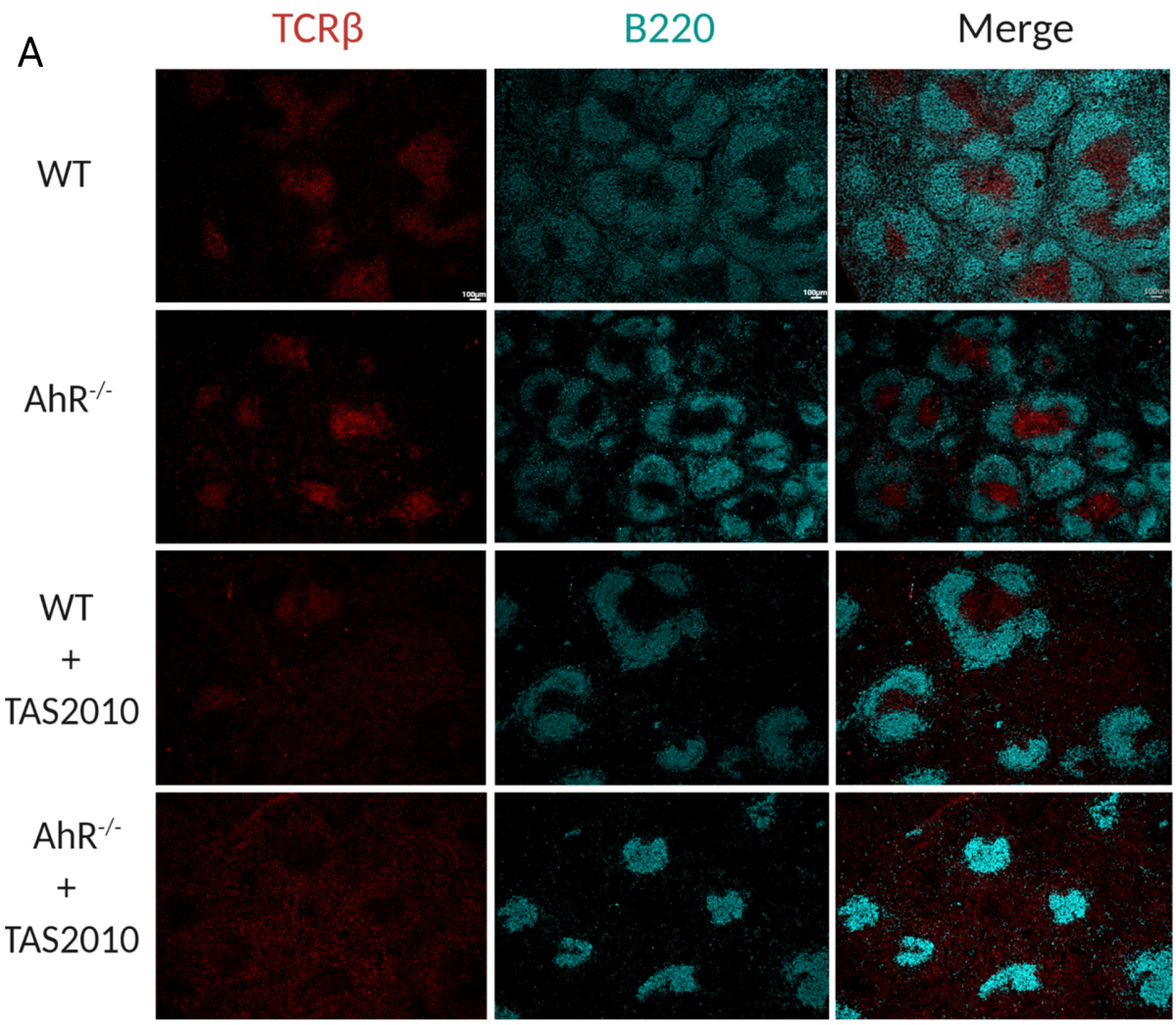


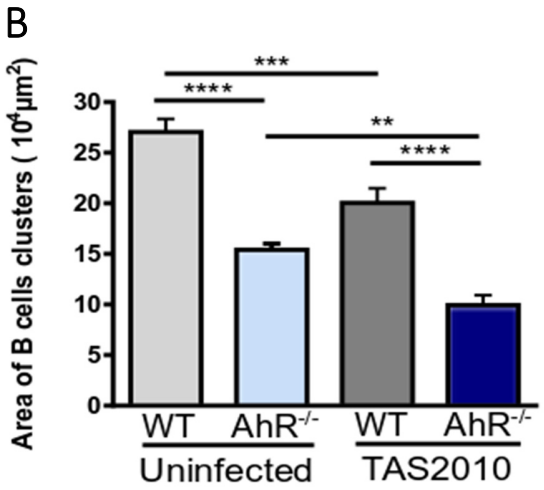


**Figure 5-18: IF analysis of the splenic WP region in WT and AhR-deficient mice**
Spleens were collected from TAS2010 infected WT and AhR-deficient mice, PLP fixed and cryo-embedded. Representative spleen sections were stained for TCRβ for T cells (left column) and, B220 for B cells (middle column). The merge images are shown in the right column (A*)*. Magnification :4x Scale bar: 100µm
Statistical analysis of the area covered by B cell clusters is depicted in (B) (n=3-4 mice, 3-5 images were taken from each animal and 35-80 clusters /genotype were measured). Results are shown as mean +/– SEM and significance was determined by one-way ANOVA corrected for multiple comparisons by the Bonferroni's method (****p<0.0001, *** p<0.001, ** p<0.01, *p<0.05)

## 5.4 Long-term infection of AhR-deficient mice with TAS2010

A strong decrease in bacterial counts can already be observed around 4 to 5 weeks post *S.* Typhimurium infection (Kupz et al., 2014). To test whether AhR-deficient mice can clear the bacteria at all, we performed another experiment for the duration of 5 weeks. Interestingly, 80% of the AhR-deficient mice survived TAS2010 infection up to 4 weeks, but the survival rate decreased to only 20 % by the end of the fifth week of infection. This clearly shows that AhR-deficient mice were highly susceptible to TAS2010 infection compared to WT mice (**Figure 5-19**).

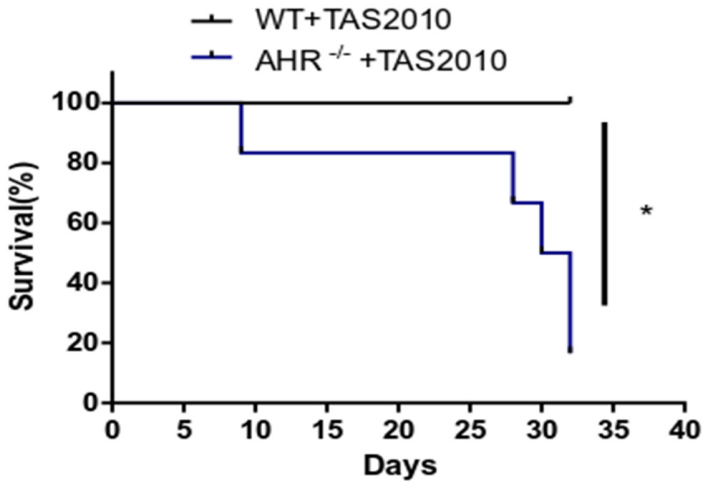


**Figure 5-19: AhR-deficient mice succumb to TAS2010, 5 weeks post infection**
WT and AhR-deficient mice were infected with TAS2010 and the survival curves were analyzed. Mice were sacrificed upon reaching high a stress level (n=4-6mice). Significant differences are depicted as *p<0.05. Significance was calculated using Log-rank (Mantel-cox) test

In line with the literature, determination of the bacterial counts in systemic organs 5 weeks post infection revealed that WT animals are in the process of clearing the infection at this time, harboring around 100 CFU or less in spleen and liver. In contrast, TAS2010 persisted in both organs in AhR-deficient mice, showing similarly high counts as seen 2 weeks post infection **(Figure 5-20 A, B)**. Moreover, AhR-deficient mice still had significantly higher serum IFNγ levels **(Figure 5-20 C)**. Furthermore, enhanced splenomegaly in AhR-deficient mice relative to WT mice was preserved **(Figure 5-20 D)**. Furthermore, TAS2010 infected AhR-deficient mice still had slightly smaller livers than infected WT mice **(Figure 5-20 E)**.

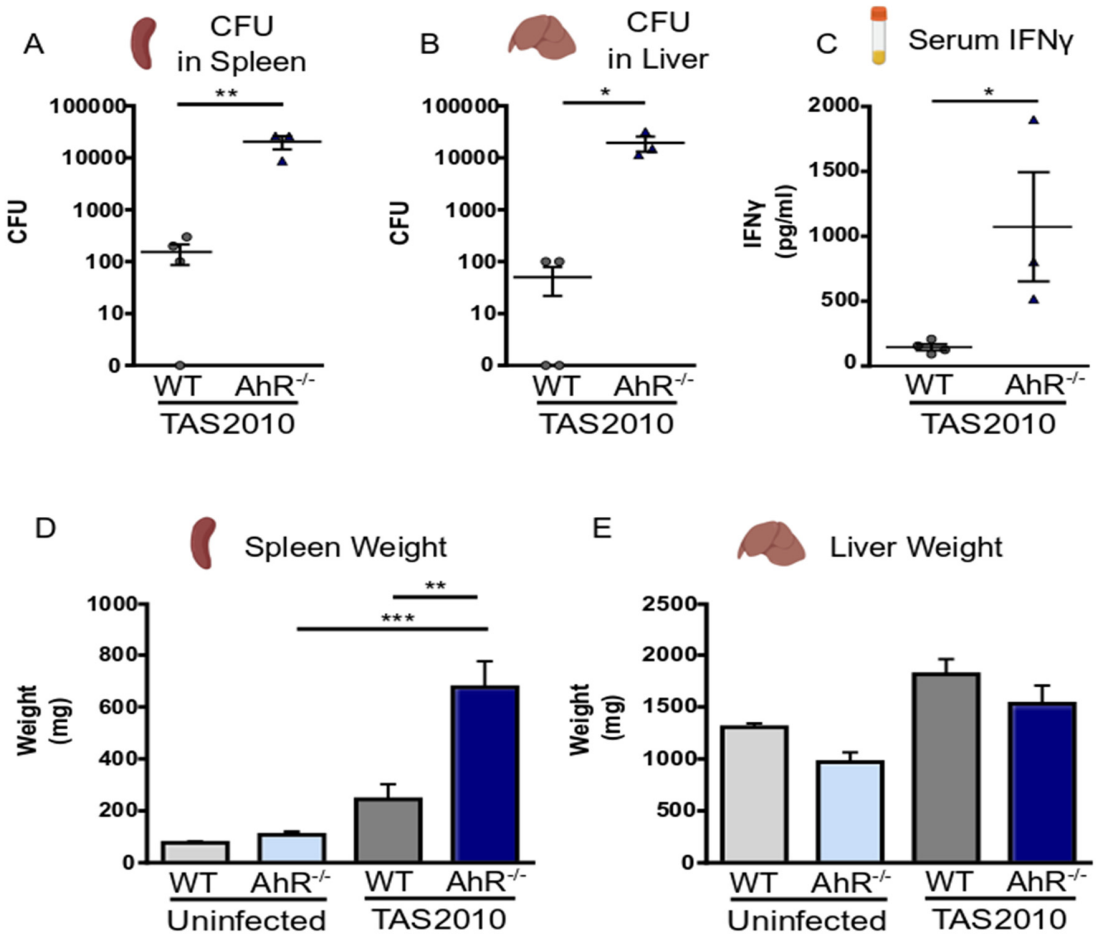


**Figure 5-20: AhR-deficient mice show persistent bacterial growth in systemic organs accompanied by high serum IFNγ and enhanced splenomegaly 5 weeks post infection**
WT and AhR-deficient mice were infected with TAS2010 and analyzed 5 weeks post infection for bacterial load (CFU) in spleen (A) and liver (B) as well as serum IFNγ levels (C). Spleen (D) and liver (E) weights were assessed. (n=3-4 mice). Results are shown as mean +/– SEM and significance was determined by unpaired students t-test (A-C) or by one-way ANOVA corrected for multiple comparisons by the Bonferroni's method (D-E) (****p<0.0001, *** p<0.001, ** p<0.01, *p<0.05).

### 5.4.1 Analysis of the presence of immune cells and RBCs in the spleen 5 weeks post infection

Since the enhanced splenomegaly was still apparent in AhR-deficient mice relative to WT mice upon infection, we again analyzed the cell types contributing to this persistent phenotype. As described above, all live splenic cells counted, and increased spleen cell numbers were observed in both genotypes upon TAS2010 infection. In comparison to 2 weeks post infection, WT and AhR-deficient mice showed slightly lower cell counts 5 weeks post infection, however, AhR-

deficient mice still exhibited increased cell counts relative to WT mice **(Figure 5-21, Figure 5-12)**.

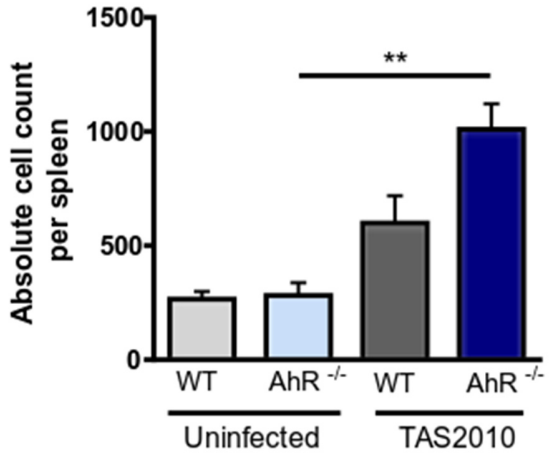


**Figure 5-21: Persistently enhanced splenomegaly in AhR-deficient mice 5 weeks post infection correlates with a preserved increase in splenic cell counts**
WT and AhR-deficient mice were infected with TAS2010 and spleens were collected 5 weeks post infection. Spleen cells were counted using a Neubauer chamber. (n=3-4 mice). Results are shown as mean +/– SEM and significance was determined by one-way ANOVA corrected for multiple comparisons by the Bonferroni's method (****p<0.0001, *** p<0.001, ** p<0.01, *p<0.05)

Further analysis of immune cell populations showed no major difference in the frequency of $CD11b^{+}F4/80^{+}$ macrophages between WT and AhR-deficient mice 5 weeks post infection. The frequency of $B220^{+}$ B cells was still lower after TAS2010 infection. The frequency of $CD8^{+}$ T cells was similar in WT and AhR-deficient mice after TAS2010 infection at both infection times while the frequency of $CD4^{+}$ T cells in AhR-deficient mice 5 weeks post infection was moderately decreased compared to WT **(Figure 5-22 A, Figure 5-13 A)**. Moreover, AhR-deficient mice had increased total $CD11b^{+}F4/80^{+}$ macrophages cell numbers 5 weeks post infection compared to WT mice. Different from the 2 week time point, AhR-deficient mice had similar $B220^{+}$ B cell numbers and only slightly increased $CD4^{+}$ and $CD8^{+}$ T cell numbers compared to WT mice **(Figure 5-22 B, Figure 5-13 B)**. This suggests that, increased immune cell numbers contributed to the increased spleen cellularity observed in AhR-deficient mice 2 weeks post infection, this did not seem to be the case 5 weeks post infection.

Next, the composition of RBCs was analyzed. The frequency of immature $Ter119^{med}CD71^{hi}$ and $Ter119^{hi}CD71^{hi}$ RBCs in WT mice at 5 weeks were lower than 2 weeks post infection, nearly reaching the levels of the naïve state. In contrast, AhR-deficient mice possessed a similar frequency of $Ter119^{med}CD71^{hi}$ and $Ter119^{hi}CD71^{hi}$ RBCs compared to 2 weeks post infection. Although

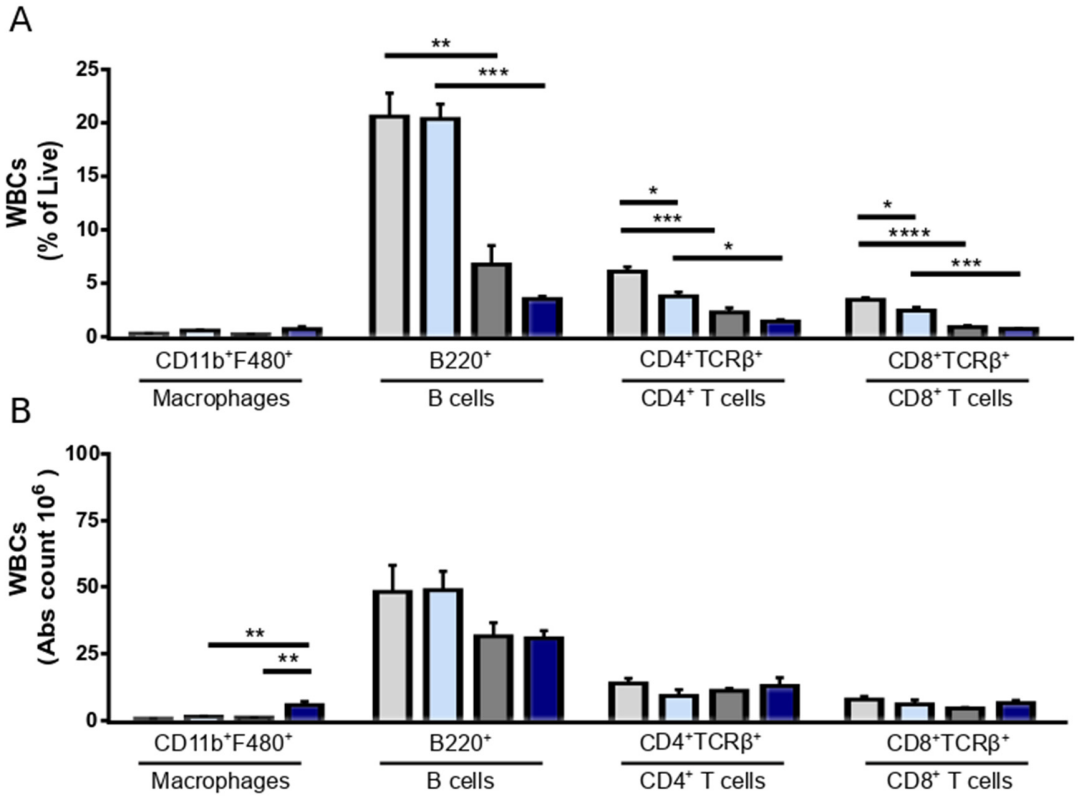


**Figure 5-22 : Analysis of immune cell populations in the spleen of WT and AhR-deficient mice 5 weeks post infection**
WT and AhR-deficient mice were infected with TAS2010 and spleens were collected 5 weeks post infection for immune cell analysis. Frequencies of $CD11b^{+}F480^{+}$ macrophages, $B220^{+}$ B cells, $CD4^{+}$ and $CD8^{+}$T cells are depicted (A). The absolute numbers of indicated immune cell subsets were shown (B). (n=3-4 mice). Results are shown as mean +/– SEM and significance was determined by one-way ANOVA corrected for multiple comparisons by the Bonferroni's method (****p<0.0001, *** p<0.001, ** p<0.01, *p<0.05)

AhR-deficient mice displayed lower immature cell numbers at 5 weeks compared to 2 weeks post infection, these populations were still significantly higher compared to WT mice **(Figure 5-23 A, Figure 5-14 B)**. Interestingly, the ratio of $Ter119^{hi}CD71^{low}$ to $Ter119^{hi}CD71^{med}$ population was 12 in WT mice at 5 weeks **(Figure 5-23 C, Figure 5-14 D)** compared to 4 at 2 weeks post infection, suggesting that the RBC maturation processes was slowly returning to the normal state. In contrast, the ratio of $Ter119^{hi}CD71^{low}$ to $Ter119^{hi}CD71^{med}$ RBC was only 2 in AhR-deficient mice 5 weeks post infection, suggesting that RBC maturation in these was still strongly impaired **(Figure 5-23 C, Figure 5-14 D)**. Taken together, these data showed that the persistently, enhanced splenomegaly and increased cellularity observed after 5 weeks of infection in AhR-deficient mice

correlates with an increased proportion of immature RBCs and ongoing impairment of RBC maturation.

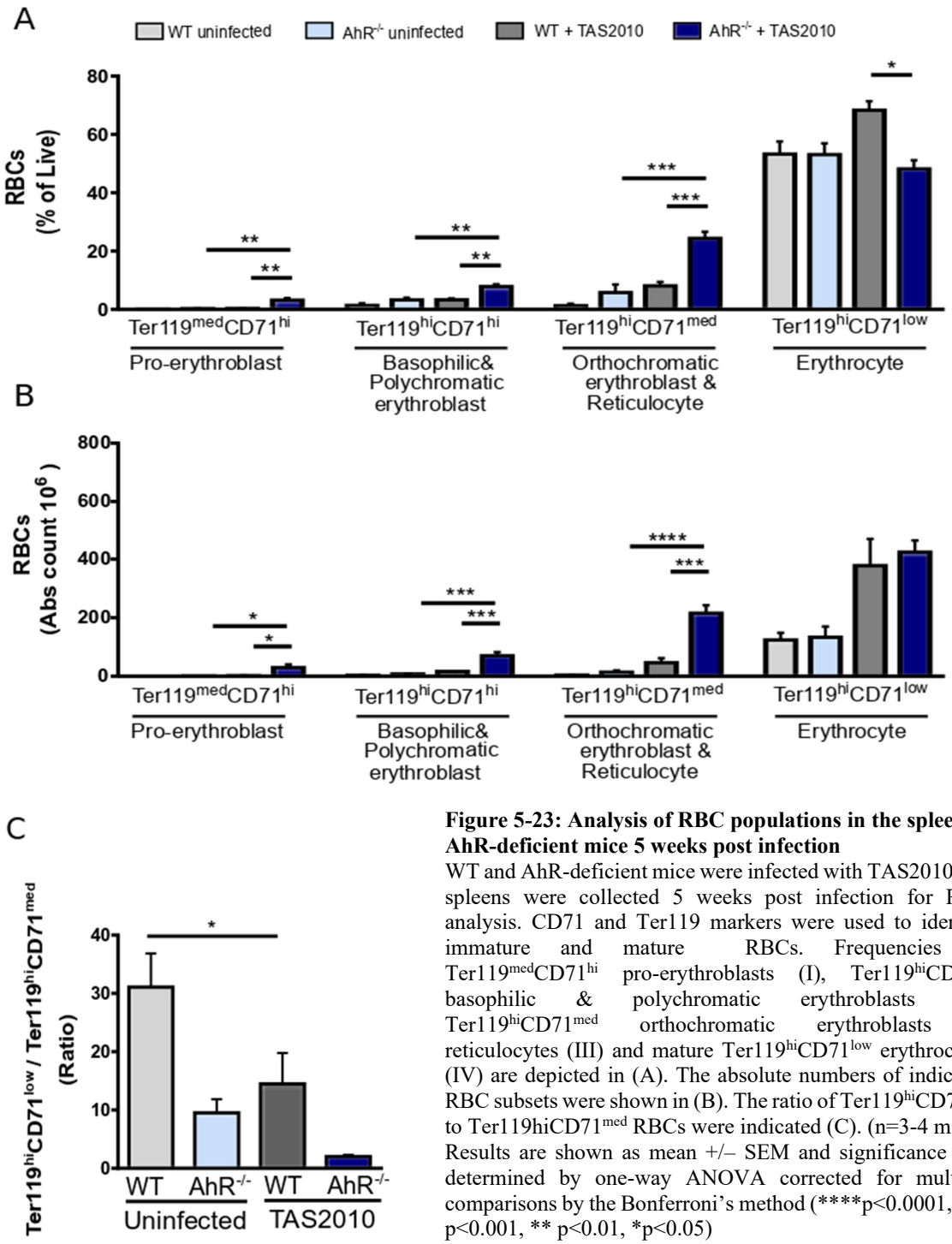


**Figure 5-23: Analysis of RBC populations in the spleen of AhR-deficient mice 5 weeks post infection**
WT and AhR-deficient mice were infected with TAS2010 and spleens were collected 5 weeks post infection for RBC analysis. CD71 and Ter119 markers were used to identify immature and mature RBCs. Frequencies of $Ter119^{med}CD71^{hi}$ pro-erythroblasts (I), $Ter119^{hi}CD71^{hi}$ basophilic & polychromatic erythroblasts (II), $Ter119^{hi}CD71^{med}$ orthochromatic erythroblasts & reticulocytes (III) and mature $Ter119^{hi}CD71^{low}$ erythrocytes (IV) are depicted in (A). The absolute numbers of indicated RBC subsets were shown in (B). The ratio of $Ter119^{hi}CD71^{low}$ to Ter119hiCD71$^{med}$ RBCs were indicated (C). (n=3-4 mice). Results are shown as mean +/– SEM and significance was determined by one-way ANOVA corrected for multiple comparisons by the Bonferroni's method (****p<0.0001, *** p<0.001, ** p<0.01, *p<0.05)

### 5.4.2 Long-term infection of AhR-deficient mice with TAS2010 leads to a further increase in the frequency of IFNγ$^+$ CD4$^+$ T cells as well as CD69$^+$ T cells and myeloid cells

To examine the activation status of T and myeloid cells 5 weeks post infection, the expression of CD69 and the presence of IFNγ-producing T cells were evaluated. WT mice exhibited 18% CD69$^+$CD4$^+$ T cells, 8% CD69$^+$CD8$^+$ T cells and 4% CD69$^+$ CD11b$^+$ myeloid cells, which was similar to the values obtained at 2 weeks post infection. Remarkably, AhR-deficient mice possessed 40% CD69$^+$ CD4$^+$ T cells, 26 % CD69$^+$ CD8$^+$ T cells and 15 % CD69$^+$CD11b$^+$ myeloid cells, which was significantly higher compared to WT mice. Moreover, the frequency of these cells was also elevated relative to 2 weeks post infection **(Figure 5-24 A, B, C, Figure 5-16 B, C, D)**. This suggests that while CD69 expression was rather stable in TAS2010 infected WT mice, AhR-deficient mice increased CD69 expression in T cells and myeloid cells over the course of infection.

Furthermore, AhR-deficient mice displayed a significant increase in the frequency of IFNγ$^+$ CD4$^+$T cells compared to WT mice 5 weeks post infection. In addition, the frequency of IFNγ$^+$ CD4$^+$T cells was also higher compared to 2 weeks post infection (**Figure 5-24 D, Figure 5-15 B**). On the other hand, the frequency of IFNγ$^+$ CD8$^+$T cells was more stable, with about 30% IFNγ$^+$ CD8$^+$ T cells at both time points after infection. Also, WT and AhR-deficient mice displayed similar frequencies of IFNγ$^+$ CD8$^+$T cells 5 weeks post infection (**Figure 5-24 E, Figure 5-15 C**). These data indicate that the regulation of CD69 expression in myeloid cells and T cells, and IFNγ expression in T cells after TAS2010 infection is probably AhR-dependent. In addition, excessive activation of these cells as well as increased production of IFNγ in T cells might contribute to the overall enhanced infection-related pathology in AhR-deficient mice.

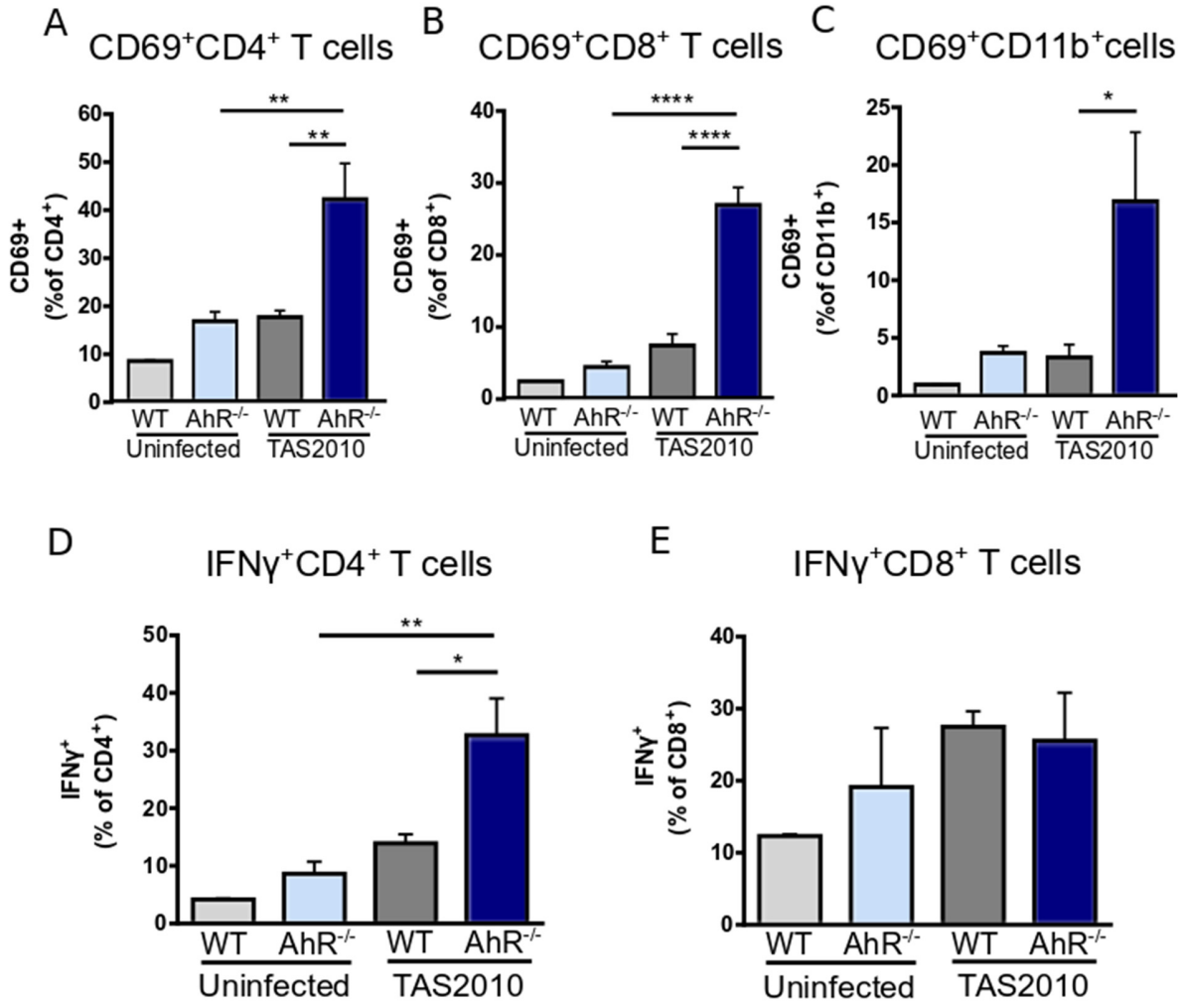


**Figure 5-24: Analysis of CD69 and IFNγ expressing immune cells in AhR-deficient mice 5 weeks post infection**

WT and AhR-deficient mice were infected with TAS2010 and spleens were collected 5 weeks post infection. The frequency of $CD69^+$ $CD4^+$ T cells (A), $CD69^+$ $CD8^+$ T cells (B) $CD69^+$ $CD11b^+$cells (C) as well as $IFN\gamma^+$ $CD4^+$ T cells (D) and $IFN\gamma^+$ $CD8^+$ T cells (E) were depicted. (n=3-4 mice). Results are shown as mean +/– SEM and significance was determined by one-way ANOVA corrected for multiple comparisons by the Bonferroni's method (****p<0.0001, *** p<0.001, ** p<0.01, *p<0.05)

### 5.4.3 AhR-deficient mice show a further decrease in B cell follicle size and sustained T cell delocalization 5 weeks post infection

We were also interested in the alterations of the WP architecture in AhR-deficient mice 5 weeks post infection. In WT mice, the B cell follicles were nearly in similar size when comparing 2 weeks and 5 weeks post infection, with a marked reduction compared to the naive state **(Figure 5-25 A- middle column, B Figure 5-18 A- middle column, B)**. Like 2 weeks post infection, some intact T cell zones were visible in WT mice. In contrast, there were no visible T cell zones and T cells were dislocated to the RP in AhR-deficient mice 5 weeks post infection and this phenotype was even more pronounced compared to the 2 weeks time point **(Figure 5-25 A-left column, B, Figure 5-18 A-left column, B)**. These findings demonstrate that while WT mice can maintain a partially intact WP structure as the infection progresses, the WP structure continues to deteriorate in AhR-deficient mice.

To summarize, we observed that most AhR-deficient mice could not survive the infection for more than 5 weeks, displaying continuously high serum IFNγ levels. WT mice were in the process of clearing the infection, since they had only few bacteria in spleen and liver, different from AhR-deficient mice, which had persistently high TAS2010 CFU in these organs. The constantly elevated frequency of immature RBC populations in AhR-deficient mice appeared to be contributing to the persevered splenomegaly 5 weeks post infection. Furthermore, the splenic architecture was even more altered at 5 weeks compared to 2 weeks post infection, since AhR-deficient mice displayed even smaller B cell follicles and continuous dislocation of T cells. Finally, T cells and myeloid cells displayed an increased activation state over the course of infection as indicated by expression of CD69 and increased proportions of IFNγ-expressing CD4+ T cells. Overall, these data showed that the processes involved in extramedullary erythropoiesis as well as immunoregulation seem to be strongly altered and thus contribute to the increased susceptibility of AhR-deficient mice to TAS2010 infection relative to WT mice.

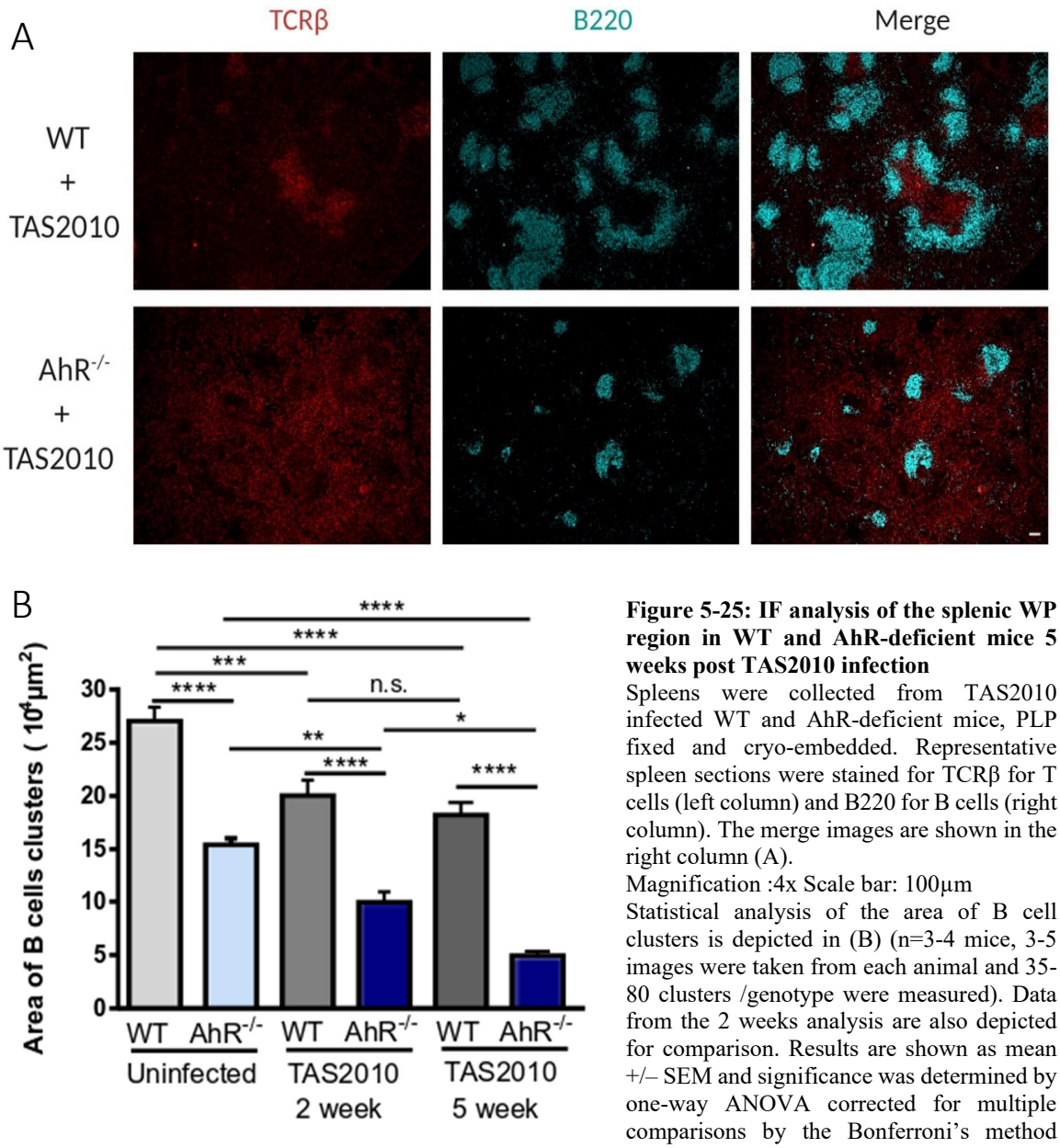


**Figure 5-25: IF analysis of the splenic WP region in WT and AhR-deficient mice 5 weeks post TAS2010 infection**

Spleens were collected from TAS2010 infected WT and AhR-deficient mice, PLP fixed and cryo-embedded. Representative spleen sections were stained for TCRβ for T cells (left column) and B220 for B cells (right column). The merge images are shown in the right column (A).

Magnification :4x Scale bar: 100µm

Statistical analysis of the area of B cell clusters is depicted in (B) (n=3-4 mice, 3-5 images were taken from each animal and 35-80 clusters /genotype were measured). Data from the 2 weeks analysis are also depicted for comparison. Results are shown as mean +/– SEM and significance was determined by one-way ANOVA corrected for multiple comparisons by the Bonferroni's method (****p<0.0001, *** p<0.001, ** p<0.01, *p<0.05)

## 5.5 Increase in immature RBCs and defects in RBC maturation in AhR-deficient mice might be due to dysregulated expression of EPO and IL-6

We showed that AhR-deficient mice had increased immature RBC numbers and a possible defect in the last erythrocyte maturation step identified by a decrease in the $Ter119^{hi}CD71^{low}$ to $Ter119^{hi}CD71^{med}$ ratio relative to WT mice after 2 and 5 weeks TAS2010 infection. We speculated that possible changes in the concentration of erythroid lineage markers could lead to this phenotype. Using Biolegend's LEGENDPLEX$^{TM}$ bead-based immunoassay, we quantified soluble TPO, IL-6, SCF, EPO and CXCL2 in serum samples using FACS. These factors contribute to different stages in the RBC maturation process, either directly or indirectly. TPO was present at similar levels in WT and AhR-deficient mice in the naïve state. At 2 weeks post infection, both genotypes slightly increased TPO levels in serum, whereas AhR-deficient mice had higher TPO levels compared to WT mice 5 weeks post infection **(Figure 5-26 A)**. In the naïve state, AhR-deficient mice had slightly lower CXCL2 levels in the serum. Although both genotypes had higher CXCL12 levels at 2 weeks compared to 5 weeks post infection, these changes were similar in WT and AhR-deficient mice **(Figure 5-26 B)**. SCF could be detected at similar levels in WT and AhR-deficient mice in the naïve state and after TAS2010 infection **(Figure 5-26 C)**. We further found that WT and AhR-deficient mice have very low concentrations of serum IL-6 in the naïve state but show a strong increase in IL-6 after infection. Interestingly, AhR-deficient mice showed nearly 3-fold increase in IL-6 levels compared to WT mice 2 weeks post infection. This increase was even more apparent 5 weeks post infection with almost 25-fold difference **(Figure 5-26 D)**. EPO, which is one of the main contributors to RBC maturation and survival was also detected in similar levels in WT and AhR-deficient mice in naïve state. Remarkably, AhR-deficient mice showed a 4-fold and nearly a 100-fold increase in serum EPO levels compared to WT mice at 2 and 5 week post infection, respectively **(Figure 5-26 E)**. These data suggest that the AhR may be involved in the regulation of EPO and IL-6 expression, leading to an increase in extramedullary erythropoiesis as well as an RBC maturation defect in AhR-deficient mice upon TAS2010 infection relative to WT mice.

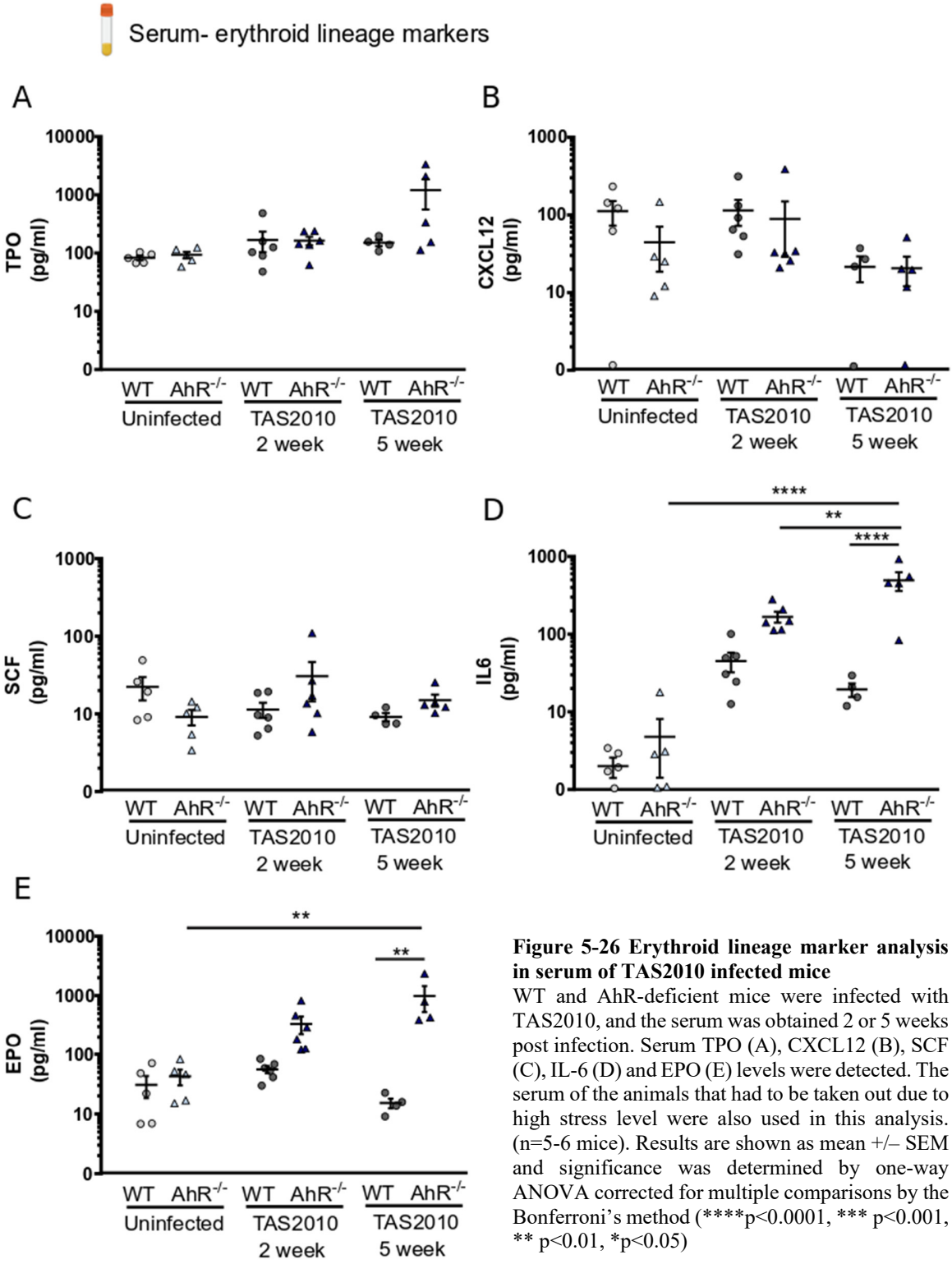


**Figure 5-26 Erythroid lineage marker analysis in serum of TAS2010 infected mice**
WT and AhR-deficient mice were infected with TAS2010, and the serum was obtained 2 or 5 weeks post infection. Serum TPO (A), CXCL12 (B), SCF (C), IL-6 (D) and EPO (E) levels were detected. The serum of the animals that had to be taken out due to high stress level were also used in this analysis. (n=5-6 mice). Results are shown as mean +/– SEM and significance was determined by one-way ANOVA corrected for multiple comparisons by the Bonferroni's method (****p<0.0001, *** p<0.001, ** p<0.01, *p<0.05)

## 5.6 Influence of the AhRR and hypoxia on *in vitro* T helper cell differentiation

Using a DSS colitis model, our group showed that AhRR-deficient mice had an enhanced Th17 and reduced Th1 cell frequency relative to WT mice. To assess whether these differences were due to T cell intrinsic actions, splenic naïve T cells were isolated and differentiated *in vitro* into Th1, Th2, Th17, Th22 and Treg cells under normoxic conditions (21% $O_2$). These data showed no significant differences in cytokine and TF expression profiles of WT and AhRR-deficient cells under normoxic conditions (Brandstätter et al., 2016). However, physiologically, the intestine is adapted to hypoxic (≤1% $O_2$) environment. Under hypoxia, some T cell subsets are enhanced due to increased expression of the hypoxia sensing transcription factor subunit, HIF-1α. HIF-1α directly interacts with RORγt and enhances Th17 cell development. In addition, HIF-1α binds to FOXP3, targeting it for degradation and thus decreasing Treg development (Dang et al., 2011). Since HIF1-*β* (ARNT) is necessary for AhR and HIF signaling, it is likely that these signaling pathways interfere (Chan et al., 1999). In light of these findings, we speculated, whether the differentiation of AhRR-deficient naïve T cells into T helper subsets would be altered when the cells were cultured in hypoxic conditions. To explore this, splenic naïve T cells of WT and AhRR-deficient mice were differentiated into Th1, Th17 and Treg cells under hypoxic conditions and cytokine & TF expression profiles were determined by ELISA and FACS analysis.

Previously, splenic naïve $CD4^+$T cells from WT and AhRR-deficient mice were isolated by magnetic separation and further purified by FACS sorting. The cells were differentiated into different subsets, using combinations of different cytokines and antibodies (listed in **Table 4-3**) for 5 days, then the cells were analyzed by FACS, and supernatants were used for detection of cytokine release by ELISA. For unknown reasons, however, we observed a relatively high cell death upon FACS sorting (data not shown). In addition, the remaining cells also did not survive culturing for 5 days in all the conditions used (data not shown). Therefore, we changed the protocol, replacing the FACS sorting by the Mojosort$^{TM}$ mouse CD4 naïve T cell isolation kit for isolating splenic naïve T cells (described in the Materials and Methods section). In addition, the cells were differentiated for 4 days instead of 5 days in culture, which improved the cell viability.

We first tested the purity of untouched $CD4^+$ naïve T cells after using the MojosortTM mouse CD4 naïve T cell isolation kit (protocol described in methods section) by FACS analysis. For this, a small aliquot of isolated cells was stained for CD3, CD4, CD8, CD44, CD62L and CD25. Naïve $CD4^+$ T cells are described as $CD3^+CD4^+CD8^-CD44^{lo}CD62L^{hi}CD25^-$ T cells. Using this assay the purity of the isolated naïve T helper cells was found to be around 91% with a viability of 85 % **(Figure 5-27)**.

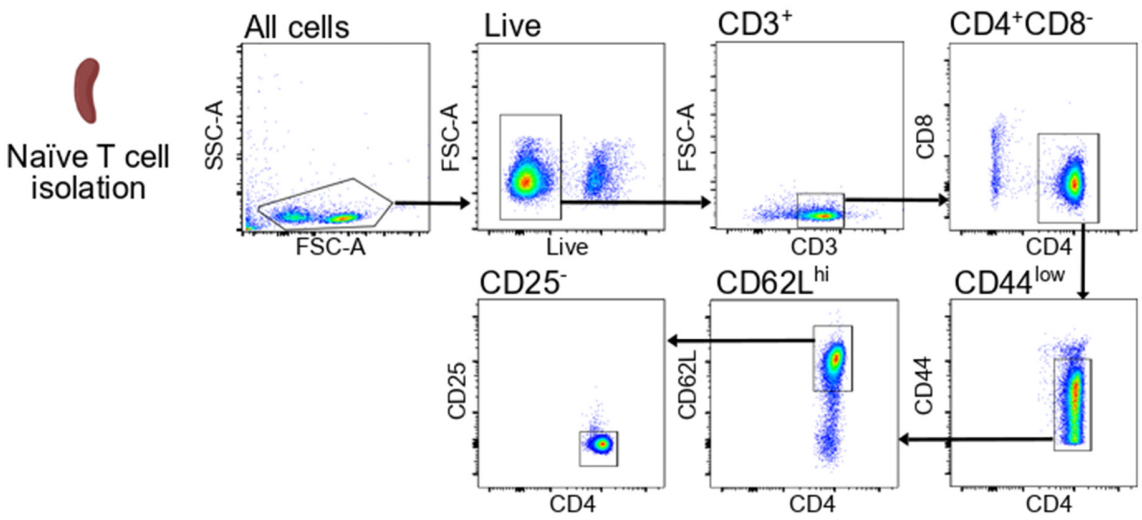


**Figure 5-27: The gating strategy for purity check of Mojosort™ mouse $CD4^+$ naïve T cell isolation kit**
The splenic cells were isolated from WT mice and $CD4^+$ naïve T cells were purified using Mojosort™ mouse $CD4^+$ naïve T cell isolation kit. The splenic naïve T cells were identified as $CD3^+CD4^+CD8^-CD44^{lo}CD62L^{hi}CD25^-$ T cells.

We next assessed the background cytokine production in undifferentiated (Th0) cells. The splenic naïve T helper cells of WT and AhRR-deficient mice were cultured with anti-IFNγ and anti-IL-4 antibodies for 4 days under normoxic or hypoxic conditions to block spontaneous Th1 and Th2 differentiation. Afterwards, the Th0 subset was analyzed for key cytokines and FOXP3. Th1 cells express IFNγ, Th17 cells express IL-17 as signature cytokines, and Tregs express FOXP3 as key TF. Th0 cells were stimulated with PMA, ionomycin and brefeldin A for 4 hours, and then IFNγ, and IL-17 expression was analyzed by FACS. In addition, unstimulated Th0 cells were used for detecting FOXP3 expression. The gating strategy is depicted in **Figure 5-28 A**. WT cells developed only 4 % and 2 % Th1 cells under normoxia and hypoxia, respectively, under Th0

culture conditions. In comparison, AhRR-deficient cells cultivated under Th0 culture conditions displayed around 5% Th1 cells in normoxia and hypoxia. Irrespective of the genotype, around 2 % Th17 cells developed under these conditions.

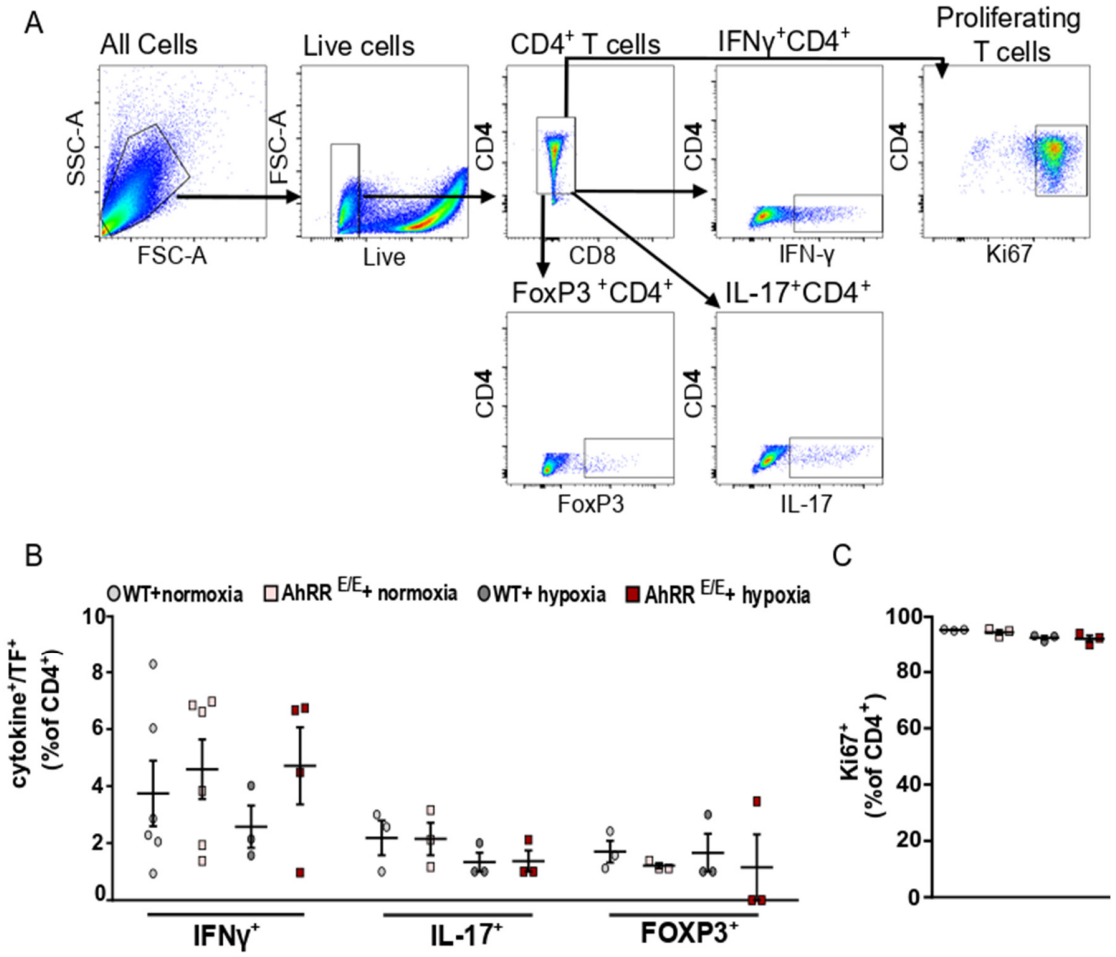


**Figure 5-28: Background frequency of cytokine- or FOXP3- expressing cells of Th0 culture conditions**
Splenic naïve T cells isolated from WT and AhRR-deficient mice were cultured under normoxic (21% $O_2$) or hypoxic conditions (1% $O_2$) with anti-IFNγ and anti-IL-4 for 4 days and later stimulated with PMA, ionomycin and brefeldin A for 4 hours. The cells were analyzed by intracellular cytokine/FOXP3 staining and FACS. The cells cultured under Th0 conditions were gated for IFNγ$^+$ CD4$^+$ (Th1), IL-17$^+$CD4$^+$ (Th17), FOXP3$^+$CD4$^+$ (Treg) and Ki67$^+$CD4$^+$ (A). Background frequencies of the indicated subsets were determined (B). The proliferative capacity of CD4$^+$ T cells under Th0 culture conditions was analyzed by Ki67 staining (C). (n=3-6 mice). Results are shown as mean +/– SEM and significance was determined by one-way ANOVA corrected for multiple comparisons by the Bonferroni's method. No significant difference between the different groups could be detected in this experiment.

The background frequencies of Th17 cells cultured under hypoxic conditions were like normoxia (1%). Only 1-2 % Treg developed under normoxic and hypoxic conditions **(Figure 5-28 B).** These data implied the existence of a weak Th1 differentiation under control conditions, whereas the observed Th17 and Treg background differentiation levels were negligible. Furthermore, the analysis of the proliferative capacity of the cells by Ki67 staining showed that these cells were highly proliferating, independent of oxygen levels and genotypes **(Figure 5-28 C)**. Aside from the FACS analysis, supernatants of the Th0 cultures were collected and analyzed for released IFNγ, IL-17 and TGFβ by ELISA. Similar to intracellular cytokine analysis, a slight background of IFNγ production, especially for AhRR-deficient cells was observed. However, the background was negligible for IL-17 and TGFβ release **(Figure 5-29)**.

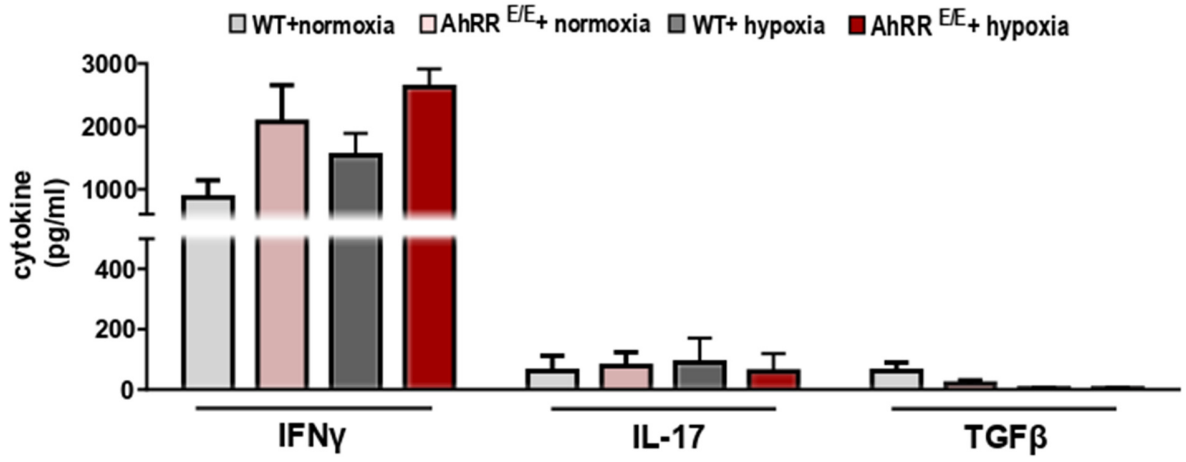


**Figure 5-29 : Background cytokine release by the cells from Th0 culture conditions**
IFNγ, IL-17 and TGFβ release from Th0 cultures of WT and AhRR-deficient mice generated under normoxic and hypoxic conditions were measured in the supernatants. Data were pooled from three independent experiments (n=3-6 mice). Results are shown as mean +/– SEM and significance was determined by one-way ANOVA corrected for multiple comparisons by the Bonferroni's method. No significant difference between the different groups could be detected in this experiment.

### 5.6.1 AhRR expression and hypoxia have only a minor influence on *in vitro* differentiation of Th1 and Th17 cells

We next assessed the influence of hypoxia and AhRR expression on the *in vitro* differentiation of different T helper cell populations. Splenic naïve $CD4^+$ T cells from WT and AhRR-deficient mice were isolated as described above. For Th1 differentiation, naïve T cells were exposed to IL-12 and

the development of Th2 cells was blocked by addition of anti-IL-4 antibody. Th17 culture conditions included IL-6, TGFβ and FICZ, and Treg differentiation was supported by adding TGFβ and retinoic acid to the culture medium. In these cultures, the development of Th1 and Th2 cells were blocked by addition of anti- IFNγ and anti- IL-4 antibodies. IL-2 was added to all subsets from the beginning on to support cell proliferation and differentiation of T helper cell subsets. After 4 days, supernatants were collected for cytokine analysis and the cells were analyzed by intracellular cytokine / TF staining by FACS. The gating strategy for all T helper cell populations is depicted in **Figure 5-30**.

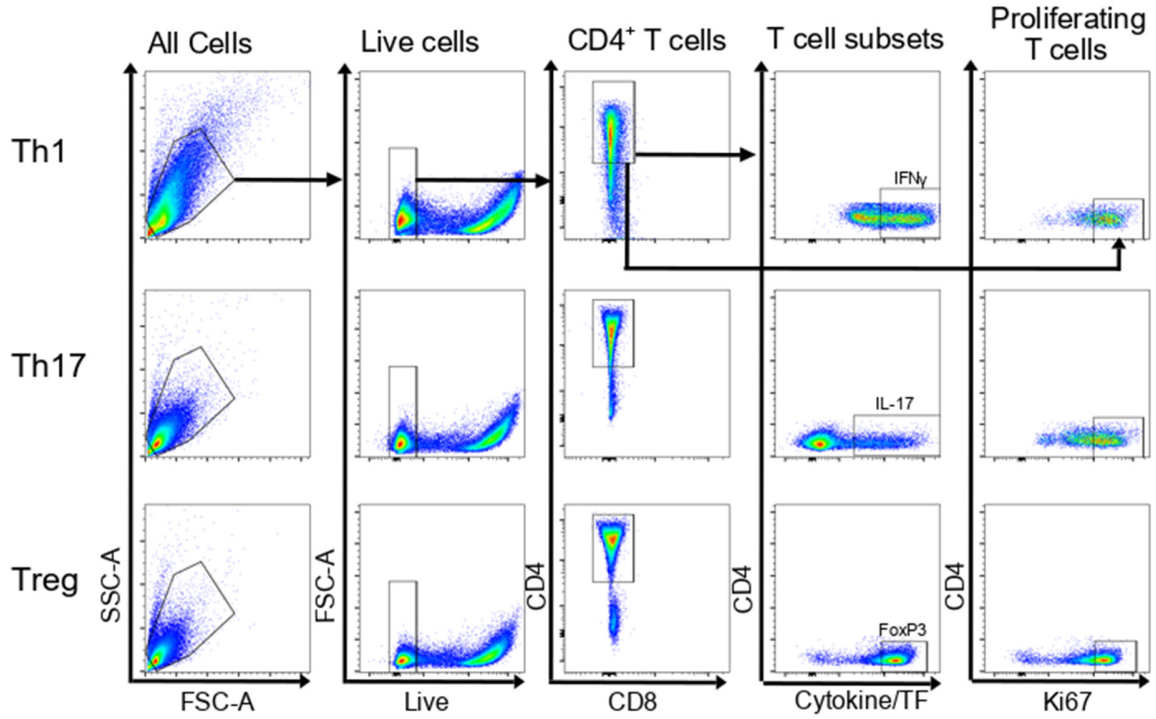


**Figure 5-30: Gating strategy for the different T helper cell subsets**
Splenic naïve $CD4^+$T cells isolated from WT mice were cultured under normoxic (21% $O_2$) or hypoxic conditions (1%$O_2$) in different cytokine/antibody milieus as described above and were stimulated after 4 days with PMA, ionomycin and brefeldin A for 4 hours followed by intracellular cytokine/TF staining and FACS analysis. Th1 cells were identified as $IFN\gamma^+CD4^+$ T cells, Th17 as $IL\text{-}17^+$ $CD4^+$ T cells and Tregs as $FOXP3^+CD4^+$ T cells. The proliferative capacity of Th1, Th17 and Treg cells was determined by Ki67 staining.

Under normoxic conditions, we observed around 60% IFNγ-producing cells in the WT background and approximately 56% in AhRR-deficient cells. Hypoxic conditions only slightly lowered the frequency of IFNγ- producing cells in the WT and AhRR-deficient background to 56% and 52 %,

respectively. In addition, the frequency of FOXP3 expressing cells differentiated under Treg conditions increased comparably in WT and AhRR-deficient cells under normoxic and hypoxic conditions compared to Th0 conditions. The frequency of IL-17 producing cells was slightly but not significantly higher in AhRR-deficient cells compared to WT cells under normoxia. Moreover, hypoxia significantly enhanced the Th17 frequency in both WT and AhRR-deficient cells. However, this increase was lower in AhRR-deficient compared to WT cells **(Figure 5-31 A)**.

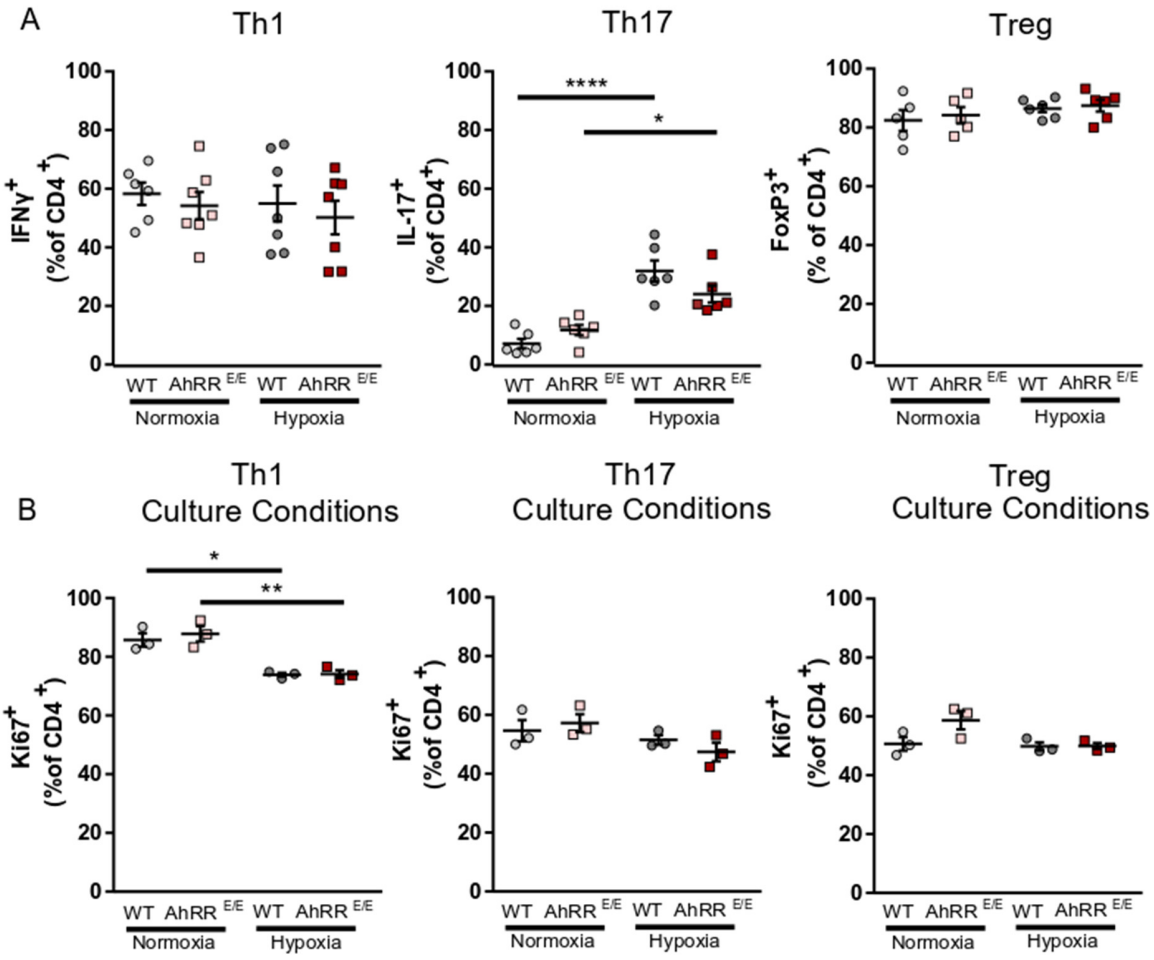


**Figure 5-31: Frequencies of cytokine$^+$ or FOXP3$^+$ CD4$^+$ T cells of the in vitro differentiated T cell subsets**
Using the gating strategy shown in **Figure 5-30**, the frequencies of WT and AhRR-deficient Th1, Th17 and Tregs under normoxic or hypoxic conditions were determined (A). The proliferative capacity was analyzed by Ki67 staining under Th1, Th17 and Treg culture conditions (B). Data describing the frequency of different T cell subsets were pooled from three independent experiments (n=5-7 mice). Data describing the frequency of Ki67$^+$ T cells in all T cell subsets were pooled from 3 mice. Results are shown as mean +/– SEM and significance was determined by one-way ANOVA corrected for multiple comparisons by the Bonferroni's method (****p<0.0001, *** p<0.001, ** p<0.01, *p<0.05)

We also checked the proliferative capacity of all $CD4^+$ T cell subsets. Interestingly, hypoxia significantly decreased the frequency of $Ki67^+$ WT and AhRR-deficient cells under Th1 culture conditions from 85% to 70%, while there was only a slight reduction under Th17 and Treg conditions. AhRR-deficient cells under Th17 culture conditions showed slightly decreased frequency of $Ki67^+$ cells under hypoxia, however this was not significant **(Figure 5-31 B)**.

Next, IFNγ release from Th1-, IL-17 from Th17- and TGFβ from Treg- cultures were analyzed. Hypoxia increased the IFNγ release in WT and AhRR-deficient cells similarly compared to normoxia **(Figure 5-32)**. IL-17 levels showed a similar trend as seen in the FACS analysis of Th17 cells. Under normoxic conditions, AhRR-deficient cells had slightly elevated IL-17 levels compared to WT cells. Whereas IL-17 levels in WT cells clearly increased under hypoxic conditions, AhRR-deficient cells failed to enhance the IL-17 release **(Figure 5-32)**. Furthermore, TGFβ production was slightly increased in hypoxia compared to normoxia, and AhRR-deficient cells showed slightly lower TGFβ levels compared to WT cells independent of the oxygen levels **(Figure 5-32)**. However, none of these differences reached statistical significance.

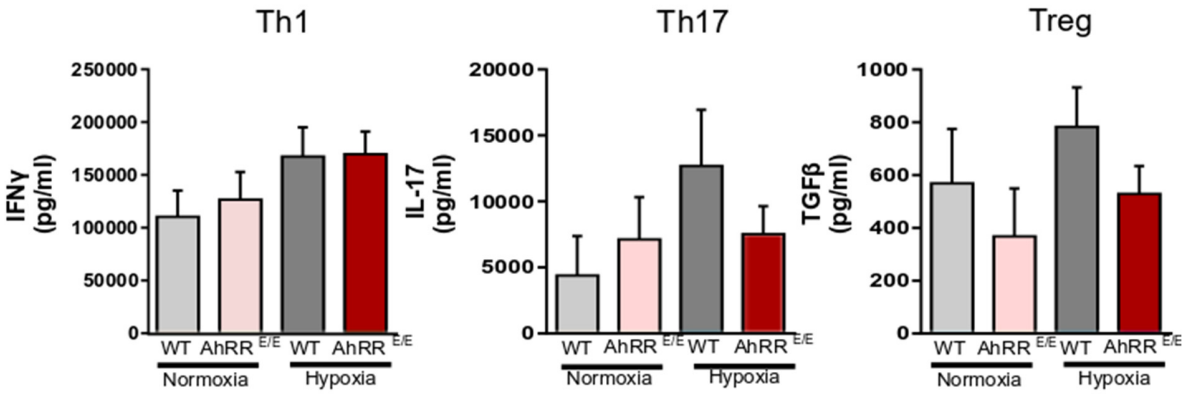


**Figure 5-32: The cytokine production of *in vitro* differentiated T helper cell subsets**
IFNγ release from Th1 cells, IL-17 from Th17 and TGFβ from Tregs cultures were measured in the supernatants of WT and AhRR-deficient cells cultured under normoxic and hypoxic conditions. Data were pooled from three independent experiments (n=3-6 mice). Background from Th0 culture conditions was subtracted. Results are shown as mean +/– SEM and significance was determined by one-way ANOVA corrected for multiple comparisons by the Bonferroni's method. No significant difference between the different groups detected in this experiment.

Together these data showed that hypoxia influences proliferative capacity of Th1 cells and regulates cytokine release from Th1, Th17 and Treg cells. However, the absence of the AhRR does not really favor a specific T helper cell subset under hypoxic conditions.

# 6 Discussion

The AhR is a highly conserved ligand-activated transcription factor that acts as a sensor of polyaromatic chemicals and is involved in the process of detoxification of environmental toxins. Although initially, the AhR was known to mediate toxicity in response to TCDD, this was only one of multiple functions of the AhR (Mandal, 2005). Due to its broad expression in an organism, as well as the identification of endogenous and dietary AhR ligands in addition to exogenous toxins, the AhR is likely also involved in the physiological regulation of gene expression (Esser & Rannug, 2015; Yi et al., 2018). Several studies indicated a role of the AhR in mediating immune responses to infections, microbiota, and nutrients. For instance, the AhR is required for immune responses against *T. gondii* by dampening excess inflammatory responses (Sanchez et al., 2010).

AhR activity is regulated by a negative feedback loop through the AhRR, which is encoded by a direct target gene of the AhR (Mimura et al., 1999). In comparison to the AhR, much less is known about the AhRR. Recently, our group shed light into the expression pattern as well as certain immunoregulatory functions of the AhRR using AhRR/eGFP-reporter and AhRR-deficient mice. Thus, our group was able to show that the AhRR is expressed mainly in immune cells of barrier organs such as skin and intestine (Brandstätter et al., 2016). One might speculate that since *Ahrr* is a target gene of the AhR, its expression correlates with AhR signaling and the two factors act antagonistically in a feedback loop. Our experimental data indicate, however, that the relationship between the AhR and the AhRR is more complex. While the AhR is expressed in a wide range of cell types throughout the body, expression of the AhRR is largely restricted to hematopoietic cells located near environmental borders. In addition, in some conditions the AhR and the AhRR worked in concert to regulate immunity. For example, analysis of a chemical-induced IBD model, DSS colitis, revealed that AhR- and AhRR-deficient mice are both more sensitive to DSS-induced colitis relative to WT mice (Brandstätter et al., 2016).

To further understand the functional roles of the AhR and the AhRR in immunoregulation, in this thesis, a *T. gondii* infection model inducing inflammatory pathology in the intestine was analyzed. Furthermore, an attenuated *S.* Typhimurium strain was used in order to examine the role of the

AhRR and the AhR in bacterial infections. Finally, an *in vitro* model was employed to study the influence of the AhRR and hypoxia on T helper cell differentiation.

## 6.1 AhRR-deficiency differentially regulates T helper cell differentiation depending on the disease context and this is not related to T cell intrinsic mechanisms

Although the DSS-induced colitis model used in our group induces some inflammatory responses in the small intestine, the main site of inflammation is the colon (Perše & Cerar, 2012). Since AhRR expression is stronger in the small intestine compared to the colon, we next addressed the question whether induction of inflammation specifically in the small intestine shows a stronger dependency on AhRR function. Oral infection of mice with *Toxoplasma gondii* triggers damage largely in the distal portion of the small intestine (ileum) (Egan et al., 2012). Moreover, the ileal inflammatory pathology induced by the parasite seems to mimic the pathology observed in human IBD, especially Crohn´s disease(Egan et al., 2012).

Previously, our group showed that AhRR-deficient mice were more susceptible to *T. gondii* infection compared to WT mice. Furthermore, examination of the ileal morphology revealed a stronger pathology which was dependent on AhRR-deficiency (König, 2016). Similarly, AhRR-deficient mice were also more susceptible to DSS-induced colitis, showing enhanced inflammation and tissue damage in the gut (Brandstätter et al., 2016). These two studies indicate that the AhRR function in regulating inflammation and tissue damage is not limited to a specific inflammation model. Furthermore, AhR-deficient mice are also prone to have stronger symptoms than WT mice, including increased intestinal tissue damage with severe inflammation following a *T. gondii* challenge (Wagage et al., 2015). Therefore, like what is known using the DSS-induced colitis model, the AhR and the AhRR act in concert to downregulate intestinal tissue damage upon *T. gondii* infection.

IFNγ is critical for survival of a *T. gondii* infection (Scharton-Kersten et al., 1996). Our study showed that the systemic IFNγ levels of AhRR-deficient mice were comparable to WT mice upon *T. gondii* infection. This is not surprising since AhR-deficient mice also had similar serum IFNγ

levels after a *T. gondii* challenge (Sanchez et al., 2010). However, AhR-deficient mice developed an exaggerated Th1 cell response with increased IFNγ production to the parasitic challenge (Wagage et al., 2015). Excess production of IFNγ by Th1 cells may enhance tissue damage through over-induction of NO and ROS by macrophages (Egan et al., 2012). Therefore, we speculated that Th1 cells might produce more IFNγ in the LP of the small intestine and this might be associated with increased ileal damage observed in AhRR-deficient mice upon *T. gondii* infection. Although Th1 cells are the major source of IFNγ upon *T. gondii* infection, Tc1 cells can also partially contribute to IFNγ induced parasite control (Sturge & Yarovinsky, 2014) and were therefore also included in our analysis. Besides activating macrophages by IFNγ, Tc1 cells do possess cytotoxic functions including the ability to kill infected cells by releasing perforins and granzymes (Khan et al., 2019), which might also contribute to intestinal damage. Our study showed that even though the survival of the mice was dependent on the AhRR, the frequency of Th1 and Tc1 cells in the ileum was only slightly enhanced in AhRR-deficient mice and can only partially explain the increased intestinal damage observed in response to *T. gondii* infection. This was unanticipated but does not rule out the idea that IFNγ may still be responsible for this phenotype, as it is possible that other IFNγ-producing cells contribute to the intestinal damage. Since our *T. gondii* infection experiment lasted only for 6 days, innate immune cells may have a big impact on regulating intestinal inflammation. Therefore it might be interesting to study NK cells, which are also a major source of IFNγ in response to *T. gondii* infection and possess cytotoxic activity (Gigley, 2016). Furthermore, AhR-deficient mice show defects in IL10 expression by NK cells, which correlates with enhanced tissue damage (Wagage et al., 2014). Since IL-10 is one of the key anti-inflammatory cytokines, defects in IL-10 production by NK cells might contribute to the intestinal pathology observed in AhRR-deficient mice after a *T. gondii* challenge.

The decrease in Th1 and Tc1 cells in AhRR-deficient mice in response to DSS-induced colitis (Brandstätter et al., 2016) stands in contrast to our observations using *T. gondii* challenge. In the DSS-induced colitis model, AhRR-deficient mice showed an enhanced Th17 and Tc17 response and hence developed an imbalance regarding the Th1/Th17 and Tc1/Tc17 ratios (Brandstätter et al., 2016). Here, it was proposed that in the absence of the AhRR, AhR ligands present in the gut may further induce Th17 cell differentiation and hence downregulate Th1 differentiation in the

DSS-induced colitis model. It might be possible that *T. gondii* reduces the amount of AhR ligands in the gut by dysregulating microbiota and might therefore favor Th1 differentiation. Furthermore, in an inflammation model which is mainly dependent on IFNγ and Th1 cells, it is also likely that myeloid cell derived cytokines that drive Th1 differentiation are indirectly induced by the absence of the AhRR. Further analysis of Th17 and Tc17 subsets might be needed to see how AhRR-deficiency regulates Th1/Th17 and Tc1/Tc17 ratios upon *T. gondii* infection.

The changes in the Th1/Th17 and Tc1/Tc17 ratios in the DSS-induced colitis model as well as the moderate increases in the Th1 response in the *T. gondii* infection model in AhRR- deficient mice might partially be due to T cell intrinsic alterations. To test this hypothesis, we used an *in vitro* cell culture model and mimicked more physiological conditions of the gut microenvironment by inducing hypoxia. Our data showed that absence of the AhRR only slightly reduced the frequency of Th1 cells in vitro, but the differences we observed between WT and AhRR-deficient mice were not as apparent as seen in the DSS colitis model and did not fit to the *T. gondii* infection model. Furthermore, we observed opposite effects of the AhRR in regulating Th17 differentiation in our *in vitro* model compared to the DSS-colitis model. This suggests that the observed differences in the DSS colitis model and *T. gondii* infection model are not due to T cell intrinsic AhRR effects, even under hypoxic conditions. On the other hand, one must note that naïve $CD4^+$ T cells from the spleen were used in this differentiation protocol. Perhaps, isolation of naïve $CD4^+$ T cells from the ileum would better model these effects. However, it is very difficult to isolate enough naïve $CD4^+$ T cells from the ileum as most of the T cells in the intestinal lamina propria represent effector T cells. Nevertheless, these data support the hypothesis that there might be a local crosstalk between AhRR-dependent myeloid cells and T cells, which may drive Th1 or Th17 differentiation depending on the disease context.

## 6.2 AhRR-deficient mice show a slight increase in ileal damage and enhanced Th1 responses upon *S.* Typhimurium infection

Above, we could show that the AhRR may partially induce protection from excess ileal damage by regulating T cell responses upon *T. gondii* infection. Next, we wanted to study the AhRR function in bacterial infections using *S.* Typhimurium. High IFNγ levels and bacterial numbers

are known to be correlated with disease severity (Kupz et al., 2014). According to our data, the peak of infection was 2 weeks post inoculation whereas Kupz *et al.* identified highest IFNγ levels around 3 weeks post infection in WT mice (Kupz et al., 2014) but similar to the findings reported here the bacterial load was highest around 2 weeks post infection. However, Kupz et.al. used the BRD509 strain in their experiments. These findings suggest that depending on the *S.* Typhimurium strain, the IFNγ response kinetics in the host may vary.

We also showed that the AhRR did not have an influence on systemic bacterial clearance since the bacterial dissemination to spleen and liver was comparable in WT and AhRR-deficient mice.

Disruptions in the villi structure in AhRR-deficient mice which were not observed in WT mice indicate that the AhRR regulates ileal tissue damage upon *S.* Typhimurium infection to some extent, but this was not as vigorous as seen after *T. gondii* infection. Similar to infection with *T.gondii*, IFNγ is also very critical during *S.* Typhimurium infection, since IFNγ-deficient mice succumb to infection at around 4 weeks post inoculation (Kupz et al., 2014). The challenge with *S.* Typhimurium showed similar serum IFNγ levels in WT and AhRR-deficient mice, which is in line with our *T. gondii* experiments. A study by Kupz et al showed that Th1 cell-produced IFNγ is more important for the antibacterial defense than Tc1 cell-produced IFNγ (Kupz et al., 2014). While $CD8^+$T cell-deficient mice cleared the infection similarly to WT mice, mice deficient in both $CD4^+$ and $CD8^+$ T cells displayed significantly higher bacterial loads in the spleen and liver compared to $CD4^+$T cell deficient mice suggesting that in the absence of $CD4^+$ T cells, $CD8^+$ T cells can help to clear the infection (Kupz et al., 2014). Our data showed a clear increase in IFNγ release by Th1 cells and partial increase in IFNγ by Tc1 cells in AhRR-deficient mice relative to WT mice upon *S.* Typhimurium infection. In contrast, the intestinal tissue damage observed in AhRR-deficient mice upon *T. gondii* infection was not accompanied by a local increase in Th1 cells.

Surprisingly, both $CD4^+$ and $CD8^+$ T cells decreased the level of AhRR/eGFP expression upon *S.* Typhimurium infection. In contrast to the *T. gondii* model, Th1 and Tc1 cells, which did not express the AhRR/eGFP reporter at all, were the major IFNγ producing cells. We initially speculated that the AhRR/eGFP expressing cells might die during *S.* Typhimurium infection,

however FACS analysis of dead cells revealed only a minor fraction of AhRR/eGFP$^+$ cells. One possibility might be that dead or apoptotic cells may leak eGFP and hence loose the eGFP fluorescence signal (Steff et al., 2001). Therefore, it would be informative to also look for the presence of the eGFP mRNA in these cells. Since epigenetic modifications play a role in regulating immune responses against pathogens and the *Ahrr* promoter is a target of CpG methylation (Obata et al., 2015; Reynolds et al., 2015), *Ahrr* gene silencing could also occur upon *S.* Typhimurium infection. Hence, it might be interesting to analyze epigenetic modifications of the *Ahrr* gene in T cells upon *S.* Typhimurium infection.

In conclusion, our results using *T. gondii* and *S.* Typhimurium infection models support the notion that AhRR-deficiency differentially regulates T cell responses in the intestine depending on the pathogen. Overall, AhRR-deficient mice appear to be more susceptible to *T. gondii* infection than WT mice, whereas their ability to cope with *S.* Typhimurium infection was rather normal.

## 6.3 High susceptibility of AhR-deficient mice to *S.* Typhimurium infection is a consequence of disruption in spleen structure and function

As the function of the AhR itself during *S.* Typhimurium infection was not really analyzed so far, we used an AhR-deficient mouse model to address this question using the TAS2010 *Salmonella* vaccine strain. The survival analysis revealed that all WT mice but only 20% of AhR-deficient mice survived *S.* Typhimurium infection up to 5 weeks, which clearly indicates that AhR-deficient mice exhibited a very high susceptibility to TAS2010 infection relative to WT mice. Furthermore, AhR-deficient mice also had a higher disease score relative to AhRR-deficient mice 2 weeks post infection. This clearly implied that the AhR but not the AhRR is necessary for the clearance of *S.* Typhimurium infection, was also supported by the high CFU counts in spleen and liver as well as very high serum IFNγ levels in AhR-deficient mice relative to WT and AhRR-deficient mice. It has been shown that the AhR is needed for the clearance of the intracellular bacterium *Listeria monocytogene* by inducing macrophage survival and ROS production (Kimura et al., 2014). Hence similar processes may be affected upon *S.* Typhimurium infection and the absence of the AhR might therefore lead to an increased bacterial load in systemic organs.

In contrast to the AhRR, the AhR is expressed broadly in an organism and the absence of the AhR influences various tissue structures and functions. For instance, naïve AhR-deficient mice have larger spleens with increased cellularity compared to WT mice but also have smaller livers, with a reduction in hepatocyte size (Lahvis et al., 2000; K. P. Singh et al., 2011). In addition, AhR deficiency leads to a developmental defect resulting in defective closure of the Ductus venosus and impaired vascularization of the liver (Walisser et al., 2005). Consistent with the literature, AhR-deficient mice in our colony also possessed slightly larger spleens and smaller livers compared to WT mice. Therefore, we speculated that changes in the spleen and liver function in AhR-deficient mice resulted in a higher susceptibility to *S.* Typhimurium challenge.

Since we observed the biggest morphological differences in the spleen of AhR-deficient mice in response to *S.* Typhimurium infection, we identified the changes in cellular composition of the spleen that were responsible for this phenotype. *S.* Typhimurium infection is known to lead to splenomegaly accompanied by extramedullary erythropoiesis and increased cell numbers in WT mice (Jackson et al., 2010), which could also be observed in our WT animals. Interestingly, splenomegaly was much more pronounced in the AhR-deficient mice, suggesting that the AhR might regulate extramedullary erythropoiesis upon *S.* Typhimurium infection.

### 6.3.1 The AhR regulates splenic extramedullary erythropoiesis during *S.* Typhimurium infection

It is known that *S.* Typhimurium infection enhances the proportion of immature RBC populations in spleen of WT mice (Jackson et al., 2010). Considering this, we speculated that the enhanced splenomegaly observed in AhR-deficient mice compared to WT mice upon TAS2010 infection could be due to an excess increase in splenic immature RBC counts. In line with the literature (Jackson et al., 2010), we could detect only a low frequency of immature RBC in uninfected WT mice , whereas AhR-deficient mice already showed slightly enhanced immature RBC proportions relative to WT mice in the naïve state. Our data further showed that the enhanced immature RBC proportions correlated with the enhanced splenomegaly detected in AhR-deficient mice. Furthermore, we confirmed that upon *S.* Typhimurium infection, WT mice enhanced splenic erythropoiesis, since the frequency of immature RBCs was increased at 2 weeks post infection

compared to naïve state(Jackson et al., 2010). However, the splenic erythropoiesis was normalized in WT mice in the later course of infection as apparent by a decrease in the frequency of immature RBCs at 5 weeks compared to 2 weeks post infection. On the contrary, AhR-deficient mice displayed a similarly high frequency of immature RBC at 2 and 5 weeks post infection, which indicated a possible role of the AhR in regulating immature RBC expansion already in naïve state, but even more so upon *S.* Typhimurium infection.

Furthermore, we propose that AhR-deficient mice might have a possible RBC maturation defect, which was especially apparent after infection. In the final stage of RBC maturation, reticulocytes lose their nuclei and obtain a biconcave shape to become fully mature erythrocytes (Dzierzak & Philipsen, 2013). Although enhanced erythropoiesis is observed after *S.* Typhimurium infection, very few of the immature cells appear to develop into mature RBCs (Jackson et al., 2010). This could suggest that reticulocytes may encounter a maturation defect upon *S.* Typhimurium infection. We observed that the erythrocyte to reticulocyte ratio was slightly higher in WT mice compared to AhR-deficient mice in the naïve state. Even though this ratio was lower 2 weeks post infection for both genotypes compared to naïve state, AhR-deficient mice displayed even lower ratios compared to WT mice. Moreover, as the infection progressed, the WT mice could restore reticulocyte maturation, whereas AhR-deficient mice could not, indicating a role of the AhR in regulating the final phase of erythropoiesis. An important step in reticulocyte maturation is the elimination of mitochondria by a process called mitophagy (Ashrafi & Schwarz, 2013) and this process might be dysregulated in AhR-deficient mice upon infection. Hence, it might be interesting to study the expression and function of mitophagy related proteins like BNIP3L/NIX (Ashrafi & Schwarz, 2013) in AhR-deficient mice upon *S.* Typhimurium infection to test this theory.

Each step of the erythropoiesis is tightly regulated by various cytokines and chemokines in the environment (Dzierzak & Philipsen, 2013). The increase in the immature RBCs as well as the low ratio of mature erythrocytes to orthochromatic erythroblasts & reticulocytes may be explained by dysregulated expression of erythroid lineage specific factors in AhR-deficient mice upon *S.* Typhimurium infection. We could not detect a major difference between WT and AhR-deficient mice in the regulators of early stages of erythropoiesis such as CXCL12 and SCF. The CFU-E and pro-erythroblasts are most sensitive to EPO, due to high expression of the EPO receptor

(EPOR) but later stages may also be partially responsive (Dzierzak & Philipsen, 2013). However, EPO is not necessary for the final stage of erythrocyte differentiation (Hattangadi et al., 2011). We observed a major increase in EPO expression in AhR-deficient mice relative to WT mice upon *S.* Typhimurium infection, which was most apparent at 5 weeks post infection. Furthermore, TPO which in stress conditions works together with EPO in order to enhance the development of early and late erythroid progenitors (Kaushansky et al., 1995) was also increased in AhR-deficient mice 5 weeks post infection. These data showed that the increase in the frequency of immature RBCs upon *S.* Typhimurium infection is likely due to uncontrolled expression of EPO and TPO in AhR-deficient mice. The absence of the AhR can stabilize HIF1α signaling resulting in increased EPO expression (Vorrink & Domann, 2014). Furthermore, *S.* Typhimurium infection induces hypoxia in tissues and thus also causes stabilization of HIF1α (Jennewein et al., 2015). Therefore, it is well possible that hypoxia induced HIF1α increases EPO expression even further upon infection in the absence of the AhR.

In addition to EPO and TPO, serum levels of IL-6 were also increased in AhR-deficient mice relative to WT mice after *S.* Typhimurium infection. IL-6 is known to impair erythrocyte maturation by decreasing the membrane potential of mitochondria in which heme biosynthesis is initiated (Mccranor et al., 2014). Excess IL-6 production could thus also contribute to the impaired RBC maturation defect observed in AhR-deficient mice upon *S.* Typhimurium infection.

### 6.3.2 Immunoregulatory functions of the AhR in the spleen during *S.* Typhimurium infection

Although the major reason for the splenomegaly in *S.* Typhimurium infected mice appears to be the increase in immature RBCs, various studies attributed this effect also to enhanced accumulation of certain immune cell populations (Mittrücker et al., 2002; Rosche et al., 2015). In addition to leucocyte infiltration, proliferation of tissue resident immune cells could also lead to enhanced cell numbers in the spleen upon infection (Tam et al., 2008). In line, we observed an increase in the total number of $CD11b^{+}F4/80^{+}$ macrophages in WT mice and this increase were even more apparent in AhR-deficient mice 2 and 5 weeks post infection. This indicates a possible

role for the AhR in regulating proliferation and/or infiltration of $CD11b^{+}F4/80^{+}$ macrophages in the spleen upon *S.*Typhimurium infection.

In another study, it was shown that *S.* Typhimurium infection induces the frequency of $F4/80^{+}$ RPMs (Rosche et al., 2015). It is widely accepted that this subset expresses CD68 but lacks CD11b on their surface (Kohyama et al., 2009). Of note, in the experiments performed in this thesis, *S.* Typhimurium did not influence the total number of $CD11b^{-}F4/80^{+}$ cells but AhR-deficient mice generally had increased number of these cells relative to WT mice. A more detailed surface expression analysis to identify different macrophage subsets in the spleen could confirm if this difference is indeed due to changes in RPMs. As EPO was shown to increase the $F4/80^{+}$ macrophage numbers in the spleen (Lifshitz et al., 2010), the significant increase in macrophage numbers in AhR-deficient mice relative to WT mice is likely also due to the enhanced EPO expression in AhR-deficient mice.

In line with the literature, B and T lymphocyte proportions were decreased in WT mice upon *S.* Typhimurium infection (Rosche et al., 2015). Since AhR-deficient mice had enlarged spleens relative to WT mice, the absolute B and T cell numbers per spleen were increased in AhR-deficient mice, even though their frequencies were similar to those of WT mice. However, the increase in the total B and T cell numbers in AhR-deficient mice relative to WT mice was only apparent at 2 weeks but not at 5 weeks post infection, implying that these cells made only a minor contribution to the enhanced splenomegaly of AhR-deficient mice.

Immune cells are activated to secrete effector cytokines in order to regulate *S.* Typhimurium infection, in particular IFNγ. Similar to *T. gondii* infection (Wagage et al., 2015), a hyperactivation of AhR-deficient T cells upon *S.* Typhimurium infection was demonstrated in this thesis by the excess production of IFNγ by Th1 and Tc1 cells. Even though IFNγ is required for activation of macrophages and the immune defense against *S.* Typhimurium infection, we confirmed that the high IFNγ levels mainly correlated with bacterial numbers and were not really an indicator of pathogen clearance. The hyperactivated state of immune cells in infected AhR-deficient mice was also reflected by a significant increase in the expression of the early activation marker CD69 on T and myeloid cells 2- as well as 5 weeks after infection. Interestingly, CD69 is induced by Type I

IFN (Shiow et al., 2006), and Type I IFNs are known to be increased in the AhR-deficient background after viral infection due to enhanced activity of the kinase TBK-1 (T. Yamada et al., 2016).

CD69 associates with the amino acid transporter complex LAT1-CD98 and by increasing LAT1 transport to the plasma membrane of T cells, it regulates amino acid uptake in activated cells (Cibrián Vera et al., 2016). For example, tryptophan entrance is mediated by LAT1 and oxidative metabolism of tryptophan generates AhR agonists (Cibrián Vera et al., 2016). Furthermore, the amino acid uptake by LAT1 induces mammalian target of rapamycin (mTOR) signaling. mTOR regulates cell metabolism growth and survival in response to environmental cues (Laplante & Sabatini, 2012). mTOR also regulates HIF-1α signaling (Cibrián & Sánchez-Madrid, 2017), which might be differentially affected in the absence of the AhR. In addition, *S.* Typhimurium targets AMP-activated protein kinase (AMPK), an important checkpoint for mTOR activity for its rapid degradation and permits mTOR activation (Ganesan et al., 2017). The activation of mTOR in turn allows *S.* Typhimurium to escape host defense by downregulating autophagy, an important mechanism for cells to induce pathogen clearance (Cibrián & Sánchez-Madrid, 2017; Ganesan et al., 2017). We speculate that the increase in CD69 expression in AhR-deficient mice upon *S.* Typhimurium infection may increase mTOR activity by activating the LAT1/CD98 signaling complex and hence decreases autophagy, which in turn might partly be responsible for increased survival of bacteria observed in spleen and liver. The association of CD69 with the LAT1/CD98 complex has been tested only in T cells so far, however, we observed an increase in CD69 expression also in myeloid cells in both WT and AhR-deficient mice upon *S.* Typhimurium infection. We are planning to test the hypothesis that enhanced CD69 expression in macrophages enhances intracellular survival of *S.* Typhimurium in AhR-deficient cells by using an *in vitro* system.

Previous studies showed that naïve AhR-deficient mice displayed an altered splenic architecture (K. P. Singh et al., 2011), however a detailed analysis of the different zones was missing. In our study, we could show that AhR-deficient mice had significantly smaller B cell follicles relative to WT mice already in naïve state. Since AhR-deficient mice possess a defect in B cell proliferation (Villa et al., 2017), this might influence the size of the B cell follicles in naïve state.

Furthermore, Rosche *et al.* showed that upon *S.* Typhimurium infection of WT mice, B cell follicles were destroyed, T cells dislocated from the white pulp to the red pulp, the marginal zone was disintegrated and F4/80$^+$ macrophages were present not only in the red but also in the white pulp (Rosche et al., 2015). We could confirm the observation of smaller B cell follicles and T cell dislocation in both WT and AhR-deficient mice upon *S.* Typhimurium infection. Of note, we observed that WT mice still contained some T cell zones after infection, whereas AhR-deficient mice seemed to completely lose the T cell follicles with most of the T cells being spread around in spleen. Furthermore, AhR-deficient mice showed even smaller B cell follicles upon *S.* Typhimurium than WT mice.

We were also interested in the localization of different macrophage subsets within the spleen upon *S.* Typhimurium infection. Our preliminary data is in line with the literature, indicating that F4/80$^+$ macrophages were present not only in the RP but also in the WP in WT mice upon *S.* Typhimurium infection, however further analysis is needed for the localization of these macrophages in AhR-deficient mice. Due to the high bacterial load as well as the increase in F4/80$^+$ macrophages, we think that the MZ is further disintegrated upon *S.* Typhimurium infection in AhR-deficient mice relative to WT mice and we are in the process of analyzing MZM as well as MMM. Another interesting point is to examine the localization of *S.* Typhimurium within the spleen and to quantify the immune cell subsets, which harbor *S.* Typhimurium. This might give additional clues about the reason for the enhanced bacterial load observed in the spleen of AhR-deficient mice upon *S.* Typhimurium infection.

### 6.3.3 The AhR moderately influences ileal damage induced by S. Typhimurium infection

In our hands, *S.* Typhimurium infection caused disruptions in the villi structure of some but not all AhR-deficient mice, while this kind of tissue pathology was not so apparent in WT mice. This is not fully consistent with the literature, since Bessede *et al.* showed extensive submucosal edema, thickened mucosa, and inflammatory cell recruitment in AhR-deficient mice upon *S.* Typhimurium infection (Bessede et al., 2014). However, they used an AroA deficient *S.*Typhimurium strain, which is more aggressive compared to TAS2010 used here and survival was monitored only for 7

days, which might be the reason for the stronger intestinal tissue damage observed. We believe that TAS2010 infection may not damage all regions in the ileum equally, which could explain the inconsistent ileal damage. Another possibility is that the bacteria are cleared from the intestine 2 weeks after infection and the ileal damage already declines. Therefore, it might be interesting to quantify the number of *S.* Typhimurium in the ileum over time. Even though AhR- and AhRR-deficient mice showed similarly enhanced tissue damage in response to *T. gondii* infection, the absence of the AhRR but not the AhR resulted in more ileal damage after *S.* Typhimurium infection. T cell analysis in the ileum indicated that only the Tc1 response was slightly higher in AhR-deficient mice upon *S.* Typhimurium infection. It is likely that AhRR-deficient mice show more ileal damage compared to AhR-deficient mice due to expansion of both Th1 and Tc1 cells upon *S.* Typhimurium infection.

# 7 Conclusion

IBD is a global emerging disease and it maybe a consequence of increased consumption of westernized diet all over the world (Alatab et al., 2020). Since it is a chronic disorder, it has a big impact on the quality of life of an individual and hence needs to be treated or better prevented. iNTS disease, which is commonly seen in malnourished children and immunocompromised adults with HIV infection is also a major cause of global mortality (Stanaway et al., 2019). Since both IBD and iNTS may cause dangerous complications or may be lethal, gain of knowledge about their mechanisms is highly crucial. Using IBD and *S.* Typhimurium mouse and infection models has given many insights into regulatory mechanisms influencing the disease outcomes, however, there is still a big lack of knowledge in both fields and hence the treatment options are either limited or not very effective.

In a meta-analysis of genome-wide association studies, a polymorphism in the *AHR locus* was identified as a risk factor for IBD (J. Z. Liu et al., 2015). While the important function of the AhR in regulating intestinal inflammation was already known from the analysis of IBD models in mice, our study for the first time investigated the importance of the AhRR in regulating intestinal tissue damage in the IBD-like *T. gondii* infection model and after oral infection with *S.* Typhimurium . We showed that the AhRR only exerts moderate effects on protection from intestinal tissue damage and excessive local production of pro-inflammatory cytokines. In contrast, genetic deletion of the AhR had a big impact on defense against *S.* Typhimurium infection. The difference in AhRR relative to AhR function during *S.* Typhimurium infection is likely due to the restricted tissue- and cell type-specific expression of the AhRR, and/or the high relevance of other AhR target genes or protein interaction partners of the AhR in regulation of immune responses and hematopoiesis in the course of infection.

# 8 References


Adhikari, A., Rauniyar, R., Raut, P. P., Manandhar, K. Das, & Gupta, B. P. (2015). Evaluation of sensitivity and specificity of ELISA against Widal test for typhoid diagnosis in endemic population of Kathmandu. *BMC Infectious Diseases*, *15*(1), 1–7.

Alatab, S., Sepanlou, S. G., Ikuta, K., Vahedi, H., Bisignano, C., Safiri, S., Sadeghi, A., Nixon, M. R., Abdoli, A., Abolhassani, H., Alipour, V., Almadi, M. A. H., Almasi-Hashiani, A., Anushiravani, A., Arabloo, J., Atique, S., Awasthi, A., Badawi, A., Baig, A. A. A., … Naghavi, M. (2020). The global, regional, and national burden of inflammatory bowel disease in 195 countries and territories, 1990–2017: a systematic analysis for the Global Burden of Disease Study 2017. *The Lancet Gastroenterology and Hepatology*, *5*(1), 17–30.

Andino, A., & Hanning, I. (2015). Salmonella enterica: Survival, colonization, and virulence differences among serovars. *Scientific World Journal*, *2015*.

Apetoh, L., Quintana, F. J., Pot, C., Joller, N., Xiao, S., Kumar, D., Burns, E. J., Sherr, D. H., Weiner, H. L., & Kuchroo, V. K. (2010). The aryl hydrocarbon receptor interacts with c-Maf to promote the differentiation of type 1 regulatory T cells induced by IL-27. *Nature Immunology*, *11*(9), 854–861.

Asai, H., Hirata, J., Hirano, A., Hirai, K., Seki, S., & Watanabe-Akanuma, M. (2016). Activation of aryl hydrocarbon receptor mediates suppression of hypoxia-inducible factor-dependent erythropoietin expression by indoxyl sulfate. *American Journal of Physiology - Cell Physiology*, *310*(2), C142–C150.

Ashrafi, G., & Schwarz, T. L. (2013). The pathways of mitophagy for quality control and clearance of mitochondria. *Cell Death and Differentiation*, *20*, 31–42.

Azmatullah, A., Qamar, F. N., Thaver, D., Zaidi, A. K. M., & Bhutta, Z. A. (2015). Systematic review of the global epidemiology, clinical and laboratory profile of enteric fever. *Journal of Global Health*, *5*(2).

Baba, T., Mimura, J., Gradin, K., Kuroiwa, A., Watanabe, T., Matsuda, Y., Inazawa, J., Sogawa, K., & Fujii-Kuriyama, Y. (2001). Structure and Expression of the Ah Receptor Repressor Gene. *Journal of Biological Chemistry*, *276*(35), 33101–33110.

Barminko, J., Reinholt, B., & Baron, M. H. (2016). Development and differentiation of the erythroid lineage in mammals HHS Public Access. *Dev Comp Immunol*, *58*, 18–29.

Batista, F. D., & Harwood, N. E. (2009). The who, how and where of antigen presentation to B cells. *Nature Reviews Immunology*, *9*(1), 15–27.

Bessede, A., Gargaro, M., Pallotta, M. T., Matino, D., Servillo, G., Brunacci, C., Bicciato, S., Mazza, E. M. C., Macchiarulo, A., Vacca, C., Iannitti, R., Tissi, L., Volpi, C., Belladonna, M. L., Orabona, C., Bianchi, R., Lanz, T. V., Platten, M., Della Fazia, M. A., … Puccetti, P. (2014). Aryl hydrocarbon receptor control of a disease tolerance defence pathway. *Nature*, *511*(7508), 184–190.

Black, M. W., & Boothroyd, J. C. (2000). Lytic Cycle of Toxoplasma gondii. *Microbiology and Molecular Biology Reviews*, *64*(3), 607–623.

Blanchette, J., Jaramillo, M., & Olivier, M. (2003). Signalling events involved in interferon-γ-inducible macrophage nitric oxide generation. *Immunology*, *108*(4), 513–522.

Bock, K. W. (2016). Toward elucidation of dioxin-mediated chloracne and Ah receptor functions. In *Biochemical Pharmacology* (Vol. 112, pp. 1–5). Elsevier Inc.

Bonyadi, M. R., & Bastani, P. (2013). Modification and Evaluation of Avidity IgG Testing for

Differentiating of Toxoplasma gondii Infection in Early Stage of Pregnancy Citation: Bonyadi MR, Bastani P. Modification and evaluation of avidity IgG testing for differentiating of toxoplasma gondii . *CELL JOURNAL(Yakhteh)*, *15*(3), 238–243.

Borges Da Silva, H., Fonseca, R., Pereira, R. M., Cassado, A. A., Álvarez, J. M., & D'Império Lima, M. R. (2015). Splenic macrophage subsets and their function during blood-borne infections. *Frontiers in Immunology*, *6*(SEP).

Brandstätter, O., Schanz, O., Vorac, J., König, J., Mori, T., Maruyama, T., Korkowski, M., Haarmann-Stemmann, T., Von Smolinski, D., Schultze, J. L., Abel, J., Esser, C., Takeyama, H., Weighardt, H., & Förster, I. (2016). Balancing intestinal and systemic inflammation through cell type-specific expression of the aryl hydrocarbon receptor repressor. *Scientific Reports*, *6*(May), 1–17.

Brenner, F. W., Villar, R. G., Angulo, F. J., Tauxe, R., & Swaminathan, B. (2000). Salmonella nomenclature. *Journal of Clinical Microbiology*, *38*(7), 2465–2467.

Bronte, V., & Pittet, M. J. (2013). The spleen in local and systemic regulation of immunity. *Immunity*, *39*(5), 806–818.

Brubaker, S. W., Bonham, K. S., Zanoni, I., & Kagan, J. C. (2015). Innate Immune Pattern Recognition: A Cell Biological Perspective. *Annual Review of Immunology*, *33*(1), 257–290.

Cardona, S. M., Garcia, J. A., & Cardona, A. E. (2013). The fine balance of chemokines during disease: Traf ficking, inflammation, and homeostasis. *Methods in Molecular Biology*, *1013*, 1–16.

Carter, P. B., & Collins, F. M. (1974). The route of enteric infection in normal mice. *Journal of Experimental Medicine*, *139*(5), 1189–1203.

Caruso, R., Warner, N., Inohara, N., & Núñez, G. (2014). NOD1 and NOD2: Signaling, host defense, and inflammatory disease. *Immunity*, *41*(6), 898–908.

Chan, W. K., Yao, G., Gu, Y. Z., & Bradfield, C. A. (1999). Cross-talk between the aryl hydrocarbon receptor and hypoxia inducible factor signaling pathways: Demonstration of competition and compensation. *Journal of Biological Chemistry*, *274*(17), 12115–12123.

Chen, I., McDougal, A., Wang, F., & Safe, S. (1998). Aryl hydrocarbon receptor-mediated antiestrogenic and antitumorigenic activity of diindolylmethane. *Carcinogenesis*, *19*(9), 1631–1639.

Chen, Y. H., Riby, J., Srivastava, P., Bartholomew, J., Denison, M., & Bjeldanes, L. (1995). Regulation of CYP1A1 by indolo[3,2-b]carbazole in murine hepatoma cells. *Journal of Biological Chemistry*, *270*(38), 22548–22555.

Cheroutre, H., Lambolez, F., & Mucida, D. (2011). The light and dark sides of intestinal intraepithelial lymphocytes. *Nature Reviews Immunology*, *11*(7), 445–456.

Cibrián, D., & Sánchez-Madrid, F. (2017). CD69: from activation marker to metabolic gatekeeper. *European Journal of Immunology*, *47*(6), 946–953.

Cibrián Vera, D., Laura Saiz, M., De La Fuente, H., Sánchez-Díaz, R., Moreno-Gonzalo, O., Cerrudo, I. J., Ferrarini, A., Vázquez, J., Punzón, C., Fresno, M., Vicente-Manzanares, M., Daudén Tello, E., Fernández-Salguero, P. M., Martín, P., & Sánchez-Madrid, F. (2016). CD69 controls L-Trp uptake through LAT1-CD98 and AhR-dependent IL-22 secretion in psoriasis Europe PMC Funders Group. *Nat Immunol*, *17*(8), 985–996.

Ciolino, H. P., Daschner, P. J., & Yeh, G. C. (1999). Dietary flavonols quercetin and kaempferol are ligands of the aryl hydrocarbon receptor that affect CYP1A1 transcription differentially. *Biochemical Journal*, *340*(3), 715–722.

Cossart, P., & Sansonetti, P. J. (2004). Bacterial Invasion: The Paradigms of Enteroinvasive Pathogens. *Science*, *304*(5668), 242–248.

Crump, J. A., Luby, S. P., & Mintz, E. D. (2004). The global burden of typhoid fever. *Bulletin of the World Health Organization*, *82*(5), 346–353.

Dang, E. V., Barbi, J., Yang, H. Y., Jinasena, D., Yu, H., Zheng, Y., Bordman, Z., Fu, J., Kim, Y., Yen, H. R., Luo, W., Zeller, K., Shimoda, L., Topalian, S. L., Semenza, G. L., Dang, C. V., Pardoll, D. M., & Pan, F. (2011). Control of TH17/Treg balance by hypoxia-inducible factor 1. *Cell*, *146*(5), 772–784.

Darcy, F., & Zenner, L. (1993). Experimental models of toxoplasmosis. *Research in Immunology*, *144*(1), 16–23.

Delves, P. J., & Roitt, I. M. (2000). The immune system. First of two parts. *New England Journal of Medicine*, *343*(1), 37–49.

Dubey, J. P., Speer, C. A., Shen, S. K., Kwok, O. C. H., & Blixt, J. A. (1997). Oocyst-Induced Murine Toxoplasmosis: Life Cycle, Pathogenicity, and Stage Conversion in Mice Fed Toxoplasma gondii Oocysts. *The Journal of Parasitology*, *83*(5), 870.

Dukaczewska, A., Tedesco, R., & Liesenfeld, O. (2015). Experimental models of ocular infection with Toxoplasma gondii . *European Journal of Microbiology and Immunology*, *5*(4), 293–305.

Dunay, I. R., & Diefenbach, A. (2018). Group 1 innate lymphoid cells in Toxoplasma gondii infection. *Parasite Immunology*, *40*(2), e12516.

Dunkelberger, J. R., & Song, W. C. (2010). Complement and its role in innate and adaptive immune responses. *Cell Research*, *20*(1), 34–50.

Dunstan, S. J., Simmons, C. P., & Strugnell, R. A. (1998). Comparison of the abilities of different attenuated Salmonella typhimurium strains to elicit humoral immune responses against a heterologous antigen. *Infection and Immunity*, *66*(2), 732–740.

Dzierzak, E., & Philipsen, S. (2013). Erythropoiesis: Development and differentiation. *Cold Spring Harbor Perspectives in Medicine*, *3*(4), 1–16.

Egan, C. E., Cohen, S. B., & Denkers, E. Y. (2012). Insights into inflammatory bowel disease using Toxoplasma gondii as an infectious trigger. *Immunology and Cell Biology*, *90*(7), 668–675.

Enan, E., & Matsumura, F. (1996). Identification of c-Src as the integral component of the cytosolic Ah receptor complex, transducing the signal of 2,3,7,8-tetrachlorodibenzo-p-dioxin (TCDD) through the protein phosphorylation pathway. *Biochemical Pharmacology*, *52*(10), 1599–1612.

Eng, S. K., Pusparajah, P., Ab Mutalib, N. S., Ser, H. L., Chan, K. G., & Lee, L. H. (2015). Salmonella: A review on pathogenesis, epidemiology and antibiotic resistance. *Frontiers in Life Science*, *8*(3), 284–293.

Esser, C., & Rannug, A. (2015). The aryl hydrocarbon receptor in barrier organ physiology, immunology, and toxicology. *Pharmacological Reviews*, *67*(2), 259–279.

Etheridge, R. D., Alaganan, A., Tang, K., Lou, H. J., Turk, B. E., & Sibley, L. D. (2014). The Toxoplasma pseudokinase ROP5 forms complexes with ROP18 and ROP17 kinases that synergize to control acute virulence in mice. *Cell Host and Microbe*, *15*(5), 537–550.

Evans, B. R., Karchner, S. I., Allan, L. L., Pollenz, R. S., Tanguay, R. L., Jenny, M. J., Sherr, D. H., & Hahn, M. E. (2008). Repression of Aryl Hydrocarbon Receptor (AHR) signaling by AHR repressor: Role of DNA binding and competition for AHR nuclear translocator.

*Molecular Pharmacology*, *73*(2), 387–398.
Fernandez-Salguero, P. M., Ward, J. M., Sundberg, J. P., & Gonzalez, F. J. (1997). Lesions of Aryl-hydrocarbon Receptor-deficient Mice. *Veterinary Pathology*, *34*(6), 605–614.
Fontenot, J. D., Gavin, M. A., & Rudensky, A. Y. (2017). Foxp3 programs the development and function of CD4+CD25+ regulatory T cells. *Journal of Immunology*, *198*(3), 986–992.
Forchielli, M. L., & Walker, W. A. (2005). The role of gut-associated lymphoid tissues and mucosal defence. *British Journal of Nutrition*, *93*(S1), S41–S48.
Foster, J. W. (1993). The acid tolerance response of Salmonella typhimurium involves transient synthesis of key acid shock proteins. *Journal of Bacteriology*, *175*(7), 1981–1987.
Fujimura, Y. (1986). Functional morphology of microfold cells (M cells) in Peyer's patches - Phagocytosis and transport of BCG by M cells into rabbit Peyer's patches. *Gastroenterologia Japonica*, *21*(4), 325–334.
Gal-Mor, O. (2019). Persistent infection and long-term carriage of typhoidal and nontyphoidal salmonellae. *Clinical Microbiology Reviews*, *32*(1).
Galanis, E., Lo Fo Wong, D. M. A., Patrick, M. E., Binsztein, N., Cieslik, A., Chalermchaikit, T., Aidara-Kane, A., Ellis, A., Angulo, F. J., & Wegener, H. C. (2006). Web-based surveillance and global Salmonella distribution, 2000-2002. *Emerging Infectious Diseases*, *12*(3), 381–388.
Galen, J. E., Buskirk, A. D., Tennant, S. M., & Pasetti, M. F. (2016). Live Attenuated Human Salmonella Vaccine Candidates: Tracking the Pathogen in Natural Infection and Stimulation of Host Immunity. *EcoSal Plus*, *7*(1).
Ganesan, R., Hos, N. J., Gutierrez, S., Fischer, J., Stepek, J. M., Daglidu, E., Krönke, M., & Robinson, N. (2017). Salmonella Typhimurium disrupts Sirt1/AMPK checkpoint control of mTOR to impair autophagy. *PLoS Pathogens*, *13*(2).
Ganesh, V., Baru, A. M., Hesse, C., Friedrich, C., Glage, S., Gohmert, M., Jänke, C., & Sparwasser, T. (2014). Salmonella enterica serovar typhimurium infection-induced CD11b+ Gr1+ cells ameliorate allergic airway inflammation. *Infection and Immunity*, *82*(3), 1052–1063.
Germain, R. N. (2002). T-cell development and the CD4-CD8 lineage decision. *Nature Reviews Immunology*, *2*(5), 309–322.
Gigley, J. P. (2016). The Diverse Role of NK Cells in Immunity to Toxoplasma gondii Infection. *PLoS Pathogens*, *12*(2).
Goswami, R., & Kaplan, M. H. (2011). A Brief History of IL-9. *The Journal of Immunology*, *186*(6), 3283–3288.
Govoni, G., Vidal, S., Gauthier, S., Skamene, E., Malo, D., & Gros, P. (1996). The Bcg/Ity/Lsh locus: Genetic transfer of resistance to infections in C57BL/6J mice transgenic for the Nramp1(Gly169) allele. *Infection and Immunity*, *64*(8), 2923–2929.
Griffith, J. W., Sokol, C. L., & Luster, A. D. (2014). Chemokines and Chemokine Receptors: Positioning Cells for Host Defense and Immunity. *Annual Review of Immunology*, *32*(1), 659–702.
Gut, A. M., Vasiljevic, T., Yeager, T., & Donkor, O. N. (2018). Salmonella infection – Prevention and treatment by antibiotics and probiotic yeasts: A review. *Microbiology (United Kingdom)*, *164*(11), 1327–1344.
Gutzeit, C., Magri, G., & Cerutti, A. (2014). Intestinal IgA production and its role in host-microbe interaction. *Immunological Reviews*, *260*(1), 76–85.

Harrison, O. J., & Powrie, F. M. (2013). Regulatory T cells and immune tolerance in the intestine. *Cold Spring Harbor Perspectives in Biology*, *5*(7).

Hattangadi, S. M., Wong, P., Zhang, L., Flygare, J., & Lodish, H. F. (2011). From stem cell to red cell: Regulation of erythropoiesis at multiple levels by multiple proteins, RNAs, and chromatin modifications. *Blood*, *118*(24), 6258–6268.

He, S. Y. (1998). Type Iii Protein Secretion Systems in Plant and Animal Pathogenic Bacteria. *Annual Review of Phytopathology*, *36*(1), 363–392.

Hohmann, E., Ohl, M. E., & Miller, S. I. (2006). Nontyphoidal Salmonellosis. *Tropical Infectious Diseases*, *1*, 241–254.

Holsapple, M. (1991). 2,3,7,8-Tetrachlorodibenzo-p-Dioxin-Induced Changes In Immunocompetence : Possible Mechanisms. *Annual Review of Pharmacology and Toxicology*, *31*(1), 73–100.

Hormaeche, C. E. (1979). Natural resistance to Salmonella typhimurium in different inbred mouse strains. *Immunology*, *37*(2), 311–318.

Hoshino, K., Takeuchi, O., Kawai, T., Sanjo, H., Ogawa, T., Takeda, Y., Takeda, K., & Akira, S. (1999). Cutting edge: Toll-like receptor 4 (TLR4)-deficient mice are hyporesponsive to lipopolysaccharide: evidence for TLR4 as the Lps gene product. *Journal of Immunology (Baltimore, Md. : 1950)*, *162*(7), 3749–3752. http://www.ncbi.nlm.nih.gov/pubmed/10201887

Jackson, A., Nanton, M. R., O'Donnell, H., Akue, A. D., & McSorley, S. J. (2010). Innate Immune Activation during Salmonella Infection Initiates Extramedullary Erythropoiesis and Splenomegaly . *The Journal of Immunology*, *185*(10), 6198–6204.

Jennewein, J., Matuszak, J., Walter, S., Felmy, B., Gendera, K., Schatz, V., Nowottny, M., Liebsch, G., Hensel, M., Hardt, W. D., Gerlach, R. G., & Jantsch, J. (2015). Low-oxygen tensions found in Salmonella-infected gut tissue boost Salmonella replication in macrophages by impairing antimicrobial activity and augmenting Salmonella virulence. *Cellular Microbiology*, *17*(12), 1833–1847.

Jones, B. D., Ghori, N., & Falkow, S. (1994). Salmonella typhlrnurium initiates murine infection by penetrating and destroying the specialized epithelial M cells of the peyer's patches. *Journal of Experimental Medicine*, *180*(1), 15–23.

Jones, S. (2004). An overview of the basic helix-loop-helix proteins. *Genome Biology*, *5*(6).

Jung, C., Hugot, J.-P., & Barreau, F. (2010). Peyer's Patches: The Immune Sensors of the Intestine. *International Journal of Inflammation*, *2010*, 1–12.

Kaplan, M. J., & Radic, M. (2012). Neutrophil Extracellular Traps: Double-Edged Swords of Innate Immunity. *The Journal of Immunology*, *189*(6), 2689–2695.

Kaushansky, K., Broudy, V. C., Grossmann, A., Humes, J., Lin, N., Ren, H. P., Bailey, M. C., Papayannopoulou, T., Forstrom, J. W., & Sprugel, K. H. (1995). Thrombopoietin expands erythroid progenitors, increases red cell production, and enhances erythroid recovery after myelosuppressive therapy. *Journal of Clinical Investigation*, *96*(3), 1683–1687.

Kazlauskas, A., Poellinger, L., & Pongratz, I. (2000). The immunophilin-like protein XAP2 regulates ubiquitination and subcellular localization of the dioxin receptor. *Journal of Biological Chemistry*, *275*(52), 41317–41324.

Kazlauskas, Arunas, Poellinger, L., & Pongratz, I. (1999). Evidence that the co-chaperone p23 regulates ligand responsiveness of the dioxin (aryl hydrocarbon) receptor. *Journal of Biological Chemistry*, *274*(19), 13519–13524.

Khan, I. A., Hwang, S., & Moretto, M. (2019). Toxoplasma gondii: CD8 T cells cry for CD4 help. *Frontiers in Cellular and Infection Microbiology*, *9*(MAY), 1–8.

Kim, C. H. (2010). Homeostatic-and-pathogenic-extramedullary-hematopoiesis. *Journal of Blood Medicine*, 1–13. www.dovepress.com

Kim, K., & Weiss, L. M. (2004). Toxoplasma gondii: The model apicomplexan. *International Journal for Parasitology*, *34*(3), 423–432.

Kimura, A., Abe, H., Tsuruta, S., Chiba, S., Fujii-Kuriyama, Y., Sekiya, T., Morita, R., & Yoshimura, A. (2014). Aryl hydrocarbon receptor protects against bacterial infection by promoting macrophage survival and reactive oxygen species production. *International Immunology*, *26*(4), 209–220.

Kiss, E. A., Vonarbourg, C., Kopfmann, S., Hobeika, E., Finke, D., Esser, C., & Diefenbach, A. (2011). Natural aryl hydrocarbon receptor ligands control organogenesis of intestinal lymphoid follicles. *Science*, *334*(6062), 1561–1565.

Klion, A. D., & Nutman, T. B. (2004). The role of eosinophils in host defense against helminth parasites. *Journal of Allergy and Clinical Immunology*, *113*(1), 30–37.

Kohyama, M., Ise, W., Edelson, B. T., Wilker, P. R., Hildner, K., Mejia, C., Frazier, W. A., Murphy, T. L., & Murphy, K. M. (2009). Role for Spi-C in the development of red pulp macrophages and splenic iron homeostasis. *Nature*, *457*(7227), 318–321.

König, J. D. (2016). *Function of the Aryl hydrocarbon Receptor Repressor during polymicrobial and parasitic infections* (Issue November).

Konstantinovic, N., Guegan, H., Stäjner, T., Belaz, S., & Robert-Gangneux, F. (2019). Treatment of toxoplasmosis: Current options and future perspectives. *Food and Waterborne Parasitology*, *15*.

Kupz, A., Bedoui, S., & Strugnell, R. A. (2014). Cellular requirements for systemic control of Salmonella enterica serovar Typhimurium infections in mice. *Infection and Immunity*, *82*(12), 4997–5004.

Kupz, A., Scott, T. A., Belz, G. T., Andrews, D. M., Greyer, M., Lew, A. M., Brooks, A. G., Smyth, M. J., Curtiss, R., Bedoui, S., & Strugnell, R. A. (2013). Contribution of Thy1+ NK cells to protective IFN- γ production during Salmonella Typhimurium infections. *Proceedings of the National Academy of Sciences of the United States of America*, *110*(6), 2252–2257.

Kurotaki, D., Uede, T., & Tamura, T. (2015). Functions and development of red pulp macrophages. *Microbiology and Immunology*, *59*(2), 55–62.

Kuvandik, C., Karaoglan, I., Namiduru, M., & Baydar, I. (2009). Predictive value of clinical and laboratory findings in the diagnosis of the enteric fever. *New Microbiologica*, *32*(1), 25–30.

Lahvis, G. P., Lindell, S. L., Thomas, R. S., McCuskey, R. S., Murphy, C., Glover, E., Bentz, M., Southard, J., & Bradfield, C. A. (2000). Portosystemic shunting and persistent fetal vascular structures in aryl hydrocarbon receptor-deficient mice. *Proceedings of the National Academy of Sciences of the United States of America*, *97*(19), 10442–10447.

Laplante, M., & Sabatini, D. M. (2012). MTOR signaling in growth control and disease. *Cell*, *149*(2), 274–293.

Leoni Swart, A., & Hensel, M. (2012). Interactions of Salmonella enterica with dendritic cells. *Virulence*, *3*(7).

Lewis, S. M., Williams, A., & Eisenbarth, S. C. (2019). Structure and function of the immune system in the spleen. *Science Immunology*, *4*(33).

Li, L. X., Benoun, J. M., Weiskopf, K., Garcia, K. C., & McSorley, S. J. (2016). Salmonella infection enhances erythropoietin production by the kidney and liver, which correlates with elevated bacterial burdens. *Infection and Immunity*, *84*(10), 2833–2841.

Li, T. H., Liu, L., Hou, Y. Y., Shen, S. N., & Wang, T. T. (2019). C-type lectin receptor-mediated immune recognition and response of the microbiota in the gut. *Gastroenterology Report*, *7*(5), 312–321.

Li, Y., Innocentin, S., Withers, D. R., Roberts, N. A., Gallagher, A. R., Grigorieva, E. F., Wilhelm, C., & Veldhoen, M. (2011). Exogenous stimuli maintain intraepithelial lymphocytes via aryl hydrocarbon receptor activation. *Cell*, *147*(3), 629–640.

Lifshitz, L., Tabak, G., Gassmann, M., Mittelman, M., & Neumann, D. (2010). Macrophages as novel target cells for erythropoietin. *Haematologica*, *95*(11), 1823–1831.

Liu, C.-H., Fan, Y., Dias, A., Esper, L., Corn, R. A., Bafica, A., Machado, F. S., & Aliberti, J. (2006). Cutting Edge: Dendritic Cells Are Essential for In Vivo IL-12 Production and Development of Resistance against Toxoplasma gondii Infection in Mice . *The Journal of Immunology*, *177*(1), 31–35.

Liu, J. Z., Van Sommeren, S., Huang, H., Ng, S. C., Alberts, R., Takahashi, A., Ripke, S., Lee, J. C., Jostins, L., Shah, T., Abedian, S., Cheon, J. H., Cho, J., Daryani, N. E., Franke, L., Fuyuno, Y., Hart, A., Juyal, R. C., Juyal, G., … Weersma, R. K. (2015). Association analyses identify 38 susceptibility loci for inflammatory bowel disease and highlight shared genetic risk across populations. *Nature Genetics*, *47*(9), 979–986.

Liu, Qi, Das Singla, L., & Zhou, H. (2012). Vaccines against Toxoplasma gondii: Status, challenges and future directions. *Human Vaccines and Immunotherapeutics*, *8*(9), 1305–1308.

Liu, Quan, Wang, Z. D., Huang, S. Y., & Zhu, X. Q. (2015). Diagnosis of toxoplasmosis and typing of Toxoplasma gondii. *Parasites and Vectors*, *8*(1).

Ma, Q., & Baldwin, K. T. (2000). 2,3,7,8-tetrachlorodibenzo-p-dioxin-induced degradation of aryl hydrocarbon receptor (AhR) by the ubiquitin-proteasome pathway. Role of the transcription activaton and DNA binding of AhR. In *Journal of Biological Chemistry* (Vol. 275, Issue 12).

Maidhof, W., & Hilas, O. (2012). Lupus: An overview of the disease and management options. In *P and T* (Vol. 37, Issue 4).

Majowicz, S. E., Musto, J., Scallan, E., Angulo, F. J., Kirk, M., O'Brien, S. J., Jones, T. F., Fazil, A., & Hoekstra, R. M. (2010). The Global Burden of Nontyphoidal Salmonella Gastroenteritis . *Clinical Infectious Diseases*, *50*(6), 882–889.

Mak, T., Saunders, M., & Jett, B. (2014). NK, γδ T and NKT Cells. In *Primer to the Immune Response*. Elsevier.

Mandal, P. K. (2005). Dioxin: A review of its environmental effects and its aryl hydrocarbon receptor biology. *Journal of Comparative Physiology B: Biochemical, Systemic, and Environmental Physiology*, *175*(4), 221–230.

Marcus, S. L., Brumell, J. H., Pfeifer, C. G., & Finlay, B. B. (2000). Salmonella pathogenicity islands: Big virulence in small packages. *Microbes and Infection*, *2*(2), 145–156.

Marshall, J. S., Warrington, R., Watson, W., & Kim, H. L. (2018). An introduction to immunology and immunopathology. *Allergy, Asthma and Clinical Immunology*, *14*(2), 49.

Matamouros, S., & Miller, S. I. (2015). S. Typhimurium strategies to resist killing by cationic antimicrobial peptides. *Biochimica et Biophysica Acta - Biomembranes*, *1848*(11), 3021–3025.

McAllister, M. M. (2005). A decade of discoveries in veterinary protozoology changes our concept of "subclinical" toxoplasmosis. *Veterinary Parasitology*, *132*(3-4 SPEC. ISS.), 241–247.

Mccranor, B. J., Kim, M. J., Cruz, N. M., Xue, Q.-L., Berger, A. E., Walston, J. D., Civin, C. I., & Roy, C. N. (2014). Interleukin-6 Directly Impairs the Erythroid Development of Human TF-1 Erythroleukemic Cells. *Blood Cells Mol Dis*, *52*(0), 126–133.

McGhee, J. R., & Fujihashi, K. (2012). Inside the Mucosal Immune System. *PLoS Biology*, *10*(9).

Mcsorley, S. J. (2014). Immunity to intestinal pathogens: Lessons learned from Salmonella. *Immunological Reviews*, *260*(1), 168–182.

McSorley, S. J., Asch, S., Costalonga, M., Lee Reinhardt, R., & Jenkins, M. K. (2002). Tracking Salmonella-Specific CD4 T Cells In Vivo Reveals a Local Mucosal Response to a Disseminated Infection 2000). A more detailed understanding of CD4 T cell biol-ogy during Development of an Adoptive Transfer System to Track Salmonella-Specific CD4 T . *Immunity*, *16*, 365–377.

McSorley, S. J., Ehst, B. D., Yu, Y., & Gewirtz, A. T. (2002). Bacterial Flagellin Is an Effective Adjuvant for CD4 + T Cells In Vivo . *The Journal of Immunology*, *169*(7), 3914–3919.

Mebius, R. E., & Kraal, G. (2005). Structure and function of the spleen. *Nature Reviews Immunology*, *5*(8), 606–616.

Medalla, F., Gu, W., Mahon, B. E., Judd, M., Folster, J., Griffin, P. M., & Hoekstra, R. M. (2017). Estimated incidence of antimicrobial drug-resistant nontyphoidal Salmonella infections, United States, 2004-2012. *Emerging Infectious Diseases*, *23*(1), 29–37.

Medzhitov, R. (2001). Toll-like receptors and innate immunity. *Nature Reviews Immunology*, *1*(2), 135–145.

Meyer, B. K., Petrulis, J. R., & Perdew, G. H. (2000). Aryl hydrocarbon (Ah) receptor levels are selectively modulated by hsp90-associated immunophilin homolog XAP2. In *Cell Stress and Chaperones* (Vol. 5, Issue 3). Cell Stress Society International.

Michael, A., & Partch, C. (2013). bHLH-PAS proteins: Functional specification through modular domain architecture. In *OA Biochemistry* (Vol. 1, Issue 2).

Mimura, J., Ema, M., Sogawa, K., & Fujii-Kuriyama, Y. (1999). Identification of a novel mechanism of regulation of Ah (dioxin) receptor function. *Genes and Development*, *13*(1), 20–25.

Mittrücker, H. W., Köhler, A., & Kaufmann, S. H. E. (2002). Characterization of the murine T-lymphocyte response to Salmonella enterica serovar typhimurium infection. *Infection and Immunity*, *70*(1), 199–203.

Mølbak, K., Gerner-Smidt, P., & Wegener, H. C. (2002). Increasing quinolone resistance in Salmonella enterica serotype Enteritidis. *Emerging Infectious Diseases*, *8*(5), 514–515.

Monteleone, I., Rizzo, A., Sarra, M., Sica, G., Sileri, P., Biancone, L., MacDonald, T. T., Pallone, F., & Monteleone, G. (2011). Aryl hydrocarbon receptor-induced signals up-regulate IL-22 production and inhibit inflammation in the gastrointestinal tract. *Gastroenterology*, *141*(1), 237-248.e1.

Mosmann, T. R., & Coffman, R. L. (1989). TH1 and TH2 cells: Different patterns of lymphokine secretion lead to different functional properties. *Annual Review of Immunology*, *7*, 145–173.

Mueller, S. N., Gebhardt, T., Carbone, F. R., & Heath, W. R. (2013). Memory T Cell Subsets, Migration Patterns, and Tissue Residence. *Annual Review of Immunology*, *31*(1), 137–161.

Murphy, K. (2011). *Janeway´s Immunobiology* (8th ed.). Garland Science.

Mweu, E., & English, M. (2008). Typhoid fever in children in Africa. *Tropical Medicine and*

*International Health*, *13*(4), 532–540.
Nanton, M. R., Way, S. S., Shlomchik, M. J., & McSorley, S. J. (2012). Cutting Edge: B Cells Are Essential for Protective Immunity against Salmonella Independent of Antibody Secretion . *The Journal of Immunology*, *189*(12), 5503–5507.
Nebert, D. W., Roe, A. L., Dieter, M. Z., Solis, W. A., Yang, Y., & Dalton, T. P. (2000). Role of the aromatic hydrocarbon receptor and (Ah) gene battery in the oxidative stress response, cell cycle control, and apoptosis. *Biochemical Pharmacology*, *59*(1), 65–85.
Neefjes, J., Jongsma, M. L. M., Paul, P., & Bakke, O. (2011). Towards a systems understanding of MHC class i and MHC class II antigen presentation. *Nature Reviews Immunology*, *11*(12), 823–836.
Nguyen, N. T., Kimura, A., Nakahama, T., Chinen, I., Masuda, K., Nohara, K., Fujii-Kuriyama, Y., & Kishimoto, T. (2010). Aryl hydrocarbon receptor negatively regulates dendritic cell immunogenicity via a kynurenine-dependent mechanism. *Proceedings of the National Academy of Sciences of the United States of America*, *107*(46), 19961–19966.
Obata, Y., Furusawa, Y., & Hase, K. (2015). Epigenetic modifications of the immune system in health and disease. *Immunology and Cell Biology*, *93*(3), 226–232.
Ochiai, R. L., Acosta, C. J., Danovaro-Holliday, M. C., Baiqing, D., Bhattacharya, S. K., Agtini, M. D., Bhutta, Z. A., Canh, D. G., Ali, M., Shin, S., Wain, J., Page, A. L., Albert, M. J., Farrar, J., Abu-Elyazeed, R., Pang, T., Galindo, C. M., Von Seidlein, L., Clemens, J. D., … Jodar, L. (2008). A study of typhoid fever in five Asian countries: Disease burden and implications for controls. *Bulletin of the World Health Organization*, *86*(4), 260–268.
Ohl, M. E., & Miller, S. I. (2001). Salmonella: A Model for Bacterial Pathogenesis. *Annual Review of Medicine*, *52*(1), 259–274.
Ohtake, F., Baba, A., Takada, I., Okada, M., Iwasaki, K., Miki, H., Takahashi, S., Kouzmenko, A., Nohara, K., Chiba, T., Fujii-Kuriyama, Y., & Kato, S. (2007). Dioxin receptor is a ligand-dependent E3 ubiquitin ligase. *Nature*, *446*(7135), 562–566.
Patel, T. A., Armstrong, M., Morris-Jones, S. D., Wright, S. G., & Doherty, T. (2010). Imported enteric fever: Case series from the hospital for tropical diseases, London, United Kingdom. *American Journal of Tropical Medicine and Hygiene*, *82*(6), 1121–1126.
Pennock, N. D., White, J. T., Cross, E. W., Cheney, E. E., Tamburini, B. A., & Kedl, R. M. (2013). T cell responses: Naïve to memory and everything in between. *American Journal of Physiology - Advances in Physiology Education*, *37*(4), 273–283.
Perše, M., & Cerar, A. (2012). Dextran Sodium Sulphate Colitis Mouse Model: Traps and Tricks. *Journal of Biomedicine and Biotechnology*, *2012*, 13.
Petrulis, J. R., & Perdew, G. H. (2002). The role of chaperone proteins in the aryl hydrocarbon receptor core complex. *Chemico-Biological Interactions*, *141*(1–2), 25–40.
Pfefferkorn, E. R. (1984). Interferon y blocks the growth of Toxoplasma gondii in human fibroblasts by inducing the host cells to degrade tryptophan (tryptophan/kynurenine/N-formylkynurenine). In *Medical Sciences* (Vol. 81).
Pouzol, S., Tanmoy, A. M., Ahmed, D., Khanam, F., Abdullah Brooks, W., Bhuyan, G. S., Fabre, L., Bryant, J. E., Gustin, M. P., Vanhems, P., Carman, B., Weill, F. X., Qadri, F., Saha, S., & Endtz, H. (2019). Clinical Evaluation of a Multiplex PCR for the Detection of Salmonella enterica Serovars Typhi and Paratyphi A from Blood Specimens in a High-Endemic Setting. *American Journal of Tropical Medicine and Hygiene*, *101*(3), 513–520.
Priyodip, P., Prakash, P. Y., & Balaji, S. (2017). Phytases of Probiotic Bacteria: Characteristics

and Beneficial Aspects. *Indian Journal of Microbiology*, *57*(2), 148–154.

Qin, L., Waseem, T. C., Sahoo, A., Bieerkehazhi, S., Zhou, H., Galkina, E. V., & Nurieva, R. (2018). Insights into the molecular mechanisms of T follicular helper-mediated immunity and pathology. *Frontiers in Immunology*, *9*(AUG), 1.

Quintana, F. J., Basso, A. S., Iglesias, A. H., Korn, T., Farez, M. F., Bettelli, E., Caccamo, M., Oukka, M., & Weiner, H. L. (2008). Control of Treg and TH17 cell differentiation by the aryl hydrocarbon receptor. *Nature*, *453*(7191), 65–71.

Raffatellu, M., Santos, R. L., Verhoeven, D. E., George, M. D., Wilson, R. P., Winter, S. E., Godinez, I., Sankaran, S., Paixao, T. A., Gordon, M. A., Kolls, J. K., Dandekar, S., & Bäumler, A. J. (2008). Simian immunodeficiency virus-induced mucosal interleukin-17 deficiency promotes Salmonella dissemination from the gut. *Nature Medicine*, *14*(4), 421–428.

Ramakrishnan, C., Maier, S., Walker, R. A., Rehrauer, H., Joekel, D. E., Winiger, R. R., Basso, W. U., Grigg, M. E., Hehl, A. B., Deplazes, P., & Smith, N. C. (2019). An experimental genetically attenuated live vaccine to prevent transmission of Toxoplasma gondii by cats. *Scientific Reports*, *9*(1).

Rannug, A., Rannug, U., Rosenkranz, H. S., Winqvist, L., Westerholm, R., Agurell, E., & Grafstrom, A. K. (1987). Certain photooxidized derivatives of tryptophan bind with very high affinity to the Ah receptor and are likely to be endogenous signal substances. *Journal of Biological Chemistry*, *262*(32), 15422–15427.

Reynolds, L. M., Wan, M., Ding, J., Taylor, J. R., Lohman, K., Su, D., Bennett, B. D., Porter, D. K., Gimple, R., Pittman, G. S., Wang, X., Howard, T. D., Siscovick, D., Psaty, B. M., Shea, S., Burke, G. L., Jacobs, D. R., Rich, S. S., Hixson, J. E., … Liu, Y. (2015). DNA Methylation of the Aryl Hydrocarbon Receptor Repressor Associations with Cigarette Smoking and Subclinical Atherosclerosis. *Circulation: Cardiovascular Genetics*, *8*(5), 707–716.

Robert-Gangneux, F., & Dardé, M. L. (2012). Epidemiology of and diagnostic strategies for toxoplasmosis. *Clinical Microbiology Reviews*, *25*(2), 264–296.

Rock, K. L., Reits, E., & Neefjes, J. (2016). Present Yourself! By MHC Class I and MHC Class II Molecules. *Trends in Immunology*, *37*(11), 724–737.

Rosche, K. L., Aljasham, A. T., Kipfer, J. N., Piatkowski, B. T., & Konjufca, V. (2015). Infection with Salmonella enterica serovar typhimurium leads to increased proportions of F4/80+ red pulp macrophages and decreased proportions of B and T lymphocytes in the spleen. *PLoS ONE*, *10*(6).

Russ, B. E., Prier, J. E., Rao, S., & Turner, S. J. (2013). T cell immunity as a tool for studying epigenetic regulation of cellular differentiation. *Frontiers in Genetics*, *4*(NOV), 1–10.

Rydström, A., & Wick, M. J. (2007). Monocyte Recruitment, Activation, and Function in the Gut-Associated Lymphoid Tissue during Oral Salmonella Infection . *The Journal of Immunology*, *178*(9), 5789–5801.

Salazar-Gonzalez, R.-M., Srinivasan, A., Griffin, A., Muralimohan, G., Ertelt, J. M., Ravindran, R., Vella, A. T., & McSorley, S. J. (2007). Salmonella Flagellin Induces Bystander Activation of Splenic Dendritic Cells and Hinders Bacterial Replication In Vivo . *The Journal of Immunology*, *179*(9), 6169–6175.

Salisbury, R. L., & Sulentic, C. E. W. (2015). The AhR and NF-κB/Rel Proteins Mediate the Inhibitory Effect of 2,3,7,8-Tetrachlorodibenzo-p-Dioxin on the 3' Immunoglobulin Heavy Chain Regulatory Region. *Toxicological Sciences*, *148*(2), 443–459.

Sanchez, Y., De Dios Rosado, J., Vega, L., Elizondo, G., Estrada-Muñiz, E., Saavedra, R., Júarez, I., & Rodríguez-Sosa, M. (2010). The unexpected role for the aryl hydrocarbon receptor on susceptibility to experimental toxoplasmosis. *Journal of Biomedicine and Biotechnology*, *2010*, 15.

Sarma, J. V., & Ward, P. A. (2011). The complement system. In *Cell and Tissue Research* (Vol. 343, Issue 1, pp. 227–235).

Scharton-Kersten, T. M., Wynn, T. A., Denkers, E. Y., Bala, S., Grunvald, E., Hieny, S., Gazzinelli, R. T., & Sher, A. (1996). In the absence of endogenous IFN-gamma, mice develop unimpaired IL-12 responses to Toxoplasma gondii while failing to control acute infection. *Journal of Immunology (Baltimore, Md. : 1950)*, *157*(9), 4045–4054. http://www.ncbi.nlm.nih.gov/pubmed/8892638

Schmidt, J. V., & Bradfield, C. A. (1996). Ah Receptor Signaling Pathways. *Annual Review of Cell and Developmental Biology*, *12*(1), 55–89.

Schmidt, J. V., Su, G. H. T., Reddy, J. K., Simon, M. C., & Bradfield, C. A. (1996). Characterization of a murine Ahr null allele: Involvement of the Ah receptor in hepatic growth and development. *Proceedings of the National Academy of Sciences of the United States of America*, *93*(13), 6731–6736.

Schnekenburger, M., Peng, L., & Puga, A. (2007). HDAC1 bound to the Cyp1a1 promoter blocks histone acetylation associated with Ah receptor-mediated trans-activation. *Biochimica et Biophysica Acta - Gene Structure and Expression*, *1769*(9–10), 569–578.

Schulz, S. M., Köhler, G., Schütze, N., Knauer, J., Straubinger, R. K., Chackerian, A. A., Witte, E., Wolk, K., Sabat, R., Iwakura, Y., Holscher, C., Müller, U., Kastelein, R. A., & Alber, G. (2008). Protective Immunity to Systemic Infection with Attenuated Salmonella enterica serovar Enteritidis in the Absence of IL-12 Is Associated with IL-23-Dependent IL-22, but Not IL-17 . *The Journal of Immunology*, *181*(11), 7891–7901.

Searle, L. E. J., Best, A., Nunez, A., Salguero, F. J., Johnson, L., Weyer, U., Dugdale, A. H., Cooley, W. A., Carter, B., Jones, G., Tzortzis, G., Woodward, M. J., & La Ragione, R. M. (2009). A mixture containing galactooligosaccharide, produced by the enzymic activity of bifidobacterium bifidum, reduces salmonella enterica serovar typhimurium infection in mice. *Journal of Medical Microbiology*, *58*(1), 37–48.

Shiow, L. R., Rosen, D. B., Brdičková, N., Xu, Y., An, J., Lanier, L. L., Cyster, J. G., & Matloubian, M. (2006). CD69 acts downstream of interferon-α/β to inhibit S1P 1 and lymphocyte egress from lymphoid organs. *Nature*, *440*(7083), 540–544.

Sibley, L. D., & Boothroyd, J. C. (1992). Virulent strains of Toxoplasma gondii comprise a single clonal lineage. *Nature*, *359*(6390), 82–85.

Sibley, L. D., Mordue, D. G., Su, C., Robben, P. M., & Howe, D. K. (2002). Genetic approaches to studying virulence and pathogenesis in Toxoplasma gondii. *Philosophical Transactions of the Royal Society B: Biological Sciences*, *357*(1417), 81–88.

Sinal, C. J., & Bend, J. R. (1997). Aryl hydrocarbon receptor-dependent induction of Cyp1a1 by bilirubin in mouse hepatoma hepa 1c1c7 cells. *Molecular Pharmacology*, *52*(4), 590–599.

Singh, K. P., Garrett, R. W., Casado, F. L., & Gasiewicz, T. A. (2011). Aryl hydrocarbon receptor-null allele mice have hematopoietic stem/progenitor cells with abnormal characteristics and functions. *Stem Cells and Development*, *20*(5), 769–784.

Singh, K. P., Wyman, A., Casado, F. L., Garrett, R. W., & Gasiewicz, T. A. (2009). Treatment of mice with the Ah receptor agonist and human carcinogen dioxin results in altered numbers

and function of hematopoietic stem cells. *Carcinogenesis*, *30*(1), 11–19.
Singh, V. K., Saini, A., & Chandra, R. (2014). Role of Erythropoietin and Other Growth Factors in Ex Vivo Erythropoiesis . *Advances in Regenerative Medicine*, *2014*, 1–8.
Sojka, D. K., Bruniquel, D., Schwartz, R. H., & Singh, N. J. (2004). IL-2 Secretion by CD4 + T Cells In Vivo Is Rapid, Transient, and Influenced by TCR-Specific Competition . *The Journal of Immunology*, *172*(10), 6136–6143.
Soshilov, A., & Denison, M. S. (2008). Role of the Per/Arnt/Sim domains in ligand-dependent transformation of the aryl hydrocarbon receptor. *Journal of Biological Chemistry*, *283*(47), 32995–33005.
Spees, A. M., Kingsbury, D. D., Wangdi, T., Xavier, M. N., Tsolis, R. M., & Bäumler, A. J. (2014). Neutrophils are a source of gamma interferon during acute Salmonella enterica serovar typhimurium colitis. *Infection and Immunity*, *82*(4), 1692–1697.
Srinivasan, A., Foley, J., & McSorley, S. J. (2004). Massive Number of Antigen-Specific CD4 T Cells during Vaccination with Live Attenuated Salmonella Causes Interclonal Competition . *The Journal of Immunology*, *172*(11), 6884–6893.
Stanaway, J. D., Parisi, A., Sarkar, K., Blacker, B. F., Reiner, R. C., Hay, S. I., Nixon, M. R., Dolecek, C., James, S. L., Mokdad, A. H., Abebe, G., Ahmadian, E., Alahdab, F., Alemnew, B. T. T., Alipour, V., Allah Bakeshei, F., Animut, M. D., Ansari, F., Arabloo, J., … Crump, J. A. (2019). The global burden of non-typhoidal salmonella invasive disease: a systematic analysis for the Global Burden of Disease Study 2017. *The Lancet Infectious Diseases*, *19*(12), 1312–1324.
Steff, A. M., Fortin, M., Arguin, C., & Hugo, P. (2001). Detection of a decrease in green fluorescent protein fluorescence for the monitoring of cell death: An assay amenable to high-throughput screening technologies. *Cytometry*, *45*(4), 237–243.
Sturge, C. R., & Yarovinsky, F. (2014). Complex immune cell interplay in the gamma interferon response during Toxoplasma gondii infection. *Infection and Immunity*, *82*(8), 3090–3097.
Stutte, S., Quast, T., Gerbitzki, N., Savinko, T., Novak, N., Reifenberger, J., Homey, B., Kolanus, W., Alenius, H., & Förster, I. (2010). Requirement of CCL17 for CCR7- and CXCR4-dependent migration of cutaneous dendritic cells. *Proceedings of the National Academy of Sciences of the United States of America*, *107*(19), 8736–8741.
Subauste, C., & Remington, J. (2001). Animal Models for Toxoplasma gondii Infection . *Current Protocols in Immunology*, 1–18.
Szabo, S. J., Kim, S. T., Costa, G. L., Zhang, X., Fathman, C. G., & Glimcher, L. H. (2000). A novel transcription factor, T-bet, directs Th1 lineage commitment. *Cell*, *100*(6), 655–669.
Sztein, M. B., Salerno-Goncalves, R., & McArthur, M. A. (2014). Complex adaptive immunity to enteric fevers in humans: Lessons learned and the path forward. *Frontiers in Immunology*, *5*(OCT).
Takahashi, K., Mitsui, K., & Yamanaka, S. (2003). Role of ERas in promoting tumour-like properties in mouse embryonic stem cells. *Nature*, *423*(6939), 541–545.
Tam, M. A., Rydström, A., Sundquist, M., & Wick, M. J. (2008). Early cellular responses to Salmonella infection: Dendritic cells, monocytes, and more. *Immunological Reviews*, *225*(1), 140–162.
Taylor-Robinson, A. W., & Phillips, R. S. (1992). Functional characterization of protective CD4+ T-cell clones reactive to the murine malaria parasite Plasmodium chabaudi. *Immunology*, *77*(1), 99–105.

Tkachenko, A., Henkler, F., Brinkmann, J., Sowada, J., Genkinger, D., Kern, C., Tralau, T., & Luch, A. (2016). The Q-rich/PST domain of the AHR regulates both ligand-induced nuclear transport and nucleocytoplasmic shuttling. *Scientific Reports*, *6*.

Uche, I. V., MacLennan, C. A., & Saul, A. (2017). A Systematic Review of the Incidence, Risk Factors and Case Fatality Rates of Invasive Nontyphoidal Salmonella (iNTS) Disease in Africa (1966 to 2014). *PLoS Neglected Tropical Diseases*, *11*(1).

Van Belle, T. L., Coppieters, K. T., & Von Herrath, M. G. (2011). Type 1 diabetes: Etiology, immunology, and therapeutic strategies. *Physiological Reviews*, *91*(1), 79–118.

Villa, M., Gialitakis, M., Tolaini, M., Ahlfors, H., Henderson, C. J., Wolf, C. R., Brink, R., & Stockinger, B. (2017). Aryl hydrocarbon receptor is required for optimal B-cell proliferation. *The EMBO Journal*, *36*(1), 116–128.

Vogel, C. F. A., Ishihara, Y., Campbell, C. E., Kado, S. Y., Nguyen-Chi, A., Sweeney, C., Pollet, M., Stemmann, T. H., & Tuscano, J. M. (2019). A protective role of aryl hydrocarbon receptor repressor in inflammation and tumor growth. *Cancers*, *11*(5).

Vogel, C. F. A., Khan, E. M., Leung, P. S. C., Gershwin, M. E., Chang, W. L. W., Wu, D., Haarmann-Stemmann, T., Hoffmann, A., & Denison, M. S. (2014). Cross-talk between aryl hydrocarbon receptor and the inflammatory response: A role for nuclear factor-κB. *Journal of Biological Chemistry*, *289*(3), 1866–1875.

Vorrink, S. U., & Domann, F. E. (2014). Regulatory crosstalk and interference between the xenobiotic and hypoxia sensing pathways at the AhR-ARNT-HIF1α signaling node. *Chem Biol Interact*, *0*, 82–88.

Wagage, S., John, B., Krock, B. L., Hall, A. O., Randall, L. M., Karp, C. L., Simon, M. C., & Hunter, C. A. (2014). The Aryl Hydrocarbon Receptor Promotes IL-10 Production by NK Cells. *The Journal of Immunology*, *192*(4), 1661–1670.

Wagage, S., Pritchard, G. H., Dawson, L., Buza, E. L., Sonnenberg, G. F., & Hunter, C. A. (2015). The group 3 innate lymphoid cell defect in aryl hydrocarbon receptor deficient mice is associated with T cell hyperactivation during intestinal infection. *PLoS ONE*, *10*(5).

Wahid, R., Simon, R., Zafar, S. J., Levine, M. M., & Sztein, M. B. (2012). Live oral typhoid vaccine Ty21a induces cross-reactive humoral immune responses against Salmonella enterica serovar paratyphi A and S. paratyphi B in humans. *Clinical and Vaccine Immunology*, *19*(6), 825–834.

Walisser, J. A., Glover, E., Pande, K., Liss, A. L., & Bradfield, C. A. (2005). Aryl hydrocarbon receptor-dependent liver development and hepatotoxicity are mediated by different cell types. *Proceedings of the National Academy of Sciences of the United States of America*, *102*(49), 17858–17863.

Wallon, M., Liou, C., Garner, P., & Peyron, F. (1999). Congenital toxoplasmosis: Systematic review of evidence of efficacy of treatment in pregnancy. *British Medical Journal*, *318*(7197), 1511–1514.

Wei, S., Huang, J., Liu, Z., Wang, M., Zhang, B., Lian, Z., Guo, Y., & Han, H. (2019). Differential immune responses of C57BL/6 mice to infection by Salmonella enterica serovar Typhimurium strain SL1344, CVCC541 and CMCC50115. *Virulence*, *10*(1), 248–259.

Weiss, L. M., & Dubey, J. P. (2009). Toxoplasmosis: A history of clinical observations. *International Journal for Parasitology*, *39*(8), 895–901.

WHO. (2003). Background document: The diagnosis, treatment and prevention of typhoid fever: Communicable Disease Surveillance and Response. In *Vaccines and Biologicals Department*.

www.who.int/vaccines-documents/

Wilson, C. B., Tsai, V., & Remington, J. S. (1980). Failure to trigger the oxidative metabolic burst by normal macrophages. Possible mechanism for survival of intracellular pathogens. *Journal of Experimental Medicine*, *151*(2), 328–346.

Wincent, E., Amini, N., Luecke, S., Glatt, H., Bergman, J., Crescenzi, C., Rannug, A., & Rannug, U. (2009). The suggested physiologic aryl hydrocarbon receptor activator and cytochrome P4501 substrate 6-formylindolo[3,2-b]carbazole is present in humans. *Journal of Biological Chemistry*, *284*(5), 2690–2696.

Yamada, H., Nishikawa, A., Yamamoto, T., Mizue, Y., Yamada, T., Morizane, M., Tairaku, S., & Nishihira, J. (2011). Prospective study of congenital toxoplasmosis screening with use of IgG avidity and multiplex nested PCR methods. *Journal of Clinical Microbiology*, *49*(7), 2552–2556.

Yamada, T., Horimoto, H., Kameyama, T., Hayakawa, S., Yamato, H., Dazai, M., Takada, A., Kida, H., Bott, D., Zhou, A. C., Hutin, D., Watts, T. H., Asaka, M., Matthews, J., & Takaoka, A. (2016). Constitutive aryl hydrocarbon receptor signaling constrains type I interferon-mediated antiviral innate defense. *Nature Immunology*, *17*(6), 687–694.

Yang, X. O., Pappu, B. P., Nurieva, R., Akimzhanov, A., Kang, H. S., Chung, Y., Ma, L., Shah, B., Panopoulos, A. D., Schluns, K. S., Watowich, S. S., Tian, Q., Jetten, A. M., & Dong, C. (2008). Th17 Lineage Differentiation Is Programmed by Orphan Nuclear Receptors RORα and RORγ. *Immunity*, *28*(1), 29–39.

Yi, T., Wang, J., Zhu, K., Tang, Y., Huang, S., Shui, X., Ding, Y., Chen, C., & Lei, W. (2018). Aryl Hydrocarbon Receptor: A New Player of Pathogenesis and Therapy in Cardiovascular Diseases. *BioMed Research International*, *2018*.

Yrlid, U., Svensson, M., Håkansson, A., Chambers, B. J., Ljunggren, H. G., & Wick, M. J. (2001). In vivo activåtion of dendritic cells and T cells during Salmonella enterica serovar Typhimurium infection. *Infection and Immunity*, *69*(9), 5726–5735.

Zelante, T., Iannitti, R. G., Cunha, C., DeLuca, A., Giovannini, G., Pieraccini, G., Zecchi, R., D'Angelo, C., Massi-Benedetti, C., Fallarino, F., Carvalho, A., Puccetti, P., & Romani, L. (2013). Tryptophan catabolites from microbiota engage aryl hydrocarbon receptor and balance mucosal reactivity via interleukin-22. *Immunity*, *39*(2), 372–385.

Zhao, L., Liu, L., Guo, B., & Zhu, B. (2015). Regulation of adaptive immune responses by guiding cell movements in the spleen. *Frontiers in Microbiology*, *6*(JUN), 1–6.

Zhu, J., & Paul, W. E. (2008). CD4 T cells: Fates, functions, and faults. *Blood*, *112*(5), 1557–1569.

Zudaire, E., Cuesta, N., Murty, V., Woodson, K., Adams, L., Gonzalez, N., Martínez, A., Narayan, G., Kirsch, I., Franklin, W., Hirsch, F., Birrer, M., & Cuttitta, F. (2008). The aryl hydrocarbon receptor repressor is a putative tumor suppressor gene in multiple human cancers. *Journal of Clinical Investigation*, *118*(2), 640–650.

# Acknowledgements

First and foremost, I would like to express my deepest gratitude and sincere appreciation to Prof. Dr. Irmgard Förster and PD. Dr. Heike Weighardt for accepting me in their work group and for their continuous guidance and support during my PhD project. I would also like to thank Irmgard and Heike for proofreading my thesis. Special thanks go to Heike for helping me in the beginning of my PhD with experiments, answering all my questions patiently, for stimulating discussions and for her motivational and positive spirit.

Besides my supervisors, I would like to thank Prof. Dr. Johannes Hegemann for mentoring me during this PhD project. His interesting questions always helped me to look at a different angle to my project.

I owe special thanks to Philip Hatzfeld for helping me with my S2 experiments, interesting conversations about politics, science, cats and many more. Even though he will not admit it, he was being a very good friend when I needed one. I would also like to thank Anna Erazo for showing me infection experiments in the beginning and Adrian Semeniuk for helping me with some of my experiments. Special thanks go to Michelle Mayer for working with me on parts of this project during her master thesis, which led to valuable results for both of us.

I would like to acknowledge the help of past and current members of the Förster/Weighardt group. In addition to very valuable scientific input, incredible positive energy of Yasmin, Marlene, Oliver and Judith, magnificent scientific curiosity of Lorenz, witty comments of Manja and Irina and Adrian Tobias, Fabian, Anna, Michelle, Philip made it very enjoyable to work in this group.

I am very thankful to Gökcen Nur Gözüm for being a very good friend and always being there for me in good and bad times. Being an international in Germany can be hard sometimes but she made it a lot easier. Gökcen, Nur and Dominic are my family in Germany, and I am very happy to have them in my life.

Words cannot express how grateful I am to have great parents Senol, Döndü, and Gürcan as my brother. Although they are in Turkey, I have always felt their presence with me. I am very thankful for all sacrifices they made and grateful for their inspirations for making me the person who I am today.